Methodology for Using a Non-Linear Parameter Estimation Technique for Reactive Multi-Component Solute Transport Modeling in Ground-Water Systems

Qasem Abdelal

Dissertation submitted to the faculty of the Virginia Polytechnic Institute and State University for partial fulfillment of the requirements for the degree of

Doctor of Philosophy
In
Civil Engineering

Dr. Mark Widdowson, Chair
Dr. John Novak
Dr. David F. Kibler
Dr. Tom Burbey
Dr. Daniel Gallagher

14th of November, 2006
Blacksburg, VA

Keywords: Chlorinated ethenes, SEAM3D, PEST, nonlinear optimization, model calibration, parameter estimation, ground-water

Methodology for Using a Non-Linear Parameter Estimation Technique for Reactive Multi-Component Solute Transport Modeling in Ground-Water Systems

Qasem Abdelal

Abstract

For a numerical or analytical model to be useful it should be ensured that the model outcome matches the observations or field measurements during calibration. This process has been typically done by manual perturbation of the model input parameters. This research investigates a methodology for using non linear parameter estimation technique (the Marquardt-Levenberg technique) with the multi component reactive solute transport model SEAM3D. The reactive multi-component solutes considered in this study are chlorinated ethenes. Previous studies have shown that this class of compounds can be degraded by four different biodegradation mechanisms, and the degradation path is a function of the prevailing oxidation reduction conditions.

Tests were performed in three levels; the first level utilized synthetic model-generated data. The idea was to develop a methodology and perform preliminary testing where "observations" can be generated as needed. The second level of testing involved performing the testing on a single redox zone model. The methodology was refined and tested using data from a chlorinated ethenes-contaminated site. The third level involved performing the tests on a multiple redox zone model. The methodology was tested, and statistical validation of the recommended methodology was performed.

The results of the tests showed that there is a statistical advantage for choosing a subgroup of the available parameters to optimize instead of the optimizing the whole available group. Therefore, it is recommended to perform a parameter sensitivity study prior to the optimization process to identify the suitable parameters to be chosen. The methodology suggests optimizing the oxidation-reduction species parameters first then calibrating the chlorinated ethenes model. The results of the tests also proved the advantage of the sequential optimization of the model parameters, therefore the parameters of the parent compound are optimized, updated in the daughter compound model, for which the parameters are then optimized so on. The test results suggested considering the concentrations of the daughter compounds when optimizing the parameters of the parent compounds. As for the observation weights, the tests suggest starting the applied observation weights during the optimization process at values of one and changing them if needed.

Overall the proposed methodology proved to be very efficient. The optimization methodology yielded sets of model parameters capable of generating concentration profiles with great resemblance to the observed concentration profiles in the two chlorinated ethenes site models considered.

Acknowledgments

All praise is due to Allah, our lord. I thank him for giving me the guidance, patience, and determination to finish this work. This work couldn't have been possible without his mercy and countless blessings. I hope and pray that this work will find its way to being a little step towards helping all humanity live better lives.

Many thanks are due to my advisor, Dr. Mark Widdowson for his continuing advice and words of encouragement. His friendly personality, calm character, and valuable input were my most important resource in the past four years.

To my father Mohamad and my mother Asma, you were as excited about me getting my PhD as I was, if not more! Thank you for your support, encouragement, dua'as and prayers. Thank you father for teaching me the value of following my dream, your passion for learning was your children's greatest inspiration. Thank you mother for your warm feelings, and big heart, you being the great teacher and educator you are, brought a beautiful sense of direction to children's lives. Both of you, father and mother, were and still are my greatest inspiration and role model.

To all my friends, here in Blacksburg, who helped me enjoy my college years, thank you. To my Sister Iman, brother Omar, and all my family back home, this couldn't have happened without you. From the bottom of my heart, thank you all.

Last but not least, to the one who made this past year the happiest year of my life. To the one who was there in those tough nights and stressful days. To my other half and most precious companion, to Sumaia, my lovely wife, thank you. Thank you for your continuing support, encouragement and patience. May you and little Hamza stay in the best health and stay there for me!

Table of Contents

Abstract ii
Acknowledgments iii
Table of Contents iv
List of Figures vi
List of Tables ix
1. Executive Summary 1
1.1 INTRODUCTION 1
1.2 SINGLE REDOX ZONE STUDY 2
1.3 MULTIPLE REDOX ZONE STUDY 3
2. Literature Review 5
3. Single Redox Zone Model 13
3.1 INTRODUCTION 13
3.2 METHODS, TESTING TECHNIQUES AND SITE DESCRIPTOPN 15
3.2.1 SEAM3D 15
3.2.2 PEST and nonlinear optimization theory 17
3.2.3 Description of methods and testing techniques 20
3.3 RESULTS AND DISCUSSION 25
3.3.1 Sequential versus simultaneous estimation of the model parameter 25
3.3.2 Effect of kinetic state 35
3.3.3 Optimization with noisy observations 39
3.3.4 Observation weight influence 43
3.3.5 Pensacola site model 45
3.4. CONCLUSIONS 53
4. Multiple Redox Zone Model 55
4.1. INTRODUCTION 55
4.2 METHODS, TESTING TECHNIQUES AND SITE DESCRIPTOPN 56
4.2.1 Sensitivity analysis 56
4.2.2 Parameter optimization 58
4.2.3 Site description: Kings Bay, GA 63
4.3 RESULTS AND DISCUSSION 65
4.3.1 Sensitivity analysis 65
4.3.2 Anaerobic oxidants calibration 69
4.3.3 Full versus partial parameter model 71
4.3.4 Sequential versus simultaneous estimation of the model parameters 74
4.3.5 Observation weight influence 78
4.3.6 Contribution of anaerobic direct oxidation 81
4.3.7 Calibrated Kings Bay model outcome 85

4.4 SUMMARY 89
5. Summary and Conclusions 90
References 96
Appendices 99
Appendix A: DETAILED DISCUSSION OF THE MATHEMATICS OF INVERSE MODELING 99
Appendix B: CHLORINATED ETHENES BIODEGRADAION PROCESSES 103
Reductive dechlorination 103
Aerobic oxidation 104
Anaerobic oxidation 104
Appendix C: SENSITIVITY AND UNCERTAINITY ANALYSES 106
Sensitivity analysis 106
First order analysis 108
Monte-Carlo method 108
Appendix D: STATISTICAL TESTING CALCULATION SAMPLE 110
Appendix E: DISCUSSION OF THE PEST SOFTWARE 113

List of Figures

Figure 3.1. Illustration of different kinetic representations of degradation along various zones in a reactive contaminant plume 22

Figure 3.2. An aerial view of the Pensacola WWTP with chloroethenes concentrations along the centerline of the plume. 25

Figure 3.3. Comparison between synthetic "observed" concentrations and model predictions using the sequential and simultaneous optimization techniques for PCE, TCE, DCE and VC along the centerline of a plume, optimization performed with the unit weights. 30

Figure 3.4. Comparison between synthetic "observed" concentrations and model predictions using the sequential and simultaneous techniques for PCE, TCE, DCE and VC along the centerline of a plume, optimization performed with the weights yielding same order of magnitude observations. 32

Figure 3.5. Comparison between synthetic "observed" concentrations and model predictions using the sequential and simultaneous optimization techniques for PCE, TCE, DCE and VC along the centerline of a plume, optimization performed with the weights calculated using Equation 3.9. 34

Figure 3.6. Comparison of calibrated model results versus the synthetic data set in a first order kinetic plume. 38

Figure 3.7. Comparison of calibrated model results versus the synthetic data set in a zero order kinetic plume.....38

Figure 3.8. Comparison of calibrated model results versus the synthetic data set in a transition kinetic state plume. 39

Figure 3.9. Comparison of synthetic noisy "observed" concentration data set with the simulated optimized model using SEAM3D with PEST for PCE, TCE, DCE and VC along the centerline of a plume.....42

Figure 3.10. Comparison between synthetic "observed" concentrations and model predictions using two different observation weighting mechanisms for PCE, TCE, DCE and VC along the centerline of a plume.....45

Figure 3.11. Sensitivity coefficients resulting from changing the parameters: hydraulic conductivity (1), longitudinal dispersivity (2), half saturation coefficients for each compound $\overline{K}^{e}_{TCE}$ (3), $\overline{K}^{e}_{DCE}$ (4), $\overline{K}^{e}_{VC}$ (5), rate of degradation for each compound $v^{\max}_{TCE}$ (6), $v^{\max}_{DCE}$ (7) and $v^{\max}_{VC}$ (8), and the inhibition coefficients $k_{DCE,TCE}$ (9), $k_{VC,DCE}$ (10). 50

Figure 3.12. Optimization outcome for the Pensacola site model using manual calibration, sequential and simultaneous PEST optimization. 53

Figure 4.1. Schematic of the Kings Bay landfill location and the chloroethenes plume.....63

Figure 4.2. Concentration values along the centerline of the chloroethenes plume in Kings Bay 64

Figure 4.3. PCE Sensitivity coefficient values 67
Figure 4.4. TCE Sensitivity coefficient values 67
Figure 4.5. DCE Sensitivity coefficient values.....68
Figure 4.6. VC Sensitivity coefficient values 68
Figure 4.7. Calibrated model of the Fe(II) plume. 69
Figure 4.8. Calibrated model of the sulfate data. 70
Figure 4.9. Calibrated model of the methane plume. 70
Figure 4.10. A sample of the normal probability plots used to check normality of values of SSR used in statistical t-testing for PCE full parameter model, the confidence interval lines shown are 90% C.I. 72
Figure 4.11. PCE plumes generated using a model where all the parameters are optimized (Full parameter model) and another where a partial set only was optimized (partial parameter model). 72
Figure 4.12. TCE plumes generated using a model where all the parameters are optimized (Full parameter model) and another where a partial set only was optimized (partial parameter model). 73
Figure 4.13. DCE plumes generated using a model where all the parameters are optimized (Full parameter model) and another where a partial set only was optimized (partial parameter model). 73
Figure 4.14. VC plumes generated using a model where all the parameters are optimized (Full parameter model) and another where a partial set only was optimized (partial parameter model). 74
Figure 4.15. PCE plumes generated using the three methods: B1, where the optimization is sequential without consideration for the daughter compounds, B2 where the optimization is sequential with consideration for the daughter compounds and B3 where the optimization is simultaneous 76
Figure 4.16. TCE plumes generated using the three methods: B1, where the optimization is sequential without consideration for the daughter compounds, B2 where the optimization is sequential with consideration for the daughter compounds and B3 where the optimization is simultaneous 76
Figure 4.17. DCE plumes generated using the three methods: B1, where the optimization is sequential without consideration for the daughter compounds, B2 where the optimization is sequential with consideration for the daughter compounds and B3 where the optimization is simultaneous 77
Figure 4.18. VC plumes generated using the three methods: B1, where the optimization is sequential without consideration for the daughter compounds, B2 where the optimization is sequential with consideration for the daughter compounds and B3 where the optimization is simultaneous 77

Figure 4.19. PCE plumes generated using the parameters optimized with both weighed observations and observations with a weight of one. 79
Figure 4.20. TCE plumes generated using the parameters optimized with both weighed observations and observations with a weight of one. 80
Figure 4.21. DCE plumes generated using the parameters optimized with both weighed observations and observations with a weight of one. 80
Figure 4.22. VC plumes generated using the parameters optimized with both weighed observations and observations with a weight of one. 81
Figure 4.23. DCE and VC plumes resulting form different case studies designed to assess the contribution of anaerobic direct oxidation. 84
Figure 4.24. DCE concentration profiles in three cases, 1) with R.D. only simulated, 2) with both R.D. and DOx., and 3) when no biodegradation is simulated. 84
Figure 4.25. VC concentration profiles in three cases, 1) with R.D. only simulated, 2) with both R.D. and DOx., and 3) when no biodegradation is simulated. 85
Figure 4.26. Concentration profile yielded from the calibrated PCE model 86
Figure 4.27. Concentration profile yielded from the calibrated TCE model 87
Figure 4.28. Concentration profile yielded from the calibrated DCE model 87
Figure 4.29. Concentration profile yielded from the calibrated VC model 88
Figure A.1. Optimization process of the SEAM3D parameters using PEST 102
Figure E.1. A diagram of the PEST optimization process 114
Figure E.2. Screen capture of a sample PEST control file 115
Figure E.3. Screen capture of a sample PEST instructions file 115
Figure E.4. Screen capture of a sample PEST template file 117

List of Tables

Table 3.1. The observations and associated weights of the sequential versus simultaneous parameter optimization test on the synthetic system 27
Table 3.2. Sum of squared residuals (SSR) for the sequential vs. simultaneous optimization for the three weighing mechanisms 27
Table 3.3. Parameter values and inhibition coefficients used in the first order case of optimization 37
Table 3.4. Original and optimized values of parameters under consideration for the first order case 37
Table 3.5. SSR resulting from the optimization of the three kinetic state models 37
Table 3.6. The sum of squared residuals of the weighing effect on the optimization 43
Table 3.7. List of parameters used in the sensitivity study 47
Table 3.8. Parameters selected to be optimized for calibrating the Pensacola model.....51
Table 3.9. The resulting sum of squared residual for the three optimization techniques 51
Table 4.1. Parameters used in the sensitivity analysis and the max sensitivity coefficient values. 56
Table 4.2. The group of high sensitivity coefficient parameters along with their sensitivity coefficients 66
Table 4.3. Input parameters used in the anaerobic oxidant calibration 69
Table 4.4. Summary of the optimization outcome for the full and partial models along with the statistical significance analysis 71
Table 4.5. Summary of the optimization outcome for the three optimization methods B1, B2 and B3 along with the statistical significance test results.....75
Table 4.6. Summary of the optimization outcome for the two weighing mechanisms, one where the weights are set to one and another with assigned weights other than one 78
Table 4.7. Summary of the results obtained from assessing the contribution of anaerobic oxidation to the degradation of chlorinated ethenes.....81
Table 4.8. The SSR and the % reduction due to adding the direct oxidation process, along with the liquid phase concentration removal due to the two degradation process.....85
Table 4.9. Average SSR for the C.E concentration profiles generated using the calibrated Kings Bay model.....86
Table D.1. SSR for the full vs. partial parameter estimation test. 111

Chapter 1

Executive Summary

1.1 INTRODUCTION

Groundwater solute transport models are useful for simulating the behavior of contaminant plumes at contaminated groundwater sites and are widely used in site investigation and remediation studies. In order to ensure usability of a site model, input parameters are configured such that the model outcome matches a pre-measured set of observations. This process of calibration has been traditionally done by manually perturbing input parameters until model predictions reasonably match the observations. Calibration can be lengthy and subject to a number of problems, including non-unique solutions. An alternative method that has been investigated recently is the use of an automated parameter estimation process, also known as inverse modeling process. Using automated parameter estimation, parameter values are optimized using a mathematical algorithm that searches for the best set of parameter values corresponding with the minimum error between observed and simulated data with limited human interference. This approach is designed to save time and reduces model uncertainty.

This study aims at developing a methodology for using a nonlinear parameter optimization algorithm (Levenberg-Marquardt method) for optimizing the input parameters of multi-component reactive solute transport models using the code SEAM3D (Sequential Electron Acceptor Model, 3D). The class of compounds investigated in this study is chlorinated ethenes. However, the proposed methodology is applicable to any class of compounds. The Levenberg-Marquardt method has strength in that it can generally estimate parameters using fewer model runs than any other estimation method, a definite bonus for large models whose run times may be considerable, which is typical with complex chlorinated ethenes models prepared using SEAM3D. The Levenberg-Marquardt method is the method used by the PEST software. Its purpose is to assist in data interpretation, model calibration and predictive analysis. The universal applicability of PEST lies in its ability to perform these tasks for any model that reads its input data from one or a number of ASCII (ie. text) input files and writes the outcomes of its

calculations to one or more ASCII output files (Doherty, 2004). Therefore, one of the main advantages of PEST is that it can be used independently of any model as long as it can communicate with it through its own input and output files. That, along with the fact that it is easy to learn and use, was the reason for using PEST as a non linear parameter estimation tool for this research.

Transport and degradation of chlorinated ethenes is relatively complex to simulate with a mathematical model. Four different processes are known to be responsible for the degradation of chlorinated ethenes; reductive dechlorination, aerobic oxidation, anaerobic oxidation and aerobic cometabolism (Chapelle et al., 2003). The biotransformation path of each compound (therefore, the rate and extent of biodegradation) is a function of the prevalent environmental conditions and the available electron acceptors and donors. This behavior must be captured by the model to ensure accurate simulation of the field processes. The research performed to develop the methodology was initially tested using a synthetic model-generated data. The methodology was then tested using real-world site data where a single redox condition best described the ground-watery system. The methodology was further developed, tested, and statistically validated on another real-world site with multiple redox conditions.

1.2 SINGLE REDOX ZONE STUDY

A series of tests using synthetic systems led to drafting the general guidelines for the proposed methodology. A one-dimensional model using the SEAM3D code was constructed in which tetrachloroethene (PCE) was the source contaminant. Generation of the sequential daughter products of reductive dechlorination was tracked through space and time. Thus, the synthetic data consisted for concentrations of PCE, trichloroethene (TCE), cis-1,2-dichloroethene (cisDCE), and vinyl chloride (VC). This approach provided a useful testing platform in which observations can be generated as needed. The results of tests were assessed using the sum of squared residual (SSR) criterion as well as visual resemblance of the generated concentration profiles to the observed concentration profile.

The results showed that sequential estimation of the parameters of the model starting from the parent compound and ending with the daughter compound has an advantage over the simultaneous estimation of parameters of the all the compounds together. Another test investigated at the impact of the kinetic state of the plume showed no impact of the kinetic state of the plume on the optimization process. A third test where the observations were contaminated by a random noise showed that the optimization process was robust to the applied noise. An additional test showed that setting the observation weights to one has an advantage over applying any kind of weights to the observations. The findings from the tests using synthetic data demonstrated the robustness of the methodology for using the nonlinear parameter optimization algorithm with SEAM3D.

The methodology was then tested using data from a chloroethene-contaminated site in Pensacola, Florida. A site model was constructed and a sensitivity analysis study was conducted on 10 of the model parameters, from which a group of five parameters were chosen in the optimization process. Those five were the maximum specific rate of substrate utilization for the three compounds (TCE, DCE, and VC) and the inhibition coefficients of VC by DCE and of DCE by TCE. These five parameters were optimized and the model calibrated using the optimized parameters proved to produce concentration profiles that are in better match with the observations than the ones generated using a previously-reported, manually-calibrated model.

1.3 MULTIPLE REDOX ZONE STUDY

The methodology developed as a result to the studies performed on the single redox zone case primarily focused on the chloroethenes and did not consider electron acceptors and donors. The methodology was expanded and tested on a more general case in which more than one redox zone is present in an anoxic ground-water system. As a result, rates of reductive dechlorination may vary within the plume and anaerobic oxidation may be a significant attenuation process. The methodology for optimization included redox components in which the model calibration steps sequentially from terminal electron accepting processes (TEAPs) that yield the most energy in an anoxic system, i.e., Fe(III), all the way to methanogenesis. Tests were designed so that multiple optimization runs

are performed, and the statistical significance of the recommendations was tested. The study included a sensitivity analysis process on 30 of the model parameters, from which a subgroup of 13 parameters was chosen for the chlorinated ethenes optimization process. The tests showed a statistical advantage to optimizing a subgroup of the parameters over optimizing the whole set of parameters. The tests also showed an advantage for sequential optimization over simultaneous optimization. As for the observation weight factors to be used for the optimization process, it is recommended to start by using a unit weight for the observations instead of applying any other weight formula, if the optimization led to poor results, another weighing mechanism can be investigated.

As a result, the outline of the methodology suggested for applying nonlinear optimization methods for parameter estimation of multi-component reactive solute model can be summarized as follows:

1. Build a conceptual model then a numerical model.

2. Perform sensitivity analysis on the model parameters and isolate the parameters with highest sensitivity coefficients for each compound.

3. Calibrate the model so that electron donor/electron acceptor species are properly simulated; this is done by performing optimization on the parameters of the SEAM3D Biodegradation Package.

4. Optimize the chosen parameters of the source chlorinated ethenes compound (typically PCE or TCE), and then optimize parameters for the direct daughter compound.

5. Repeat Step 4 above for all the chlorinated ethenes compounds.

Chapter 2

Literature Review

The automated parameter optimization process (also referred to as the inverse modeling process) is where an algorithm searches for a set of parameters that minimize the difference between the model predicted values and observed / measured data. Inverse modeling techniques for groundwater flow and contaminant transport modeling have been used since the 1980s (Yeh, 1986). The procedure is still being refined, and the applications of the inverse modeling tools are still being widened. Most of the approaches for solving the inverse problem are based on derivative based optimization methods (Hill, 1998; Dai and Samper, 2004;Doherty, 2004). These derivative-based optimization methods have a definite superiority in cases where the objective function is convex; therefore, single global optima can be found (Mugunthan et al., 2005). A detailed discussion of the mathematics of inverse modeling and one of the derivative based optimization software (PEST) in the appendix section of this dissertation.

Another class of optimization methods that has been historically used for groundwater model calibration is the heuristic methods and genetic algorithms. For example, Ritzel et al. (1994) used genetic algorithms to find a set of optimal solutions for combining reliability and cost for a hydraulic contaminant system. The decision variables were how many wells to install, where to install them and how much to pump from each. Another example on the use of these algorithms is the work of Reed et al. (2000). The author used genetic algorithms to identify cost-effective sampling plans that accurately quantify the total mass of dissolved contaminant in a contaminated site monitoring and sampling plan. Other examples of the use of genetic algorithms include, but are not limited to, Harrouni et al.(1996) and Wu et al. (2006). These algorithms tend to require numerous model runs to obtain a suitable set of model parameters (Mugunthan et al., 2005). This poses a problem with many groundwater and solute transport models where the computational cost of a single forward run is high.

The third class of algorithms are the function approximation algorithms, these use a mathematical model as a surrogate of the optimization objective function to guide the

search for suitable parameters (Mugunthan et al., 2005). The surrogate functions can be thin plate splines, cubic splines, Gaussian and multi-quadratic functions. These methods have the advantage of being able to optimize the parameters while performing parallel model runs instead of serial model runs.

One of the applications of inverse modeling in contaminant transport was a study by Sciortino et al. (2000), in which a procedure was developed to identify the source location and dimensions of a single component dense non aqueous phase liquid (DNAPL) plume. The inverse code was developed based on the Levenberg-Marquardt method (a derivative based algorithm), and the solute transport model was a three dimensional analytical model describing the transport of the solute from a DNAPL pool. The robustness of the process to normally-distributed noise was tested by comparing the sensitivity of the parameter estimate to the weighted observations using three different weighing mechanisms. The best results obtained were with weighted concentrations; the weights being obtained by adding a constant value for the observed concentrations. Non-uniqueness in the parameter estimates was noted.

Leijnse et al. (2002) showed rather different results in which the effect of weighting the observations on parameter estimates in groundwater modeling was tested. Four different approaches of increased complexity were used for weighting the observations. The study found that the parameters estimated by a weighted least squares approximation were not very sensitive to the weights that were assigned to the different observations. As a result, it was recommended to use the simplest way of assigning weights to the observations. Hill (2000) provided a comprehensive study that investigated four issues related to weighting observations in inverse modeling application to groundwater models. The study revealed the importance of assigning weights in regression to represent observation error.

One of the other studies that dealt with inverse modeling from a different angle was presented by Anderman and Hill (1999). The goal of the study was to evaluate a 3-stage process in which the advective front location was used as a surrogate to concentration in estimating flow and transport parameters; specifically, hydraulic conductivities, recharge,

boundary conditions and dispersivities. It was hypothesized that this would reduce the computation time that the simulations require. The procedure was tested on a synthetic 2D analytical model, and the effect of error in the data was investigated using Monte-Carlo analysis. The study compared the proposed three-stage procedure to typical simultaneous estimation and found the performance of the simultaneous procedure to be better than the three-stage procedure. It also anticipated that the performance of the new method was less likely to be better with numerical models than it was with analytical models.

Many of the model calibration studies that dealt with reactive solutes still rely on the traditional trial and error techniques for parameter estimation. Dai and Samper (2004) performed one of the few inverse problem studies on multi-component reactive solute transport. Their proposed methodology was developed and tested on a synthetic system, and the theory was tested on a small scale column experiment dealing with cation exchange and kinetically-controlled calcite dissolution. The Gauss-Newton-Levenberg-Marquardt method was implemented in an inverse code which solves both the forward and inverse problems. The inverse modeling techniques proved to work well in estimating flow and transport parameters. Accurate solution could not be found, however, when the synthetic concentrations were contaminated with log normally distributed random noise.

Tebes-Stevens and Valocchil. (2000a) developed two codes to estimate reaction rate sensitivity coefficients for a multi component solute. One of the codes solved the fully-coupled system of sensitivity equations while the other code applies the operator splitting approach. Three types of sensitivity were presented. The first type was the typical perturbation techniques which have the advantage of being easy to calculate but the two disadvantages of being too computationally intensive, and that the size of the parameter perturbation factor has to be optimally chosen to avoid round off error. The second type was the direct method, in which the original model was derived with respect to the parameter considered. The advantage of this technique was that it was less numerically intensive than the perturbation method, because the typical non linear PDE used for reactive solute transport modeling simplified to a linear PDE. The third technique was the

adjoint method in which the direct sensitivity equations are manipulated to obtain an efficient algorithm, this algorithm is used for the calculation of the sensitivity of a set of performance functions with respect to each of the system parameters. Tebes-Stevens and Valocchil. (2000a) concluded that the use of the operator splitting approach significantly reduced the computational time. These comparisons also demonstrated that solution of the sensitivity equation was more efficient than a traditional direct perturbation sensitivity analysis. The sensitivity coefficients helped gain insight into the relative significance of the reaction process and to rank the individual reaction parameters in terms of importance.

Tebes-Stevens et al. (2001) compared the effect the uncertainty of flow and transport parameters have over the results of the solute transport model. This was done by comparing the local sensitivity coefficients for transport and reaction parameters. They concluded that both reaction and transport parameters were equally important.

Essaid and et al. (2003) conducted a study in which the USGS solute transport and biodegradation code BIOMOC was used in conjunction with the universal inverse modeling code UCODE to estimate the field scale hydrocarbon dissolution and biodegradation. The input parameters were recharge rate, hydraulic conductivity, dissolution rate coefficient, individual first-order BTEX anaerobic degradation rates, and transverse dispersivity. The method was able to reproduce the general plume behavior, but did not reproduce the observed small scale spatial and temporal variability in concentrations.

Suna et al. (2001b) conducted a study to use inverse modeling techniques for estimating the first order reaction rate of multi-component reactive solute using data obtained from a field site. The authors used an analytical solution to a field site contaminated with chlorinated ethenes, and estimated the biodegradation rate parameters sequentially, first for the parent compound, then for each the subsequent compounds. The reaction rate for the source compound (perchloroethene, PCE) was identified, and used to predict the PCE concentration. The concentration of the source compound was used in the direct daughter compound (trichloroethene, TCE) formulation, then the reaction rate for TCE was

estimated, and the concentration distribution of TCE was calculated. The process was repeated for the next two daughter compounds dichloroethene (DCE) and vinyl chloride (VC). The optimization tool that was used was a subroutine within MATLAB that relies on the Golden section method and the Parabolic interpolation method (both being non-gradient optimization techniques). The study concluded that using the proposed method the multi-dimensional optimization problem can be simplified to be a series of one dimensional search problems. This conclusion, however, was only applicable to first order kinetics with uniform groundwater flow conditions.

Breukelena et al. (2004) conducted a study in which the biodegradation of a landfill leachate was simulated using a 1D reactive transport model and simulating the biodegradation of DOC assuming first order oxidations. The reason for this assumption was to reduce the number of sensitive and unknown parameters. Breukelena et al. (2004) used the non linear parameter estimation program PEST to estimate some of the parameters for cation exchange, proton buffering, kinetic precipitation of carbonate minerals, and degassing. The authors referred to those processes as secondary processes (as opposed to the primary processes) of biodegradation of organic carbon coupled to iron reduction. The study demonstrated the importance of the secondary processes in simulating the leachate plume. The problem encountered, however, was the non-uniqueness of the modeling processes; that is, the model would still behave reasonably if certain processes were replaced by other processes.

In Ling and Rafai (2003) the uncertainty in model predictions for a site contaminated with a chlorinated ethenes spill was investigated. The goal was to simulate the effect of contamination source cleanup on the contaminant plume and to determine the effect of parameter uncertainty on model predictions of the plume length, maximum concentration and persistence time. The model was run a number of times using Monte Carlo analysis procedure while varying the most sensitive parameters. The results obtained from the study were believed to provide a better assessment and verification of the effectiveness and feasibility of the site remedies.

Yager (2000) documented a modeling study designed to validate the National Research Council (NRC) procedure for assessing remedial strategy and to identify major sources of uncertainty in the modeling procedure. Two fate and transport models were used for the study; MOC3D for three dimensional transport of a single species (TCE), and BIOMOC for 2D transport of multiple species. The transport models were built to simulate the extent of the plume during pre-pumping and pumping conditions and estimate the amount of mass of contaminants removed by pumping. UCODE was used for transport model parameter estimation, and five different models were used for plume simulation. One using Monod kinetics and the rest using first order kinetics. Both steady state and transient states were simulated and log the concentrations were used to unify the weights of the observations. The models underestimated the extent of the TCE plume and over estimated the extent of DCE and VC plumes; this may in part be due to the two different models used. In addition, some transport processes may not have been accurately represented in the simulation. The processes represented were advection, diffusion, point sources and sinks, first order and Monod reaction rates, zero order microorganisms growth rate, and linear exchange coefficients. The effect of inhibitors and lack of secondary substrates was neglected in that study as well. The study concluded that biodegradation of chloroethenes at that site can be represented as first order reactions, because the uptake rates computed using first order kinetics were nearly equivalent to those computed from first order approximation, and that the computed concentrations are generally less than the half saturation coefficients.

One recent concept in groundwater modeling is the concept of multi-model ranking and averaging (Poeter, 2006; Poeter and Anderson, 2005; Jakeman et al., 2006a). This concept emerged from the need to consider alternative plausible models for a certain study instead of a single model. This is due to the uncertainty in the hydrogeologic conditions and because running multiple models became much easier to do due to the advancements in the computational power and inverse modeling capabilities (Poeter and Anderson, 2005). Generally more than one model could yield similar acceptable fit to the observations; therefore inference should be made from multiple models. Multi-model averaging help captures model uncertainty (Poeter, 2006). Therefore, hydrogeologists should routinely consider several models to maintain an open mind about the system

given the uncertainty in the site conditions. Those alternative models could vary in the structure of hydrogeologic units, boundary conditions or parameter fields and all models considered should be calibrated before the models can be compared. Poeter and Anderson (2005) did some research in this field. The premise was that upon comparing multiple models, if one model is clearly superior to the rest, it is reasonable to use the model for prediction. But in cases where no one model is clearly superior, then it is reasonable to weigh all predictions. In the cases where different models yield substantially different results, then additional data need to be collected. The work of Poeter and Anderson (2005) had multiple objectives. One of which was to come up with a simple effective approach for selecting the best model. Another objective was to provide a method for making formal multimodal inference. A computer-generated example was used to illustrate the method. Choosing the best model according to the authors can be done based on an estimator called the Akaike Information Criterion (AICc), which is a function of the estimated residual variance (the result of dividing the weighed sum of squared residuals by the number of observations), number of observations, and number of estimated parameter of the model. AICc is calculated for each of the models and the model with lowest value is the best.

A look at the previously discussed studies reveals that the interest in the use of inverse modeling tools in groundwater contaminant transport is rather recent. A collection of models (analytical, BIOMOC, MOC3D) and inverse modeling tools (UCODE, PEST, MATLAB's Golden section method) was used. None of the studies used PEST to estimate the parameters of the SEAM3D model. In many of the investigated studies, the use of inverse modeling was only a part of a complete modeling project, not as a stand-alone study. The research proposed here investigates inverse modeling as a valuable tool for estimating the parameters of the SEAM3D model and address the attenuation processes and the impact of redox conditions. The current research couples the application of the inverse modeling tool on a synthetic system with the application on two field site. The former gives more flexibility in testing the tool and assessing its success while the later assures the practical applicability of the theory.

A methodology is proposed for undertaking model calibration for multi-component reactive contaminants in multiple oxidation reduction conditions. This methodology is refined by performing multiple tests, some of which are similar to those found in the literature presented above, and some are unique to this study. These tests are 1) studying the effect of applying weights to the observations on the quality of parameter optimization, 2) the effect of observation noise on the quality of the parameter optimization, 3) the advantage (if any) for optimizing the parameters sequentially over optimizing them simultaneously, and 4) the advantage (if any) for optimizing some of the most sensitive model parameters over optimizing the all the possible parameters. The results of all of these tests and site applications will follow.

Chapter 3

Single Redox Zone Model

3.1 INTRODUCTION

Chlorinated solvents, particularly perchloroethene (PCE) and trichloroethene (TCE), are recognized as ubiquitous contaminants of concern in groundwater systems due to widespread use in industrial processes worldwide (EPA, 1998). Once thought to be recalcitrant in aquatic systems, chlorinated ethenes are now recognized as subject to several biotic and abiotic attenuations mechanisms. At many sites the most significant attenuation process is microbially-mediated reductive dechlorination, in which PCE and TCE are sequentially reduced under anaerobic conditions to cis-1, 2-dichloroethene (cis-DCE), vinyl chloride (VC) and further to ethene and ethane (Maymo-Gatell et al., 1997). It is known that dehalogenating microorganisms must be present along with two related factors; highly reducing conditions and an ample supply of organic carbon are needed to sustain reductive dechlorination (Bradley, 2000).

Computational models for simulating the field-scale transport of reactive solutes in the environment such as chlorinated ethenes include analytical and numerical solutions. Some of those models incorporate first-order kinetics (Sun et al., 1999; Clement et al., 1998) while other models include either Michaelis-Menten or Monod kinetics in equations of mass balance to simulate the biotransformation of parent compounds and formation of daughter compounds (Widdowson and Waddill, 1998; Willis and Shoemaker, 2000; Widdowson, 2004). Governing equations that incorporate first-order kinetics are suited for analytical solutions. Numerical methods such as the method of characteristics are required for solving advection, dispersion and source/sink terms in the transport equation. Codes such as BIOPLUMEIII, BIOMOC, MT3DMS, RT3D and SEAM3D rely on finite difference schemes for solving the partial differential equations of contaminant transport (Bennett and Zheng, 2002). The choice of the appropriate model depends primarily on the contaminant characteristics and nature in addition to the goal of the modeling project (Zheng and Bennett, 2002).

From the viewpoint of parameterization, first-order decay models have the advantage of requiring one parameter (decay rate) per species relative to models with Michaelis-Menten kinetics, which require at least two parameters per species (decay rate and half-saturation constant). Despite the convenience and wide spread of the use of first order models, the accuracy of the model results depend on the assumption that the maximum concentration of the rate limiting compound is much less than the values of half saturation coefficient. Bekins et al. (1998) demonstrated the superiority of a two-parameter model relative to single-parameter decay models (zero and first order) in simulating contaminant concentrations along the length of an aqueous chloroethenes plume, where the range in concentration from source to the plume toe can be several orders of magnitude.

Parameter estimation techniques are needed to improve the use of comprehensive numerical models for simulating the transport and reductive dechlorination of chlorinated solvents in aquifers. Suna et al. (2001b) presented a method to optimize reaction rate values for a first-order analytical solution of multiple sequentially (serial) reactive contaminants. An analytical model was developed, and the contaminants simulated were chlorinated ethenes. The method was first tested using synthetic data generated using RT3D and then applied to published field data. Reaction rate values were optimized with a MATLAB subroutine that uses the Golden Section optimization method. The study was successful in optimizing the reaction rate parameters for the first order analytical solution of the transport formulas using both the theoretical and field data.

The purpose of this study is to develop a parameter estimation methodology that would aid in solving equations for a multi-species, multi-parameter reactive transport model. Instead of the limited applicability analytical solution, a general purpose numerical solution for the transport formula will be used. SEAM3D (Sequential Electron Acceptor Model, 3 Dimensional) is a numerical model that enables one to numerically simulate the transport and reductive dechlorination of chlorinated ethenes in a reducing groundwater system (Widdowson and Waddill, 2000). This model uses Monod kinetics for quantifying the mass loss of chlorinated ethenes, which does not constrain the model. This approach enables simulation of spatially-varying zero order, first order, and Michaelis-Menten

kinetics within a plume. The general-purpose parameter estimation software tool PEST (Doherty, 2004) will be used for estimating the model parameters needed for proper calibration of the solute transport model. PEST uses the Gauss-Marquardt-Levenberg method. The strength of this method lies in the fact that it can generally estimate parameters using fewer model runs than any other estimation method (Doherty, 2004). This approach potentially offers advantages relative to manual calibration, especially for a multi-dimensional and multi-species reactive solute transport model. In this chapter, results of method testing for optimizing parameters using PEST with SEAM3D are presented for several scenarios in which PCE is the source compound. Multiple tests were designed and performed using synthetically-generated observed data to validate the robustness of the method. The procedure was then tested using monitoring well data from a chlorinated ethane-contaminated site in which TCE is the source compound.

3.2 METHODS, TESTING TECHNIQUES AND SITE DESCRIPTOPN

3.2.1 SEAM3D

SEAM3D is a numerical model and code for simulating three-dimensional solute transport with aerobic and sequential anaerobic biodegradation and dissolution of compounds from non-aqueous phase liquids (NAPLs) in saturated porous media. The code MT3DMS 4.00, used in conjunction with MODFLOW-2000, is the base code for simulating physical transport with SEAM3D. In addition to the original MT3DMS packages, SEAM3D has additional modules including the Biodegradation, NAPL Dissolution, and Reductive Dechlorination Packages. SEAM3D is capable of simulating the transport and biotransformation of a parent chlorinated solvent compound, PCE or TCE, along with the generation, transport, and biotransformation of daughter products resulting from reductive dechlorination (i.e., cis-DCE and VC). Because the rate and extent of reductive dechlorination is dependent on the redox conditions, the simulated biotransformations are linked to the Biodegradation Package, which is used to simulate electron donor and electron acceptor mass and energy balances.

For the purpose of this study, the equation of mass balance for chlorinated ethenes (PCE, TCE, DCE, and VC; lc = 1-4, respectively) and reductive dechlorination end productions

(ethene and chloride; *lc* = 5 and 6, respectively) takes the form in Equation 3.1

$$-\frac{\partial}{\partial x_i}\left(v_i C_{lc}\right)+\frac{\partial}{\partial x_i}\left(D_{ij}\frac{\partial C_{lc}}{\partial x_j}\right)-R_{\sin k,lc}^{bio,EA}+R_{source,lc}^{bio}=R_{lc}\frac{\partial C_{lc}}{\partial t} \tag{3.1}$$

where C_{lc} is the chlorinated ethene/ reductive dechlorination end product concentration [$M_{lc}L^{-3}$]; R_{lc} is the retardation factor; $R_{\sin k,lc}^{bio,EA}$ is a biodegradation sink term to account for the reduction of a chlorinated ethene [M_{lc} L^{-3} T^{-1}]; $R_{source,lc}^{bio}$ is a biodegradation source term to account for the production of TCE, *cis*DCE, VC, ethene, and chloride [M_{lc} L^{-3} T^{-1}], v is the average pore water velocity [L T^{-1}]; D_{ij} is the tensor for the hydrodynamic dispersion coefficient [L^2 T^{-1}].

The source/sink biodegradation terms are written in terms of Monod kinetics that include inhibition coefficients. This allows simulation of the preferential use of higher energy-yielding chlorinated ethenes as electron acceptors by chlororespiring bacteria. Further, given that hydrogen (electron donor) is not generally limiting in a strongly reducing groundwater system, the general formula for the biodegradation sink term is expressed in terms of the chlorinated ethene (*lc* = 1, 2, 3, and 4):

$$R_{\sin k,lc}^{bio,EA}=\frac{M_y}{\theta}\nu_{lc}^{\max,EA}\left[\frac{\overline{C}_{lc}}{\overline{K}_{lc}^{e}+\overline{C}_{lc}}\right]I_{lc,li} \tag{3.2}$$

where M_y is the microbial biomass concentration of chlorinated ethene reducers [M_b L_{pm}^{-3}]; $\nu_{lc}^{\max,EA}$ is the maximum rate of reductive dechlorination for a chlorinated ethene *lc* [M_{lc} M_b^{-3} T^{-1}]; $\overline{K}_{lc}^{e}$ is the effective half saturation constant for a chlorinated ethene (serving as an EA) *lc* [M_{lc} L^{-3}]; θ is aquifer porosity [L^o]; $\overline{C}_{lc}$ is the effective concentration of a chlorinated ethene *lc* [M_{lc} L^{-3}]; and $I_{lc,li}$ is an inhibition function defined by

$$I_{lc,lj} = \prod_{lj=1}^{lc-1}\left[\frac{\kappa_{lc,lj}}{\kappa_{lc,lj} + \overline{C}_{lj}}\right] \text{ for } lc = 2, 3, \text{ or } 4 \tag{3.3}$$

where $\kappa_{lc,lj}$ is the EA inhibition coefficient [$M_{le}\ L^{-3}$] representing inhibition of the use of a chlorinated ethene *lc* (as an EA) by a higher molecular weight chlorinated ethene *lj*. It is assumed that the microbial population will only gain energy by reducing chlorinated ethenes.

Production of a chlorinated daughter product (TCE, cisDCE and VC) and end products of reductive dechlorination (ethane and Cl) is expressed in terms of the rate of reduction of the parent compound

$$R^{bio}_{source,lc} = \zeta^{dau}_{lc,lc-1} R^{bio,EA}_{sink,lc-1} \tag{3.4}$$

where $\zeta^{dau}_{lc,lc-1}$ is the daughter product generation coefficient [$M_{lc}\ M_{lc-1}^{-1}$].

3.2.2 PEST and nonlinear optimization theory

The purpose of an optimization process is to reduce an objective function. The objective function for solute transport models represents the difference between field observed concentrations and model generated concentrations at the same location and time. Mathematically, the objective function Φ for discrete observations can be represented by (Suna et al., 2001b):

$$\Phi = \sum_{j=1}^{m} w_j \left| \hat{c}_i^{\,j} - c_i^j \right| \quad \forall i = 1,.....,m \tag{3.5}$$

where w_j is the weight of the *j*th observation, $\hat{c}_i$ and c_i are the observed and simulated concentrations of species *i* respectively.

The optimization process is performed by upgrading a set of parameters according to a certain algorithm and running the model to generate a set of new concentrations, which are then compared to the observed concentrations. Doherty, (2004) provides comprehensive discussion of the mathematics of linear and nonlinear optimization. A

detailed discussion of non-linear optimization can be found in Appendix A; however a concise description of the process will follow. The parameter upgrade method used in this study is called the Gauss-Marquardt-Levenberg method. The parameters upgrade vector *u* takes the following form:

$$u = (J^T Q J)^{-1} J^T Q (b - b_o) \tag{3.6}$$

where *J* is the Jacobian matrix, which is a diagonal matrix in which each diagonal element represents the change in the response values relative to change in one of the parameters, in other words the parameter sensitivity coefficients. *Q* is a square diagonal matrix whose ith diagonal element is the square of the weight attached to the ith observation. This weight factor is introduced to account for the difference in orders of magnitude between the various parameters due to unit differences, *b* and b_o represent the concentrations generated using the original set of parameters and the upgraded set of parameters, respectively.

For better numerical performance, the above formula can be adjusted by introducing a parameter named the Marquardt parameter and a scaling matrix. The Marquardt parameter (α) helps in preventing a phenomenon called "hemstitching" in which the parameter set jumps from one side of a valley of minimum Φ to another without actually reaching a minimum. The scaling matrix (*S*) is a diagonal matrix that takes care of the vast difference in the magnitudes of the components of the Jacobian matrix due to difference in the types of the parameters. This magnitude difference introduces great round off errors in the parameter upgrade vector. The scaling matrix is a function of the Jacobian matrix (*J*) and the (*Q*) matrix discussed earlier. The final form of the parameter upgrade vector after adjusting for the two previous factors, which is equivalent but far numerically superior to the form in Equation (3.6), is:

$$S^{-1}u = \left((JS)^T QJS + \alpha S^T S\right)^{-1} (JS)^T Q(b - b_o) \tag{3.7}$$

where the S is a diagonal scaling matrix whose elements take the form:

$$S_{ii} = \left(J^T Q J\right)_{ii}^{-1/2} \tag{3.8}$$

and the largest element of the term $\alpha S^T S$ is denoted as (λ) the "Marquardt Lambda".

The calculation of the derivatives (the components of the Jacobian matrix) is the most time consuming step in the optimization process (Doherty, 2004). Finite difference techniques are typically used to approximate the actual values of the derivatives. Forward difference techniques in which the value of the model outcome is calculated as a response to a fine increase in one of the model parameters. The ratio of the model response change to change in the parameter value represents an approximation of the derivative called forward difference.

The optimization software package used in this study is Parameter Estimation (PEST) (Doherty, 2004). In PEST the user specifies the command line that the package needs to use in order to run the model on its own. The package then runs the model using a user specified input starting parameter, and then it extracts the simulated value from the model output files for each observation point. The sum-of squared-weighted residuals (objective function) is calculated.

To calculate sensitivities of the simulated values to the parameters, the model is executed once more for each parameter, and each time the value of one parameter is slightly perturbed. The differences between perturbed simulated values and the unperturbed simulated values are used to calculate forward-difference sensitivities for each parameter. Once the residuals and the sensitivities are calculated, they are used in the Levenberg – Marquardt method as described by Doherty, (2004) to find a parameter upgrade vector, and the parameters are adjusted accordingly, then the model is rerun with the new set of parameters. The last step of each parameter-estimation iteration involves comparing two quantities against the convergence criteria, these two are: (1) the relative changes in the parameter values and (2) the change in the sum-of-squared-weighted residuals.

PEST has a very powerful regularization tool, which allows it to estimate more parameters than otherwise believed possible. It can for example identify regions for

uniform spatial hydraulic properties in a very numerically stable way. Another tool is what is called the SVD- Assist (Singular Value Decomposition assistant), it helps reduce the parameter space thereby allow having unique solution to the parameter estimation problem as well as reducing the required computation time by factors between two and ten (Doherty, 2004).

3.2.3 Description of methods and testing techniques

The method of parameter estimation was initially tested using synthetic model-generated data. A one-dimensional groundwater and contaminant transport model was constructed for this purpose. The model consisted of 150 cells (1.0 m by 1.0m), with a hydraulic conductivity value of 8.5 m/d, therefore, for simplicity purposes homogeneity is assumed. Constant head boundary conditions were set at the first and last cells of the model to simulate the desired hydraulic gradient. The model was run to steady state for a period of 20 years. Ground water velocity ranged between 6 and 15 cm/day depending on the test assumptions. The porosity value used in the model was 0.25. Nine monitoring points were set at uniform distances, and these serve the purpose of monitoring concentrations that can be used later as synthetic observations. A longitudinal dispersivity of 3.1m was used.

The parameter values used in the synthetic model were based on a previous modeling application using SEAM3D. The synthetic model used was a single redox zone model in which redox conditions did not change with time and space. The parent chlorinated ethene compound was PCE, and all the daughter compounds generated through biodegradation were simulated. The model-generated concentrations based on the original set of parameters were used as "observations" for the optimization process. The parameters to be optimized were randomly perturbed, and PEST was used with SEAM3D to calculate simulated concentrations that best-fit the "observations". All concentrations below 0.001mg/L were discarded because in practice the minimum detectable concentration is around that range. The synthetic plume was allowed to reach steady state, and it is assumed that H_2 never limited reductive dechlorination.

3.2.3.1 Sequential versus simultaneous estimation of the model parameter

The first step in the optimization process involved parameter estimation and calibration to the parent compound. Using the optimized input parameters for the parent compound, the next step was parameter optimization of the immediate daughter compound. This pattern was continued until the final end product of reductive dechlorination (ethene) was reached. A similar approach was used in previous studies (Suna et al., 2001b). This sequential approach was tested against a simultaneous approach in which the parameters of the four compounds were optimized simultaneously.

Three optimization runs were performed, one with observation weights of 1.0, another with observation weight calculated using a formula based on the work of Anderman and Hill (1999). And a third run used weight values that are multiples of 10 and chosen such that all the observation – weight products are within the same order of magnitude. In each of these three runs, the optimization was performed twice, once in a sequential manner, starting from the parent compound and ending with the daughter compound and the other in a simultaneous manner in which all the parameters for the four compounds are optimized in the same run. To evaluate the advantage of one method over the other, the sum of squared residuals for each optimization was calculated (SSR), and the visual match of the generated concentration profile with the observed concentrations was noted. The computational time was monitored as well but was excluded as a comparison criterion because of the observed lack of correlation between the run time and accuracy of model output.

3.2.3.2 Effect of kinetic state

Another test of the methodology was to examine the effect of the "kinetic state" of the contaminant plume on the quality of the parameter optimization process. The key parameter for differentiating between the different kinetic states is the ratio of the aqueous concentration of the parent compound to the half saturation coefficient. By adjusting this ratio, plumes with various kinetic states were synthetically generated. Parameter optimization was performed on three kinetic states (zero- and first-order and mixed kinetics). This concept is better illustrated in Figure 3.1:

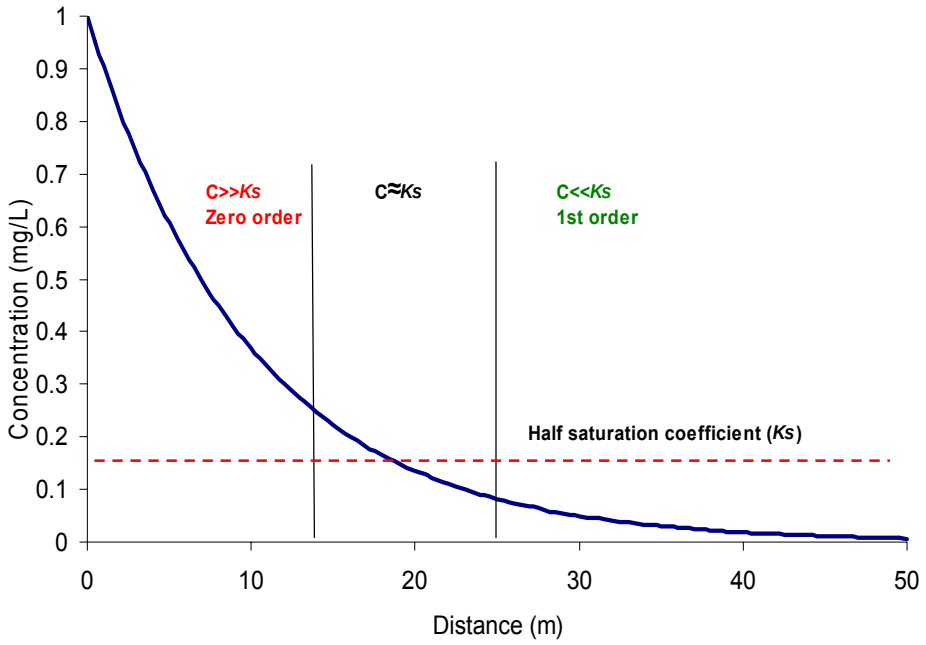

Figure 3.1. Illustration of different kinetic representations of degradation along various zones in a reactive contaminant plume

The three kinetic cases were created by adjusting the source compound concentration relative to the assigned half saturation coefficient. For a zero order kinetic simulation the source compound's concentration was set 10 times larger than the half saturation coefficient, the observations monitored were the ones within the region were the $C>>K_s$. As for the first order simulation, the initial source compound concentration was set such that it is almost 10 times smaller than the half saturation coefficient K_s. Similarly, the mixed kinetic simulation was done by setting the initial parent compound concentration to a value comparable to the half saturation coefficient.

If proven to work in a satisfactory matter regardless of the kinetic state of the plume, this optimization method would facilitate the use of more sophisticated models that are numerical and capable of simulating multiple kinetic scenarios (such as SEAM3D) in simulating complex solute transport cases.

3.2.3.3 Optimization with noisy observations

The effect of noisy observations was also studied. The goal was to study the robustness of the optimization methodology to noise in the data. This was performed by first generating

noiseless concentration data using a set of known model parameters. These concentration data sets were then contaminated with noise generated using a formula initially used by Anderman and Hill (1999).The contaminated concentrations were used as the new set of "observations" in the optimization process and a comparison between the generated plumes and the noisy plumes was made. The ability of the method to produce parameters capable of regenerating the noiseless concentrations is assessed using SSR criterion as well as the visual resemblance.

3.2.3.4 Observation weight influence

A fourth test performed using the synthetic system was the effect of the observation weights. Two weighing mechanisms were tested; the first was setting all the weights to one. In this case, the concentration values with higher magnitude impose more influence on the optimization process simply because of their larger magnitude. The second weighing mechanism was described in Anderman and Hill (1999). The weights generated using these approaches are a function of the concentration values and the coefficient of variation of the observations. Due to the lack of information about the sampling and measurements process of the observations, a value of 0.25 was used for the purpose of this study.

3.2.3.5 Site application

All of the tests mentioned above aimed at providing an assessment of the applicability of this optimization approach to reactive solute modeling using SEAM3D. A test on a chlorinated ethenes site was a necessary next step. The site studied was at the Waste-Water Treatment Plant (WWTP), Naval Air Station, Pensacola, Florida (Chapelle and Bradley 1999). The WWTP has been in operation since 1941. During the 1950's and 60's, the WWTP received industrial waste from paint and electroplating operations. A separate industrial waste-water treatment facility was built in 1971 which included an unlined holding pond. From the early 1970's to the mid-80's organic solvents, metals and other contaminants entered the aquifer through this pond. In 1985, the lateral and vertical extent of chlorinated solvent contamination was investigated during a RCRA ground water assessment of the site. The findings of the RCRA assessment resulted in the

installation of a groundwater recovery system to remediate contaminated groundwater in 1986, and the excavation and removal of large volumes of contaminated soil to a depth of 6 ft (2 m) at several locations. The excavated areas were backfilled with clean sand and capped with either 3 ft (1 m) of clay sediments or a high-density asphalt layer. In 1998, the use of the groundwater recovery system was discontinued so that the effectiveness of source remediation technologies and natural attenuation processes could be assessed. Groundwater has been monitored on a quarterly and semi-annual basis since 1987. Geochemical natural attenuation parameters have been monitored since 1997. Two chemical oxidations treatments in the source area were implemented in 1999 (Widdowson and Waddall, 2000).

Flow and solute transport models for the site were previously generated and manually calibrated. Comprehensive sensitivity analysis study to the model parameters was performed. The idea was to isolate the parameters with the highest influence on the model performance. The parameters chosen for optimization satisfy having high sensitivity and being difficult to field measure or estimate. Those parameters were then optimized and the resulting contaminant plumes were compared to the resulting plumes generated using manual calibration. To further test the recommendation of optimizing the parameters in a sequential manner instead of a simultaneous manner, two optimization runs were performed; one with the parameters optimized sequentially and one with them optimized simultaneously. The resulting concentration profiles were compared against each other and against the profile resulting from the former manual calibration. An aerial view of the study area and the chloroethenes concentrations along the flow path are shown in Figure 3.2:

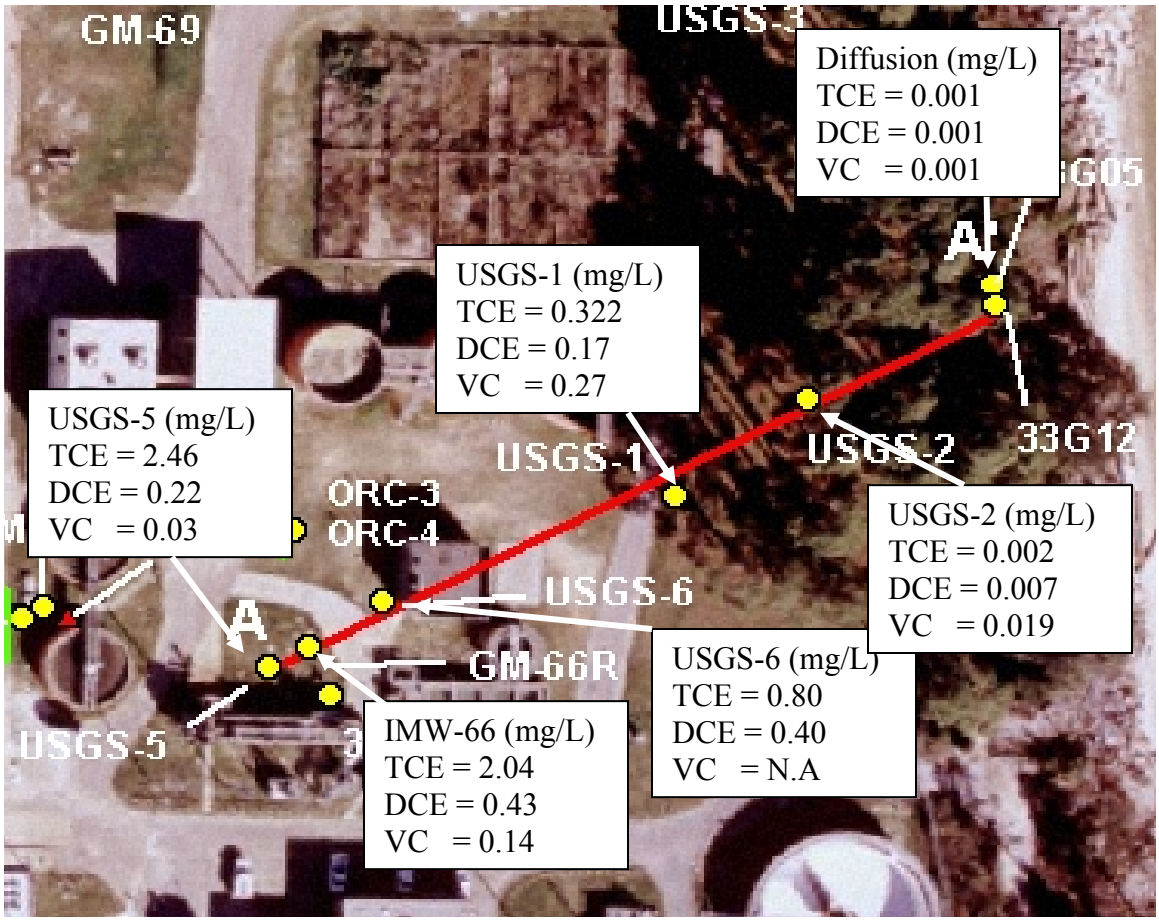

Figure 3.2. An aerial view of the Pensacola WWTP with chloroethenes concentrations along the centerline of the plume.

3.3 RESULTS AND DISCUSSION

3.3.1 Sequential versus simultaneous estimation of the model parameter

As described earlier, two approaches to parameter estimation were investigated and compared. This test studied the advantages (if any) of the sequential approach, where PEST was applied to one compound at a time, over the simultaneous approach where the input parameters of the four compounds (PCE, TCE, cis-DCE and VC) were estimated simultaneously. The later, if proven feasible, was predicted to reduce the optimization time and limit the human interference in the optimization process. For the simultaneous case, PEST was set up to estimate the parameters simultaneously, and the outcome of each run was compared to the outcome using the sequential approach.

A preliminary model parameter sensitivity study revealed a strong correlation between the maximum specific rate of reductive dechlorination and the half saturation coefficient for each compound (Equation 3.2). Therefore it was necessary to choose only one of those two parameters to be used in the optimization process. In this study the maximum specific rate of reductive dechlorination was selected. A total of seven parameters were optimized in this simulation; the maximum specific rate of reductive dechlorination $\nu^{\max,EA}$ for the four compounds (PCE, TCE, DCE and VC) and the inhibition coefficient of the daughter compound by the parent compound; inhibition of TCE by PCE($k_{TCE,PCE}$), DCE by TCE ($k_{DCE,TCE}$) and VC by DCE($k_{VC,TCE}$). As proven to be more efficient; the optimization process started by optimizing the single parameter of the parent compound (PCE) and updating $\nu_{PCE}^{\max,EA}$ in the model prior to optimizing the two TCE parameters, which in turn are updated in the model prior to optimization of the DCE parameters and so on. A similar approach was used by Suna et al. (2001b).

In the first optimization run, the observation weights were set to one. The two techniques yielded similar results for the first three compounds (Figure 3.2). However, for VC; the sequential approach yielded much better results. The optimization run was repeated with the observation weights set so that all the observation-weight products are within the same order of magnitude, thereby larger weight applied to smaller concentration values (Figure 3.3.). A third run was a one where the weights were calculated according to the Equation 3.9. This equation was used by Anderman and Hill (1999)

$$W_i = 1 / (C_v C_i)^2 \tag{3.9}$$

where W_i = is the weight to be assigned for the concentration C_i, C_v = is the coefficient of variation which is set to a value of 0.25, the results of this run is shown in Figure 3.4.

The observations along with their associated applied weights are listed in table 3.1 below:

Table 3.1. The observations and associated weights of the sequential versus simultaneous parameter optimization test on the synthetic system

Obs.	Value	Unit wt.	Same order of magnitude wt.	Formula wt.
PCE 1	3.097103	1	1	1.668048
PCE 2	0.000509	1	10000	61876337
PCE 3	6.17E-08	1	0	0
PCE 4	7.04E-12	1	0	0
PCE 5	8.28E-16	1	0	0
PCE 6	1.07E-19	1	0	0
PCE 7	1.71E-23	1	0	0
PCE 8	2.17E-27	1	0	0
PCE 9	3.24E-31	1	0	0
TCE 1	26.74875	1	0.1	0.022362
TCE 2	0.255683	1	10	244.7468
TCE 3	4.90E-05	1	0	0
TCE 4	8.62E-09	1	0	0
TCE 5	1.56E-12	1	0	0
TCE 6	3.11E-16	1	0	0
TCE 7	7.62E-20	1	0	0
TCE 8	1.48E-23	1	0	0
TCE 9	3.38E-27	1	0	0
DCE 1	2.04187	1	1	3.837636
DCE 2	12.63292	1	0.1	0.100257
DCE 3	5.237559	1	1	0.58326
DCE 4	1.369375	1	1	8.532479
DCE 5	0.340526	1	10	137.9808
DCE 6	0.089819	1	100	1983.282
DCE 7	0.028535	1	100	19650.41
DCE 8	0.007063	1	1000	320698.3
DCE 9	0.002013	1	1000	3950346
VC 1	0.003023	1	1000	1751239
VC 2	0.273094	1	10	214.5339
VC 3	2.763563	1	1	2.094987
VC 4	3.584525	1	1	1.245251
VC 5	3.278921	1	1	1.488189
VC 6	2.357667	1	1	2.878426
VC 7	0.957509	1	10	17.45156
VC 8	0.077571	1	10	2659.046
VC 9	0.00238	1	1000	2825631

The sum of squared residuals (SSR) results for the three tests are provided in Table 3.2.

Table 3.2. Sum of squared residuals (SSR) for the sequential vs. simultaneous optimization for the three weighing mechanisms

	Sequential optimization				Simultaneous optimization			
	PCE	TCE	DCE	VC	PCE	TCE	DCE	VC
Unit weights	0.35	7.73	8.01	0.82	1.02	4.96	6.21	4.27
Formula weights	0.16	57.51	9.94	9.94	9.47	35.57	21.86	32.52
Same order of magnitude weights	0.14	12.79	5.16	0.44	9.47	35.69	22.04	32.55

It was evident after doing those tests that, overall, the simultaneous parameter estimations yielded a bad match between the synthetic observations and the optimized concentrations relative to that obtained using the sequential estimation. This can be justified when understanding the nature of the SEAM3D model, were the concentration of the parent compound has a direct impact on that of the daughter compound; therefore, any alteration of the parameters of the compound will ultimately influence the concentrations of its subsequent daughter compounds. In the sequential approach of estimation, the parameters of the parent compound X_1 are optimized, fixed, loaded in the model for the subsequent daughter compound X_2. Then the parameters of the compound X_2 are optimized without changing X_1 parameters. This insured fixed concentration of the compound X_1 throughout the estimation of the X_2 parameters, and so on.

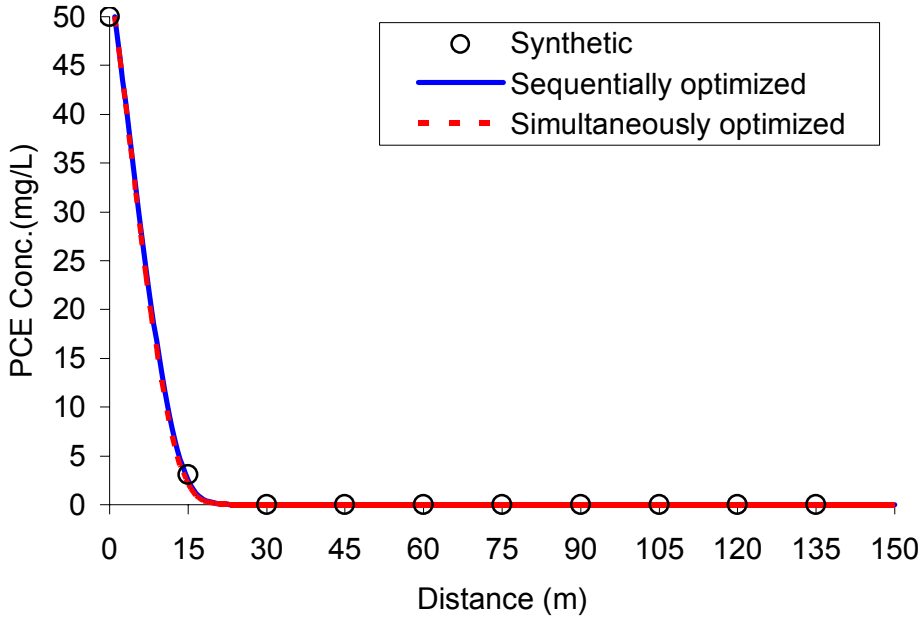

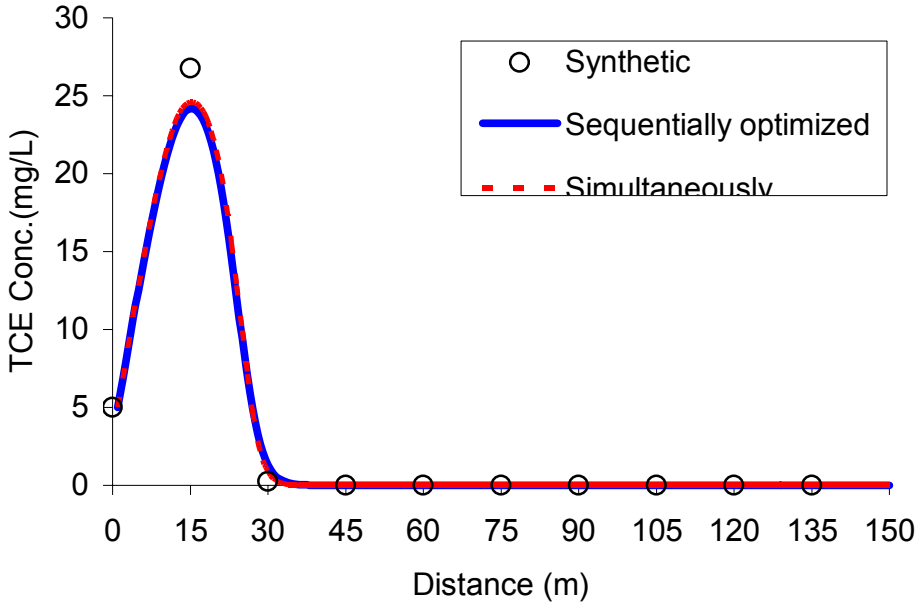
30
25
20
15
10
5
0
TCE Conc.(mg/L)
0
15
30
45
60
75
90
105
120
135
150
Distance (m)
Synthetic
Sequentially optimized
Simultaneously

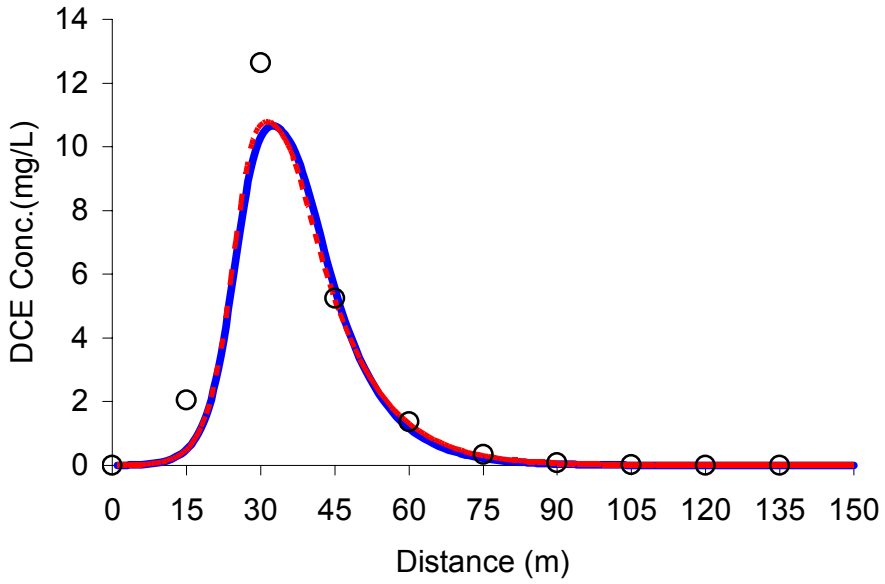
14
12
10
8
6
4
2
0
DCE Conc.(mg/L)
0
15
30
45
60
75
90
105
120
135
150
Distance (m)

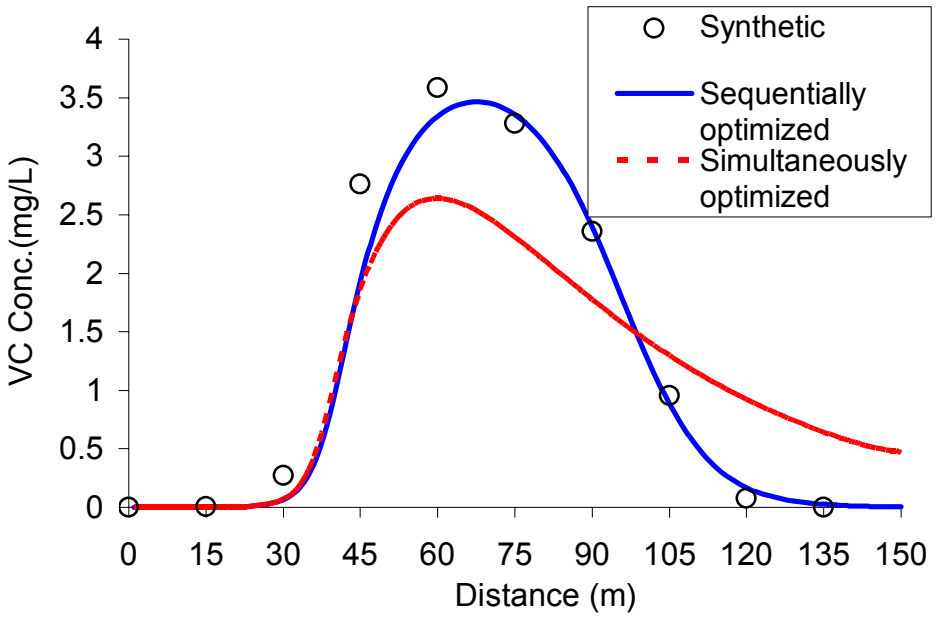

Figure 3.3. Comparison between synthetic "observed" concentrations and model predictions using the sequential and simultaneous optimization techniques for PCE, TCE, DCE and VC along the centerline of a plume, optimization performed with the unit weights.

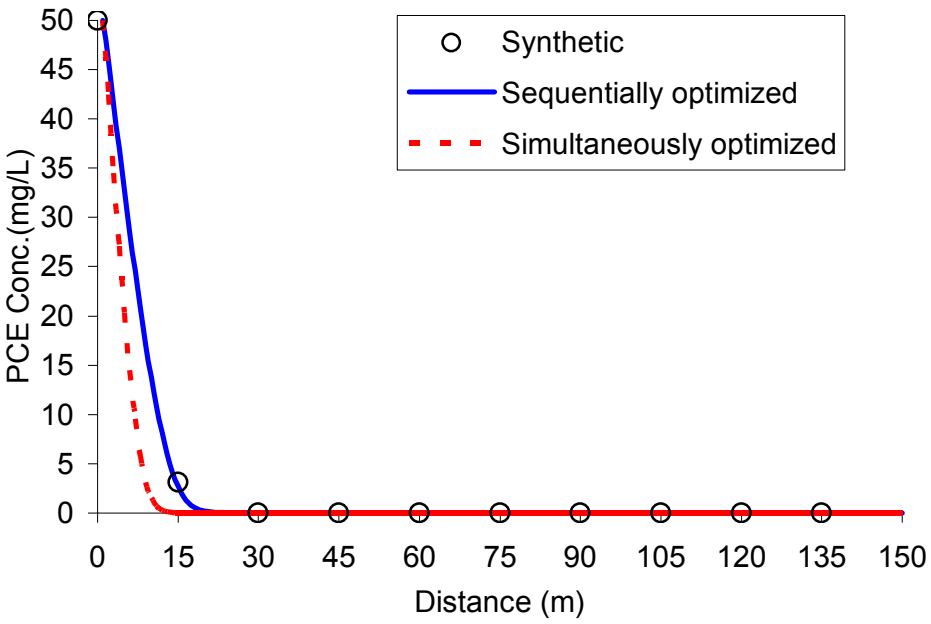
Synthetic
Sequentially optimized
Simultaneously optimized
PCE Conc.(mg/L)
Distance (m)
0
5
10
15
20
25
30
35
40
45
50
0
15
30
45
60
75
90
105
120
135
150

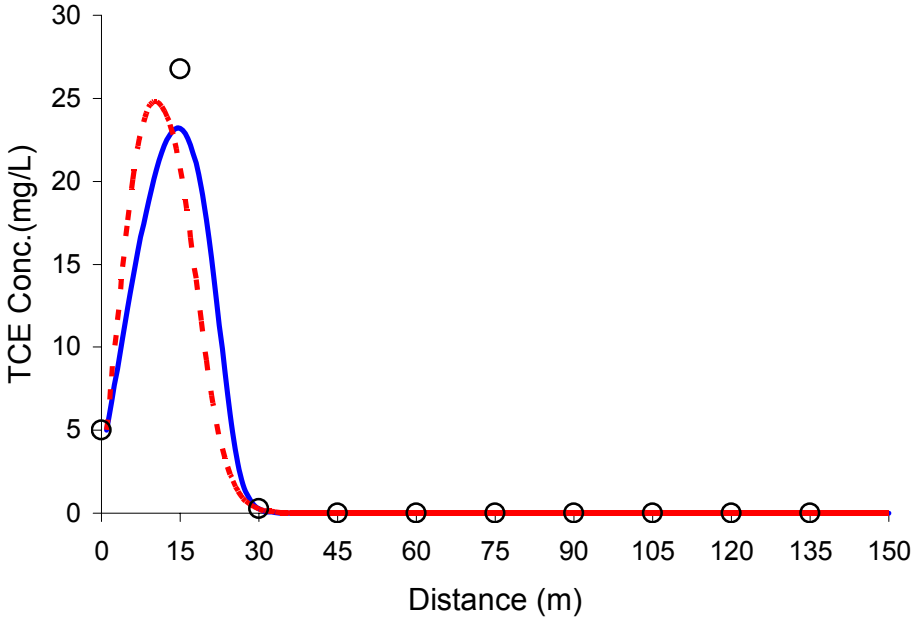
TCE Conc.(mg/L)
Distance (m)
0
5
10
15
20
25
30
0
15
30
45
60
75
90
105
120
135
150

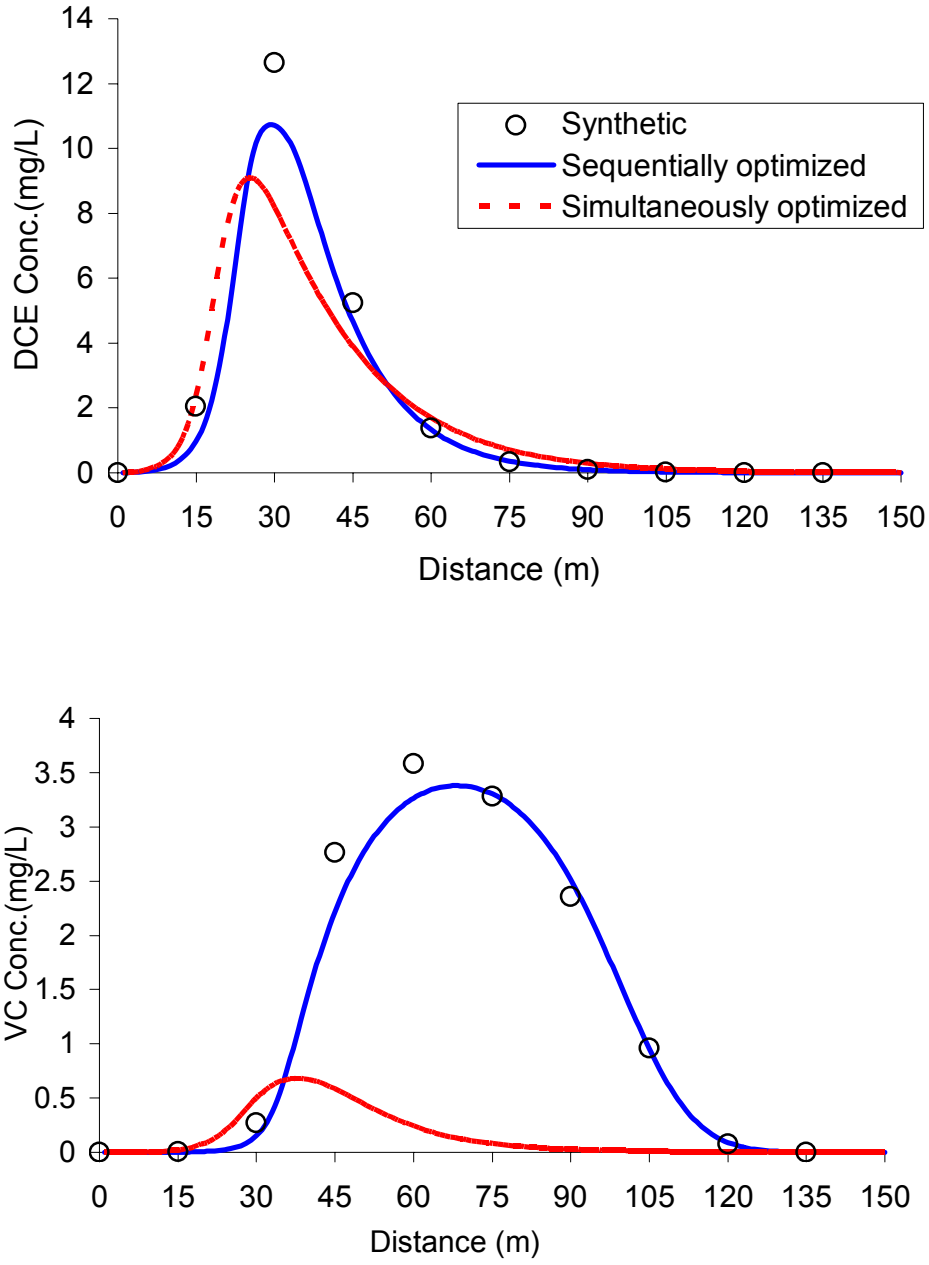

Figure 3.4. Comparison between synthetic "observed" concentrations and model predictions using the sequential and simultaneous techniques for PCE, TCE, DCE and VC along the centerline of a plume, optimization performed with the weights yielding same order of magnitude observations.

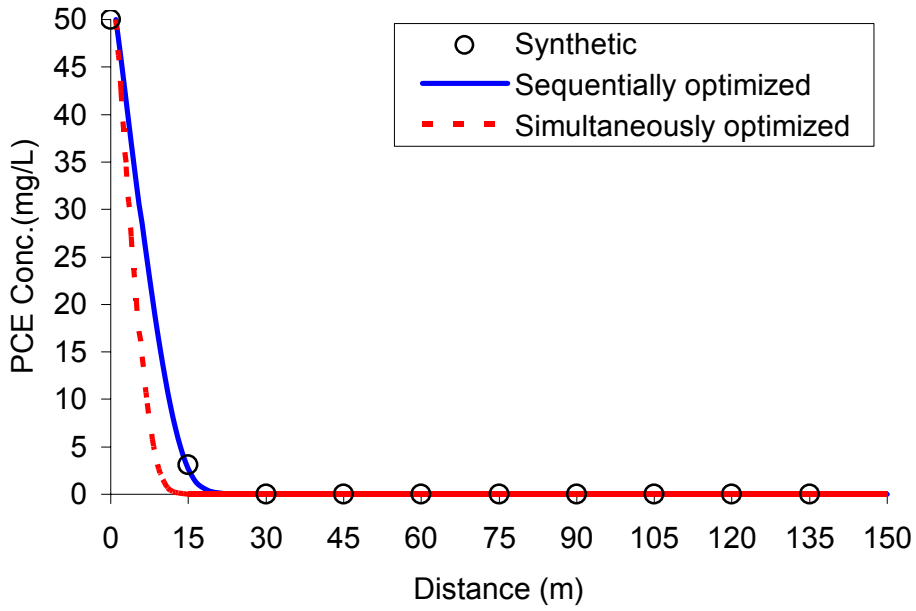
Synthetic
Sequentially optimized
Simultaneously optimized
PCE Conc.(mg/L)
Distance (m)
0
5
10
15
20
25
30
35
40
45
50
0
15
30
45
60
75
90
105
120
135
150

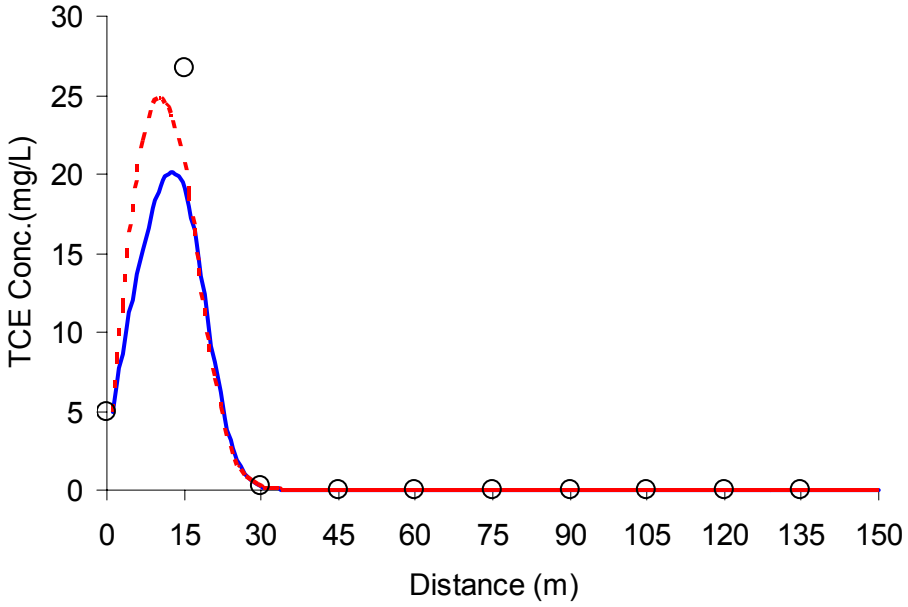
TCE Conc.(mg/L)
Distance (m)
0
5
10
15
20
25
30
0
15
30
45
60
75
90
105
120
135
150

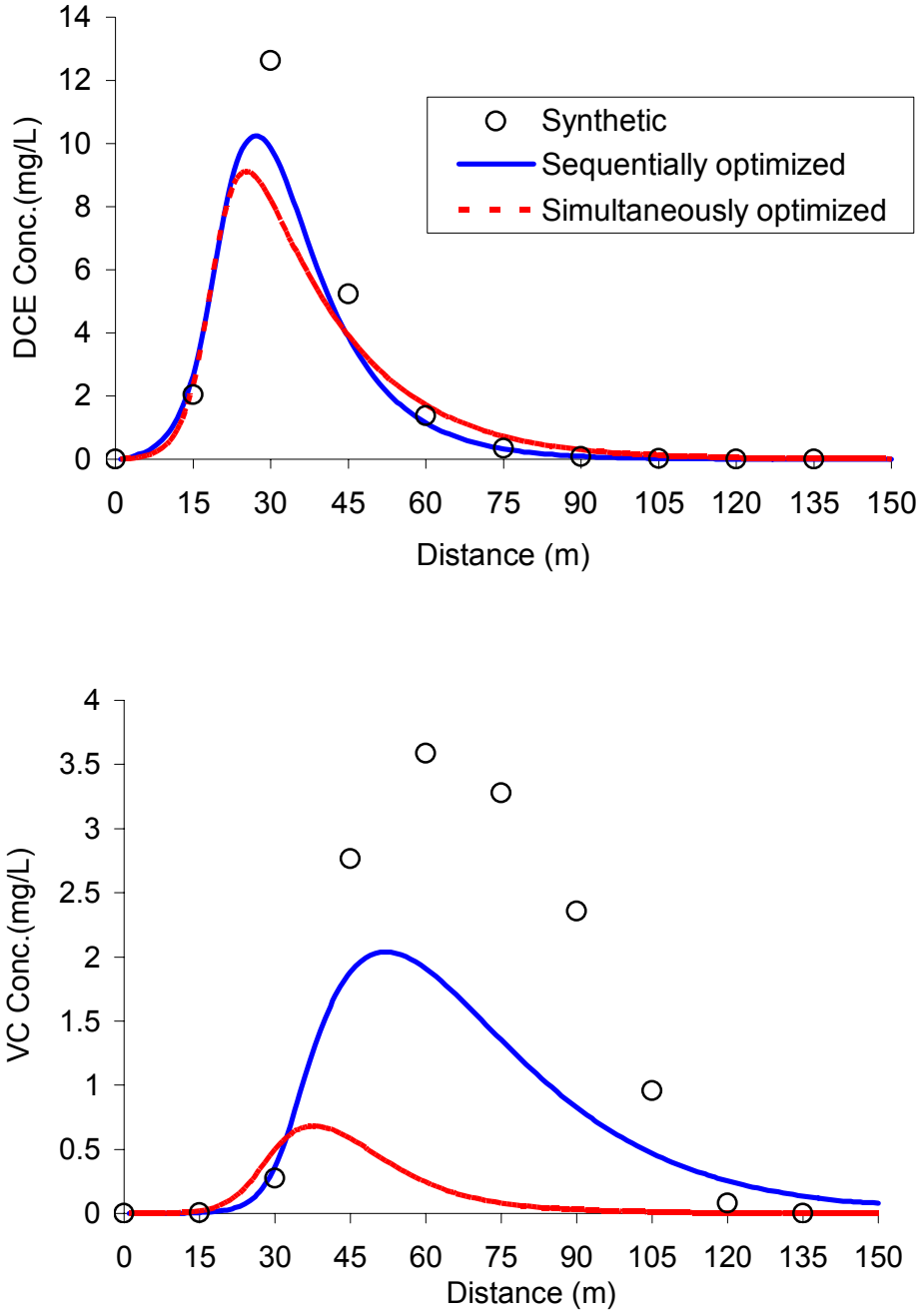

Figure 3.5. Comparison between synthetic "observed" concentrations and model predictions using the sequential and simultaneous optimization techniques for PCE, TCE, DCE and VC along the centerline of a plume, optimization performed with the weights calculated using Equation 3.9.

In the case of the simultaneous optimization, on the other hand, all the parameters are in one pool. They all are being optimized at the same time, therefore in each optimization cycle, the parameter upgrade matrix changes all of them simultaneously. So while PEST is trying to optimize the parameters of compound X_2 for example, the parameters of X_1 also change, leading to a change in the concentration of X_1, which destroys the base on which the X_2 parameters are being optimized, so PEST keeps moving in cycles of adjusting the parameters on the daughter compound based on the concentrations of parent compound while these concentrations keep changing from one optimization cycle to another. The poor match between the observed and modeled observations when the simultaneous approach is used, may also be attributed to lack of convergence. This may be demonstrated by the fact that upon using the parameter values optimized using the sequential approach as starting values for optimization using the simultaneous approach; the model regenerated the same set of observations. It stopped after one optimization iteration indicating reaching an optimal set of parameters. This shows that in theory, the simultaneous approach may be capable of coming up with the set of parameters similar to that obtained using the sequential, if there wasn't a convergence problem. However, in practice, it is much easier for the sequential approach to reach that optimal set of parameters than it is for the simultaneous approach.

It can be demonstrated, therefore, that for the case of reactive multi-component solute transport parameter estimation, the sequential optimization of the parameters of the parent compound then the daughter compounds will yield a much better result than the alternative approach of simultaneous optimization of the parameters of all the solutes. It is unclear why with TCE as the modeled compound; the simultaneous optimization yielded a better match with the synthetic than the sequential. This test was also performed on a model of an actual TCE contaminated site, the results emphasized that the sequential approach is far better that than the simultaneous one.

3.3.2 Effect of kinetic state

Choosing the correct kinetic rate of biodegradation is essential for accurate prediction of the natural attenuation capacity (Bekins et al., 1998). The kinetic rate within a contaminant plume can be represented using zero order, first order, or Monod kinetics,

each of which is function of the ratio of the concentration to the half saturation coefficient. Zero order kinetic representation is appropriate in situations where the concentration is much higher than the half saturation coefficient. In cases where contaminant concentration is much lower value than the half saturation coefficient, first order kinetic representation is appropriate (Suarez and Rifai 1999). The third scenario (Monod kinetics) is when contaminant concentration values and the half saturation coefficient are roughly similar. Many of the studies that looked into estimating essential solute transport model parameters investigated first order representations of the plume kinetics (ex. Suna et al., (2001b)), which is a good simplification that is valid only over part of the contaminant concentration range (Bekins et al., 1998). This study broadens the application by estimating essential parameters for Monod kinetics which is a kinetic setting capable of simulating the whole range of the plume.

The optimization method succeeded in finding parameters capable of generating a series of contaminant concentrations identical to those generated using the original set of parameters. Figures 3.5, 3.6 and 3.7 represent the first order kinetics, zero order and mixed kinetics, respectively. They all yielded nearly perfect match with the original synthetically generated concentration values (denoted in the figure as observed), the SSR values resulting for the optimization on the three kinetic states models is shown in table 3.5. The optimized parameters themselves were within ±10% of the original parameters, as shown in table 3.4. This difference in parameter value had no notable effect on the quality of match between the synthetically generated "observed" concentrations and the model predicted using the optimized set of parameters. It was concluded that this optimization methodology performs very well regardless of the kinetic state; optimization in the three kinetic configurations yielded a well-calibrated model. The most essential parameters used in the first order case are provided in Tables 3.3 and 3.4:

Table 3.3. Parameter values and inhibition coefficients used in the first order case of optimization

Micro-colony concentration M	0.2500
Effective porosity (θ)	0.2500
PCE Half saturation coefficient $\overline{K}^{e}_{PCE}$	10.000
TCE Half saturation coefficient $\overline{K}^{e}_{TCE}$	5.0000
DCE Half saturation coefficient $\overline{K}^{e}_{DCE}$	25.000
VC Half saturation coefficient $\overline{K}^{e}_{VC}$	5.0000
Hydraulic gradient	0.0018
Hydraulic conductivity K	8.5000
PCE Maximum specific rate $v^{\max}_{PCE}$	0.5000
TCE Maximum specific rate $v^{\max}_{TCE}$	0.1000
DCE Maximum specific rate $v^{\max}_{DCE}$	0.9000
VC Maximum specific rate $v^{\max}_{VC}$	0.6000

Inhibition of	By	
PCE	O2	0.5000
PCE	Fe(III)	100.00
PCE	SO4	50.000
TCE	O2	0.5000
TCE	Fe(III)	100.00
TCE	SO4	50.000
TCE	PCE	0.1000
DCE	O2	1.0000
DCE	Fe(III)	25.000
DCE	SO4	50.000
DCE	PCE	10.000
DCE	TCE	0.0100
VC	O2	1.0000
VC	Fe(III)	25.000
VC	SO4	50.000
VC	PCE	50.000
VC	TCE	10.000
VC	DCE	0.0100

Table 3.4. Original and optimized values of parameters under consideration for the first order case

Parameter	Original Value	Optimized Value	% Difference
Maximum specific rate of PCE	0.5000	0.5000	0.0000
Maximum specific rate of TCE	0.1000	0.0990	0.1273
Inhibition coefficient of TCE by PCE	0.1000	0.1000	0.1180
Maximum specific rate of TCE	0.9000	0.9036	0.4068
Inhibition coefficient of TCE by PCE	0.0100	0.0099	0.7056
Maximum specific rate of TCE	0.6000	0.5956	0.7245
Inhibition coefficient of TCE by PCE	0.0100	0.0101	0.9961

Table 3.5. SSR resulting from the optimization of the three kinetic state models

Kinetic state	PCE	TCE	DCE	VC
First order	2.5E-17	4.02E-08	4.81E-08	4.6E-09
Zero order	1.00E-12	2.34E-07	8.88E-04	1.48E-04
Mixed kinetics	4.16E-12	1.44E-08	1.59E-05	1.42E-06

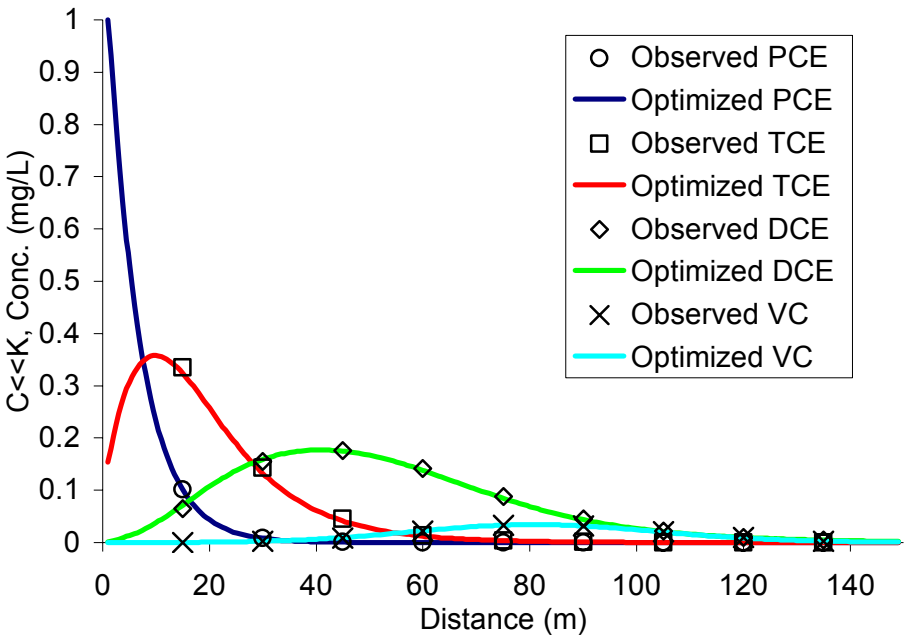

Figure 3.6. Comparison of calibrated model results versus the synthetic data set in a first order kinetic plume.

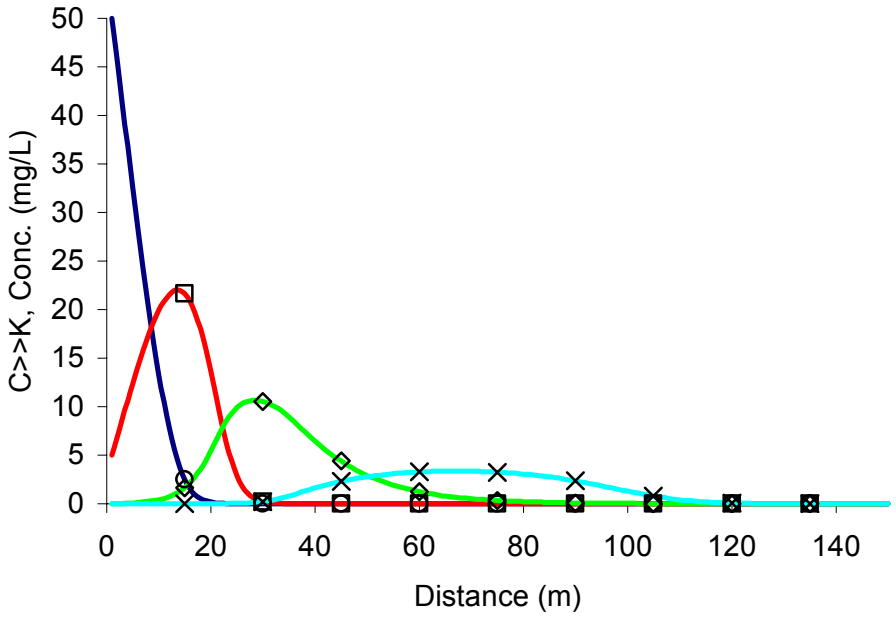

Figure 3.7. Comparison of calibrated model results versus the synthetic data set in a zero order kinetic plume.

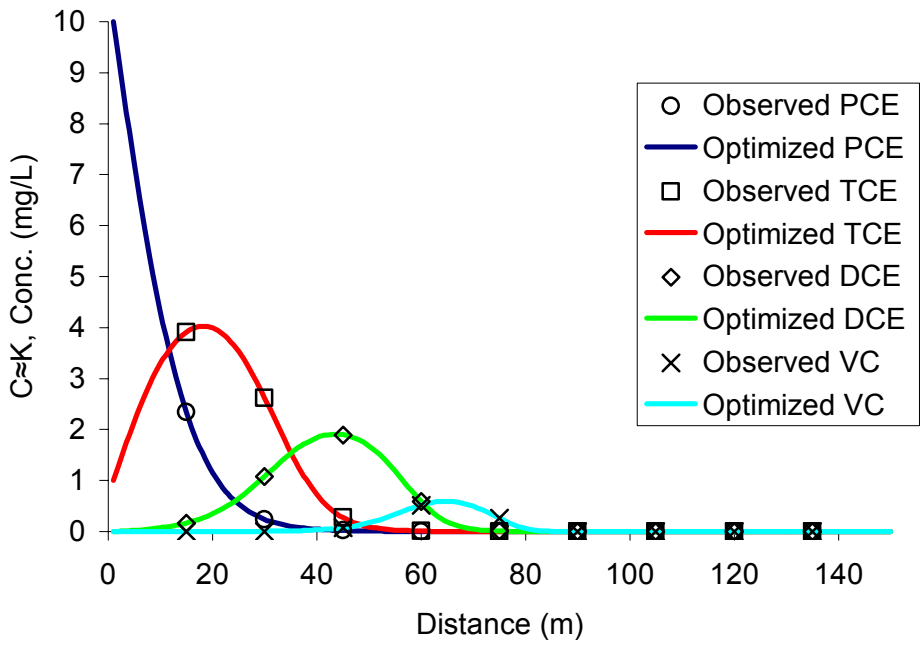

Figure 3.8. Comparison of calibrated model results versus the synthetic data set in a transition kinetic state plume.

3.3.3 Optimization with noisy observations

It is necessary to test the capability of the optimization method to handle noise in the observation data. Prior to optimization, the synthetic concentrations were adjusted using the following formula used previously by Anderman and Hill (1999).

$$C_{i,noise} = C_{i,original}\left(1 + R_i C_v\right) \tag{3.10}$$

where $C_{i,noise}$ is the noisy concentration value; $C_{i,original}$ is the original concentration value; R_i is a random number from a standard normal distribution; and C_v is the coefficient of variation (set to be = 0.25).

The approach in this test was to use the model to calculate synthetic contaminant concentration values ($C_{i,original}$) and then use Equation (3.10) to generate a set of noisy concentrations ($C_{i,noise}$). The noisy concentrations serve as the observed data set that was used with SEAM3D and PEST to calibrate the model. The estimated set of model

parameters was then compared with the input parameters used to generate the synthetic contaminant concentration data set.

Figure 3.8 shows PCE, TCE, DCE, and VC concentrations using the original and optimized sets of parameters. The PCE concentration was set to 50mg/L at the source. TCE initial concentration at the source, however, was set to three different values; zero mg/l, 5mg/l and 15 mg/l, the test was run with these three boundary conditions to assess the effect of TCE's initial concentration on the quality of fit between the modeled and 'observed' concentrations for the four compounds. The results of the test proved that the optimization method worked satisfactorily for all three initial conditions. It did perform the best, however, for the case of 5mg/L TCE initial concentration, as evident in the visual resemblance and the sum of squatted residuals (SSR). The general trend of concentrations was simulated well for all the compounds. There were some concentration points that were more off than others (i.e, DCE concentration at 30 meters). The optimized parameters were not a perfect match with the original parameter set. This was attributed to a highly-variable (and maybe unrealistic) set of observations caused by setting the randomization to an observation-by-observation basis. As a result of the variability in the observed data, SEAM3D may never be able to simulate accurately, especially with the limited number of parameters to optimize. An additional contributor to the lack of accuracy in the model estimates for daughter compounds may be the accumulative error carried over from the parent compound parameter optimization. Overall, the test proved the capability of the optimization technique to satisfactorily optimize the model parameters even in a highly random set of observations.

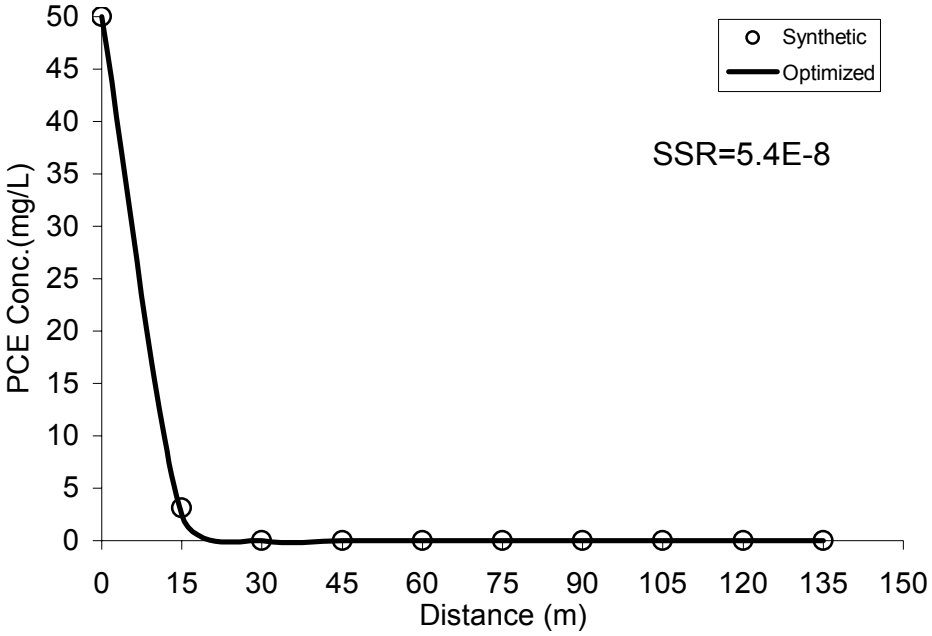
Synthetic
Optimized
SSR=5.4E-8
PCE Conc.(mg/L)
Distance (m)
0
5
10
15
20
25
30
35
40
45
50
0
15
30
45
60
75
90
105
120
135
150

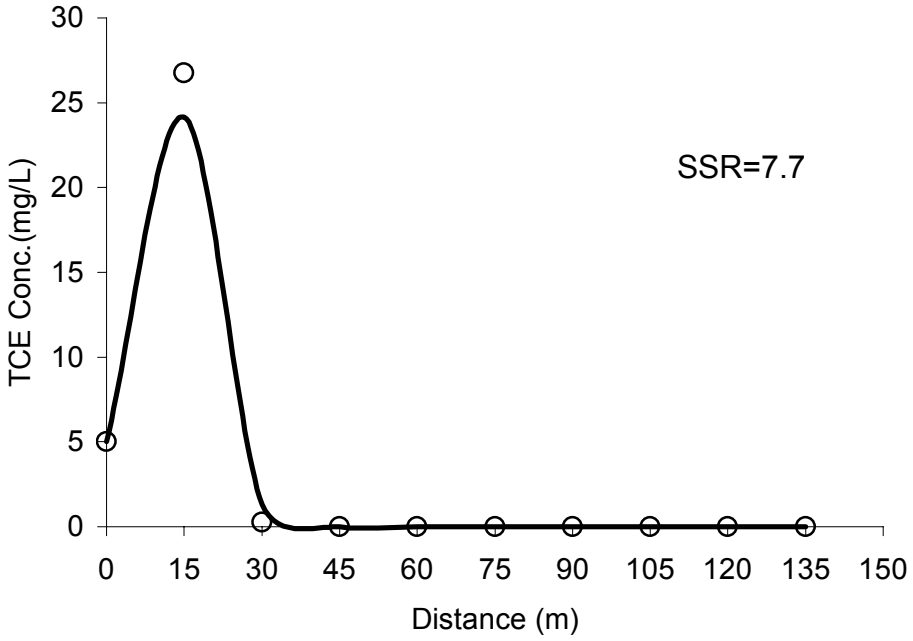
SSR=7.7
TCE Conc.(mg/L)
Distance (m)
0
5
10
15
20
25
30
0
15
30
45
60
75
90
105
120
135
150

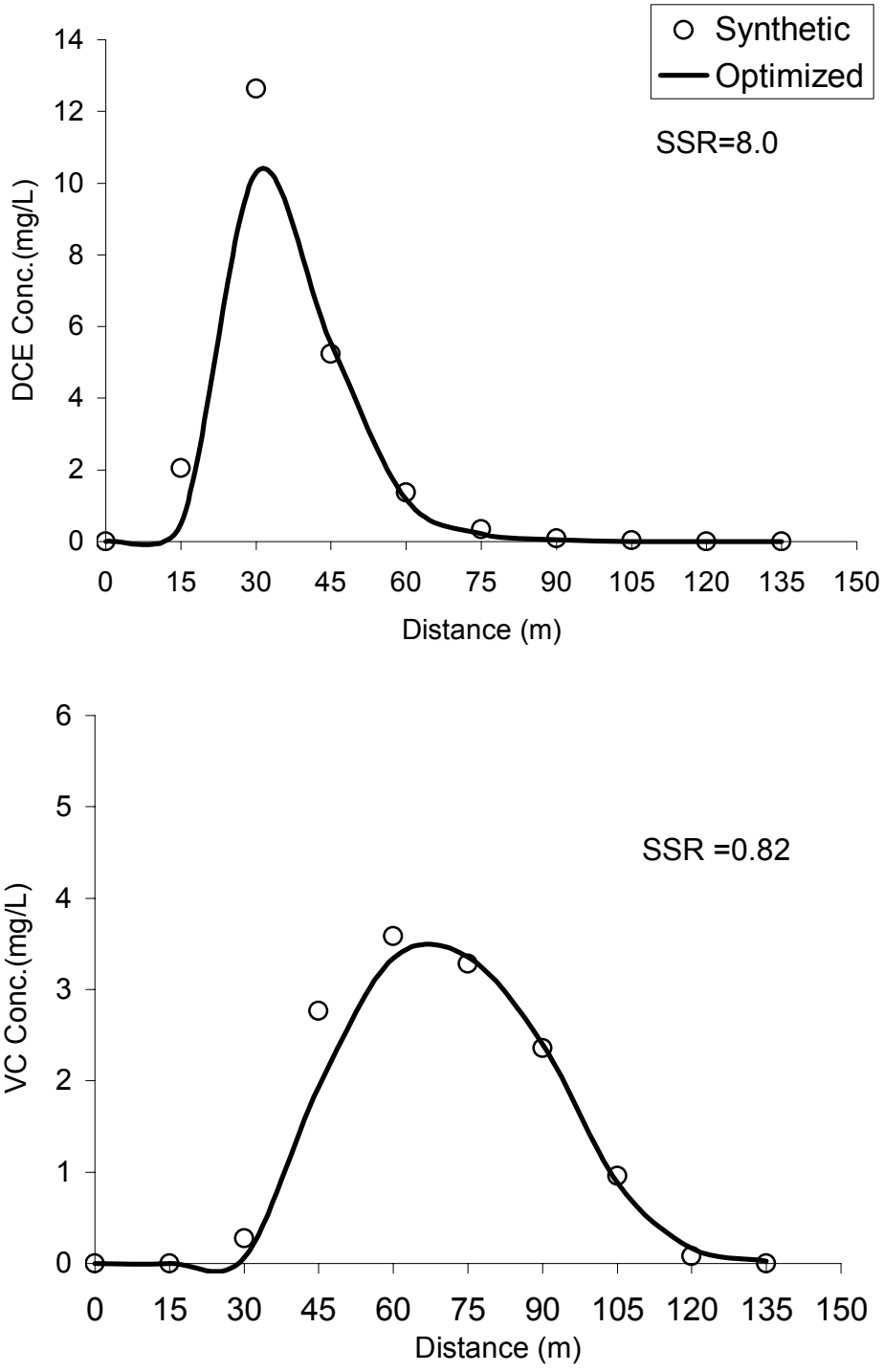

Figure 3.9. Comparison of synthetic noisy "observed" concentration data set with the simulated optimized model using SEAM3D with PEST for PCE, TCE, DCE and VC along the centerline of a plume.

3.3.4 Observation weight influence

Difference in order of magnitude of the observation values used in the optimization process makes it important to study the effect (if any) of the observations weighing mechanism applied during optimization. Two approaches for assigning weights are used. The first based on the work of Anderman and Hill, (1999) in which the weights are produced using Equation 3.9. The second approach is by keeping the default multiplier of one for all the observations.

The optimization method was performed on two model setups with the only difference being the observation weights used in optimization, the control optimization setup where all the observation weights were set to one, is referred to in Figure 3.9 as "Unity wts". The setup with the weights from the formula above is referred to as "Formula wts". In the tests, only observations values above a threshold of 0.001mg/L were considered for optimization, since that is the practical detections limit. Table 3.6 shows the SSR results for the optimization tests performed.

Table 3.6. The sum of squared residuals of the weighing effect on the optimization

	PCE	TCE	DCE	VC
Unit weights	0.35	7.73	8.01	0.82
Formula weights	0.16	57.51	9.94	9.94

The results showed a better optimization performance when all the weights are set to one, and an inferior performance for the formula-generated weights. The good performance of the unit weights can be explained by understanding that observations with larger magnitudes influence the optimization process due to their higher influence on the objective function. Therefore, values with higher magnitude force themselves indirectly to have more influence in the optimization process. Figure 3.9 shows a comparison of the simulation results using both the unity and formula observation weights.

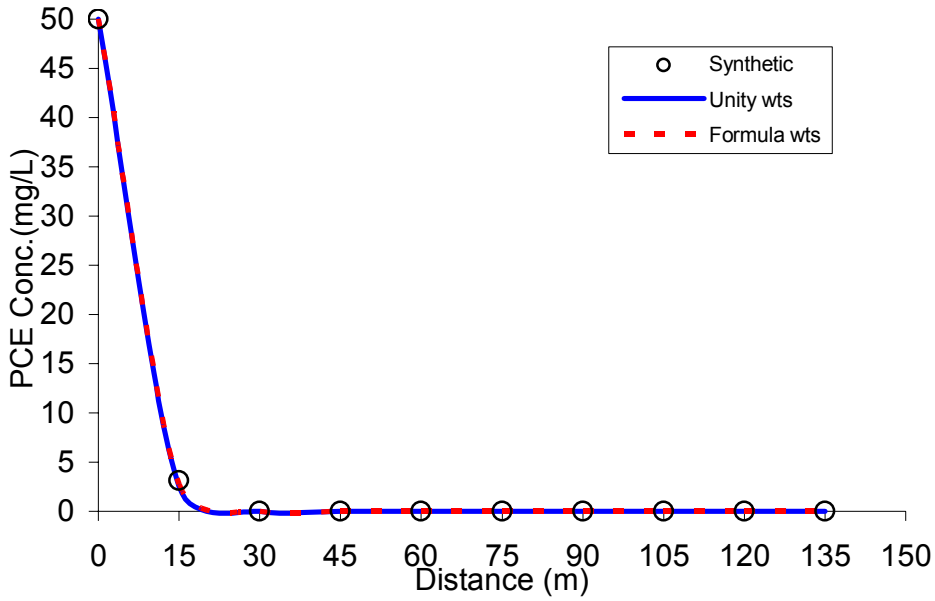
Synthetic
Unity wts
Formula wts
PCE Conc.(mg/L)
Distance (m)
0
5
10
15
20
25
30
35
40
45
50
0
15
30
45
60
75
90
105
120
135
150

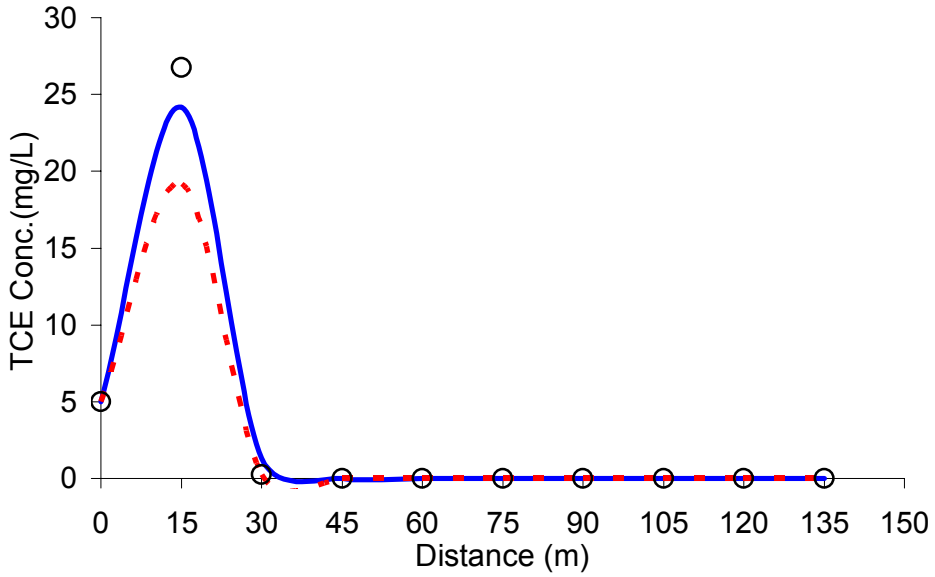
TCE Conc.(mg/L)
Distance (m)
0
5
10
15
20
25
30
0
15
30
45
60
75
90
105
120
135
150

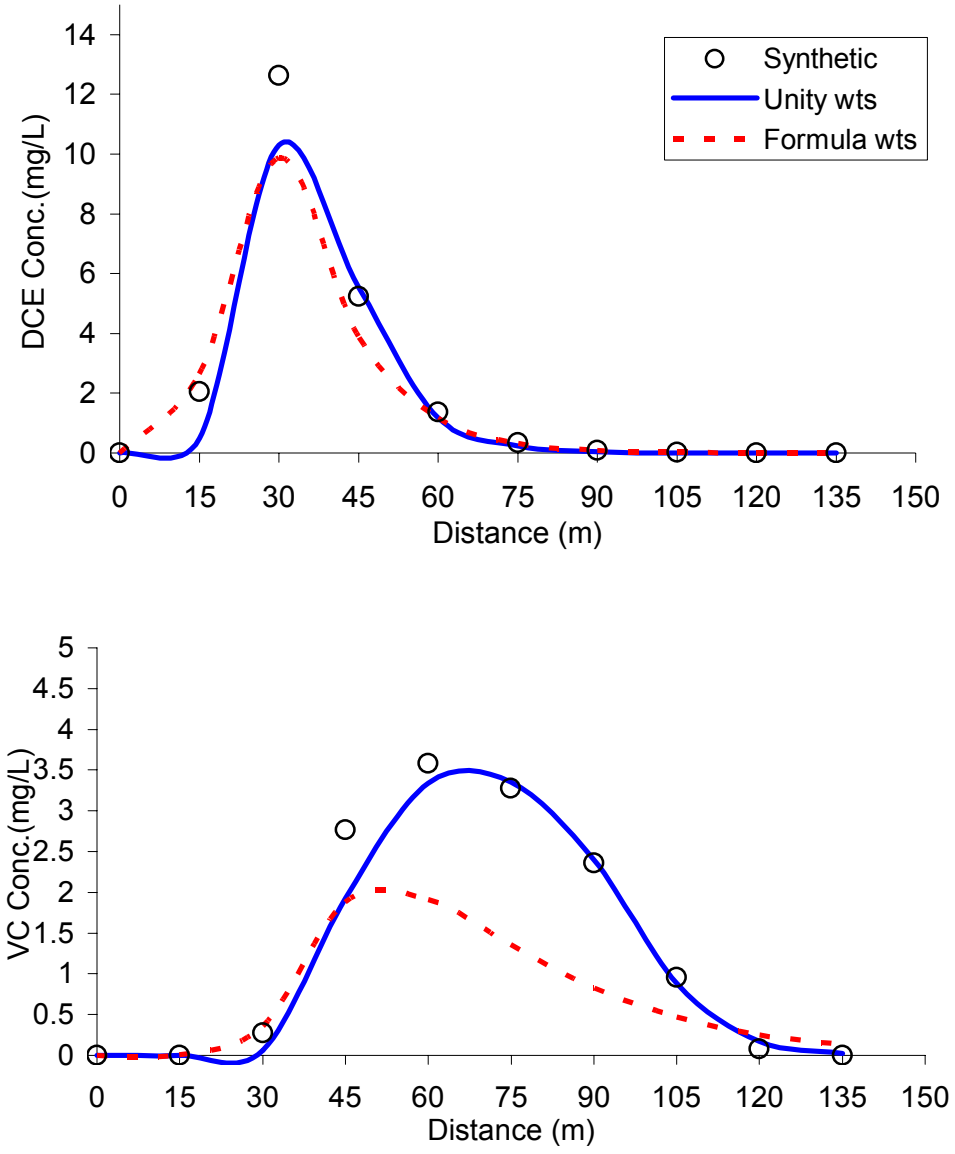

Figure 3.10. Comparison between synthetic "observed" concentrations and model predictions using two different observation weighting mechanisms for PCE, TCE, DCE and VC along the centerline of a plume.

3.3.5 Pensacola site model

The method developed and verified in the hypothetical setup was then tested using data from a chlorinated ethenes contaminated site. A mathematical model was developed to simulate the centerline plume concentrations. A one dimensional model was sufficient for simulating the behavior of the plume along the centerline. The model consisted of 150 one meter by one meter cells; the hydraulic gradient was set to 0.005 m/m, the hydraulic

conductivity set to 8.5m/d. The porosity was set to 0.25, and a total of 6 observation points set at model cells number 6, 14, 25, 46, 71, and 138. These correspond to the monitoring point locations in the field. The model was run for a period length of 4000 days to allow the concentrations to reach steady state. A TCE source concentration of 4 mg/L was observed (TCE being the parent compound) and set in the first cell of the model. The model was formerly calibrated using traditional manual trial and error techniques; recalibrating the model was attempted using the inverse modeling methods tested earlier.

Sensitivity analysis:

Performing parameter sensitivity analysis is an important precursor to the inverse modeling process; it gives a strong indication of the influence of certain parameters have over the model outcome. Multiple studies have addressed ways of performing sensitivity analysis. Deriving a model with respect to a certain parameter, performing Monte Carlo simulations and using the known perturbation methods are all sensitivity analysis tools (Tebes-Stevens et al., 2001; Tebes-Stevens and Valocchil, 2000b; Ling and Rafai, 2003). Sensitivity analysis was performed on a number of parameters, some of which can't be used as parameters in the optimization process due to their effect on the groundwater velocity. Nonetheless all are shown in the results are for comparison purposes.

The sensitivity coefficient measures the dependence of the model outcome to a certain parameter; the formula used in this study is shown in Equation 3.11

$$\text{Sensitivity coefficient} = \left| \frac{\frac{O_p - O_b}{P_P - P_b}}{\frac{}{P_b}} \right| \qquad (3.11)$$

where O_p is the model output after perturbing the input parameter, O_b is the model output for original (base) set of parameters, P_p is the perturbed parameter, P_b is the base parameter. The parameters used in the sensitivity analysis test are listed in Table 3.7.

Table 3.7. List of parameters used in the sensitivity study

Parameter #	Name and symbol
1	hydraulic conductivity K
2	longitudinal dispersivity
3	TCE half saturation coefficient $\overline{K}^{e}_{TCE}$
4	DCE half saturation coefficient $\overline{K}^{e}_{DCE}$
5	VC half saturation coefficient $\overline{K}^{e}_{VC}$
6	TCE maximum specific rate of degradation $v^{\max}_{TCE}$
7	DCE maximum specific rate of degradation $v^{\max}_{DCE}$
8	VC maximum specific rate of degradation $v^{\max}_{VC}$
9	Inhibition coefficients of DCE by TCE $k_{DCE,TCE}$
10	inhibition coefficients of VC by DCE $k_{VC,DCE}$

The parameters were perturbed by ± 50%, and the sensitivity coefficients were calculated in every cell along the plume domain. The results of the study concluded that, in general, the hydraulic conductivity and degradation rate are the most influential parameters. Hydraulic conductivity can be rather sufficiently estimated from field studies while it may be more difficult to estimate the degradation rate. Due to the high correlation between the half saturation coefficient and the degradation rate, only one can be optimized, the degradation rate is the one chosen. The inhibition coefficients fitting parameters that were shown to have an effect on the model outcome, these form some good candidate for optimization. A representation of the sensitivity coefficients for the three compounds and the two cases of parameter perturbation is shown in Figure 3.10.

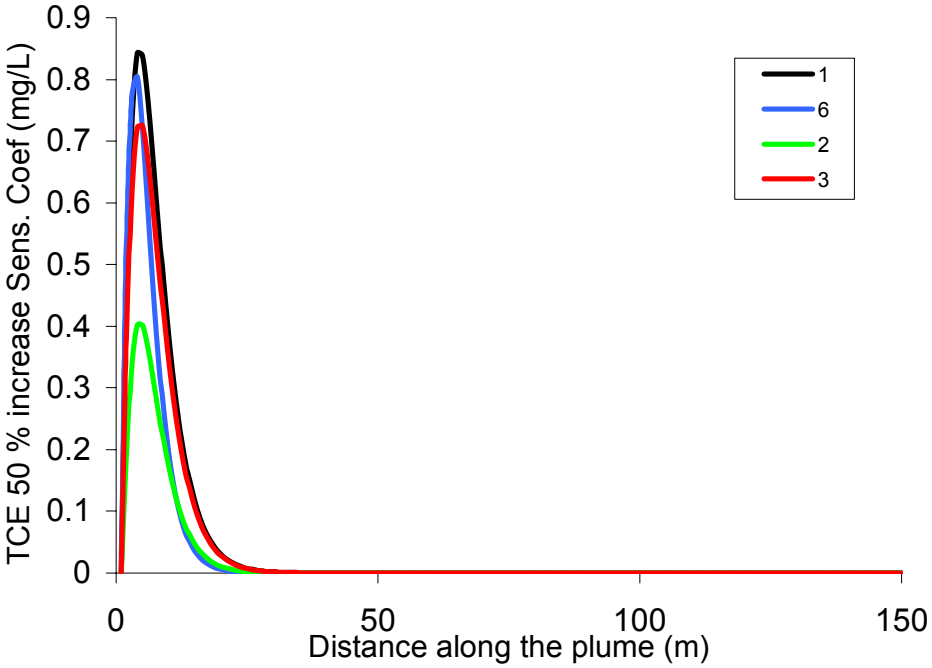
TCE 50 % increase Sens. Coef (mg/L)
0.9
0.8
0.7
0.6
0.5
0.4
0.3
0.2
0.1
0
0
50
100
150
Distance along the plume (m)
1
6
2
3

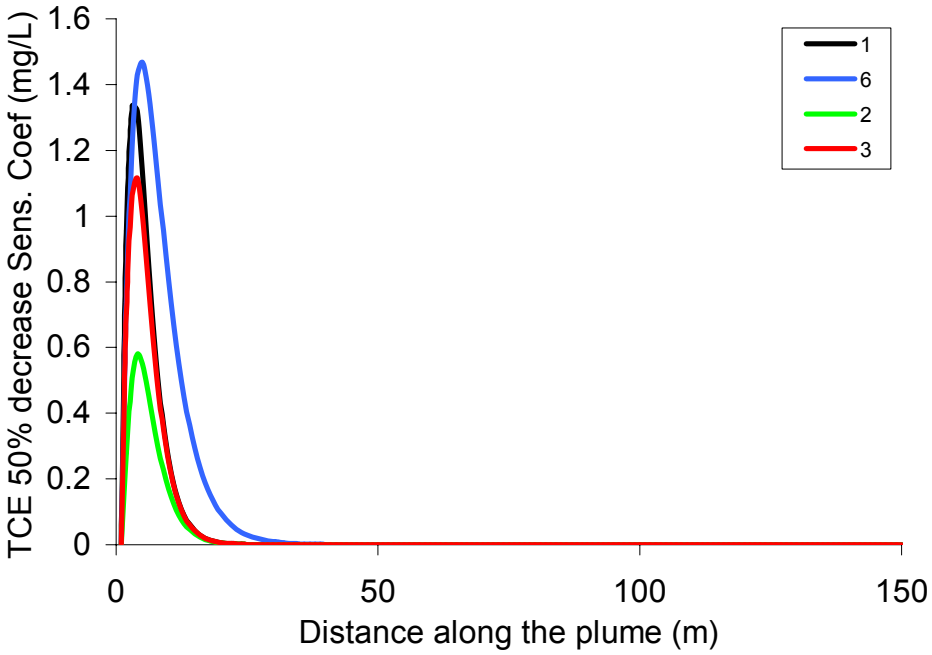
TCE 50% decrease Sens. Coef (mg/L)
1.6
1.4
1.2
1
0.8
0.6
0.4
0.2
0
0
50
100
150
Distance along the plume (m)
1
6
2
3

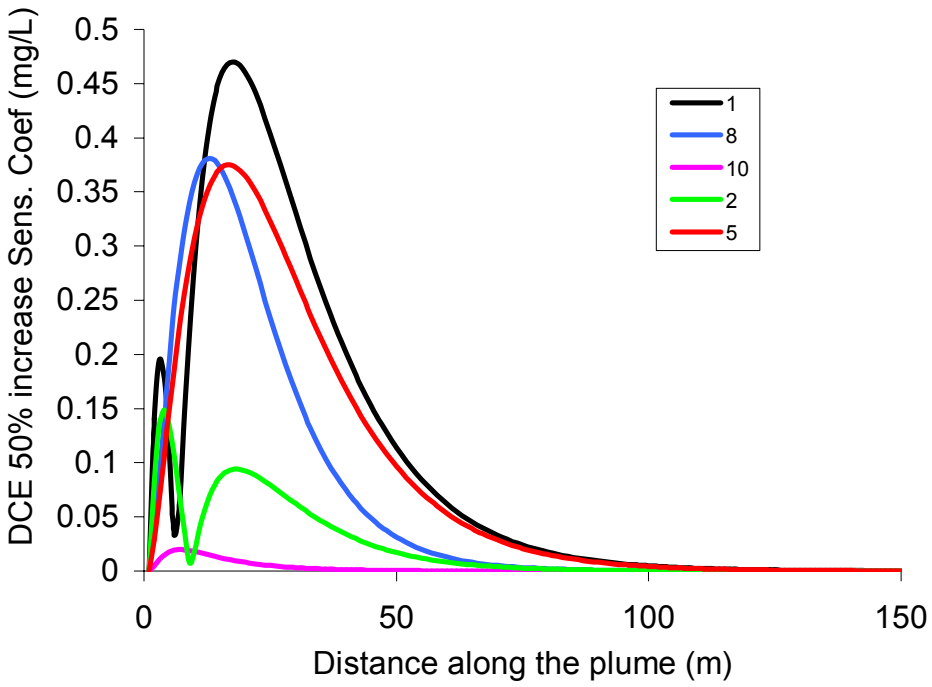
DCE 50% increase Sens. Coef (mg/L)
0.5
0.45
0.4
0.35
0.3
0.25
0.2
0.15
0.1
0.05
0
0
50
100
150
Distance along the plume (m)
1
8
10
2
5

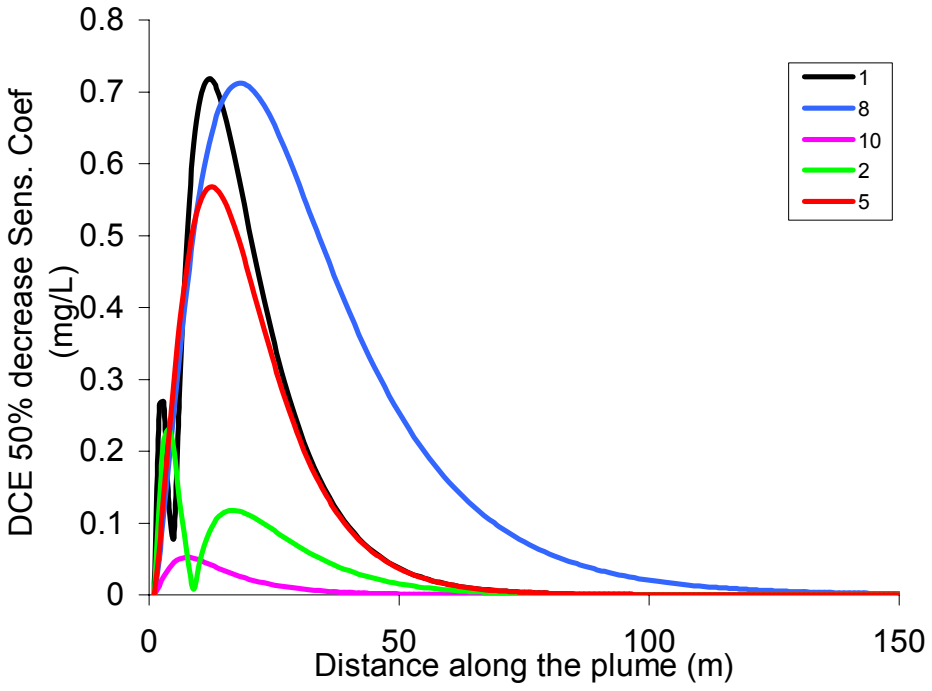
DCE 50% decrease Sens. Coef (mg/L)
0.8
0.7
0.6
0.5
0.4
0.3
0.2
0.1
0
0
50
100
150
Distance along the plume (m)
1
8
10
2
5

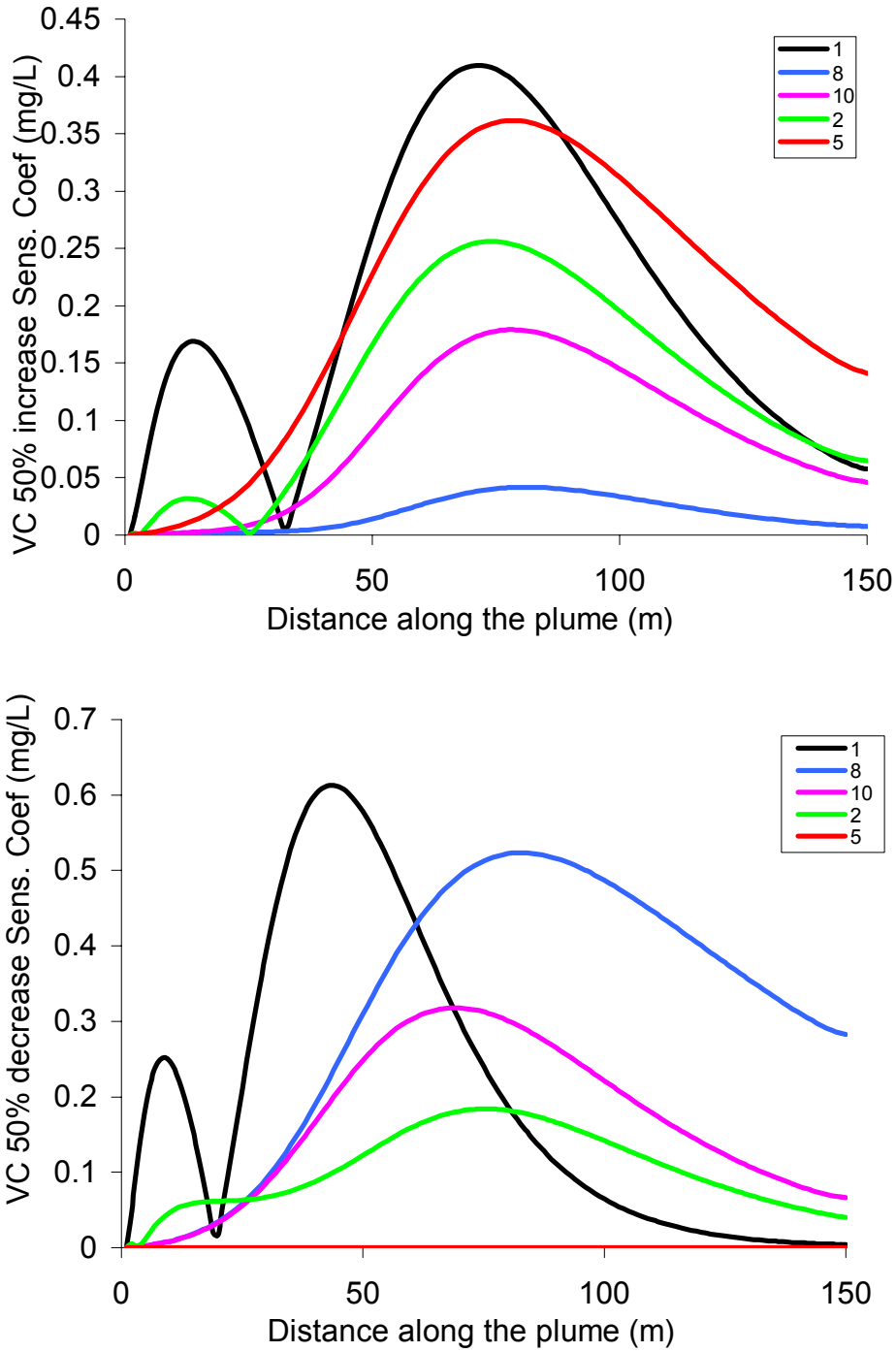

Figure 3.11. Sensitivity coefficients resulting from changing the parameters: hydraulic conductivity (1), longitudinal dispersivity (2), half saturation coefficients for each compound $\overline{K}^{e}_{TCE}$ (3), $\overline{K}^{e}_{DCE}$ (4), $\overline{K}^{e}_{VC}$ (5), rate of degradation for each compound $v^{\max}_{TCE}$ (6), $v^{\max}_{DCE}$ (7) and $v^{\max}_{VC}$ (8), and the inhibition coefficients $k_{DCE,TCE}$ (9), $k_{VC,DCE}$ (10).

Model calibration:

Table 3.7 lists the parameters selected for optimization during model calibration. Compared to the formerly performed manual calibration, the inverse modeling calibration by sequentially optimizing the model parameters produced much better match with the field observed concentrations. The same can not be said, however, about the simultaneous optimization of all the model parameters, which yielded a clear poor match between the observed and simulated concentration profiles. The sequential optimization of the parameters was performed by optimizing the parent compound's (TCE) parameters, updating the parameter values in the DCE model, optimizing the DCE parameters, updating those in the VC model and ending with optimizing the VC parameters. There was a major improvement in the calibration quality in the DCE and VC fields, limited room for improvement was available for the TCE model (Figure 3.11). It was concluded that the inverse modeling technique used by PEST proved to produce parameters that yield a better match with the observed concentration than that of the manual calibration; sequential optimization also has a great advantage over the simultaneous optimization. Table 3.9 summarizes the resulting sum of squared errors for the three calibration mechanisms, the manual, sequential, and simultaneous estimation:

Table 3.8. Parameters selected to be optimized for calibrating the Pensacola model.

TCE	**DCE**	**VC**
$v_{TCE}^{\max}$	$v_{DCE}^{\max}$	$v_{VC}^{\max}$
	$k_{DCE,TCE}$	$k_{VC,DCE}$

Table 3.9. The resulting sum of squared residual for the three optimization techniques

	TCE	DCE	VC
Manual	0.354	0.014	0.021
Sequential with PEST	0.357	0.006	0.001
Simultaneous with PEST	10.904	0.511	0.091

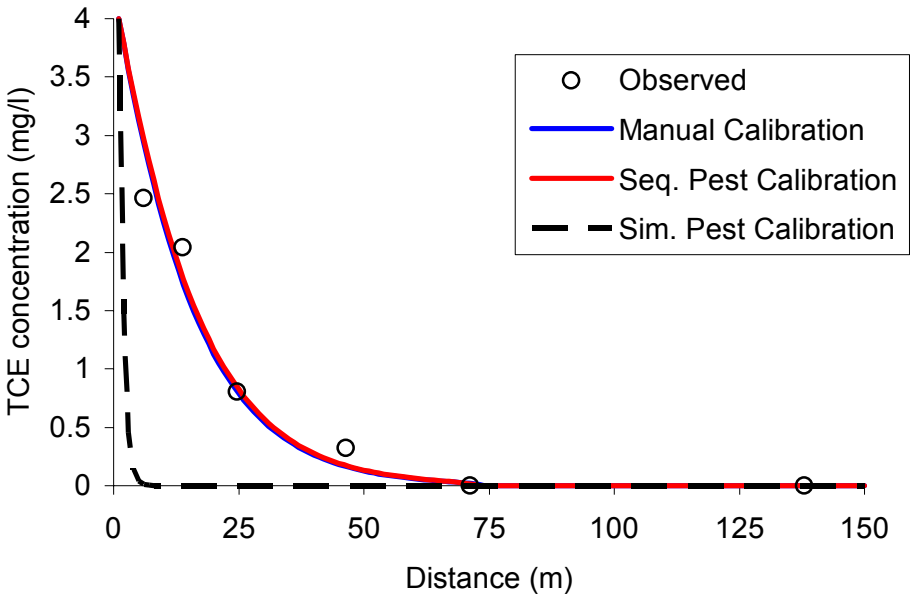
TCE concentration (mg/l)
4
3.5
3
2.5
2
1.5
1
0.5
0
0
25
50
75
100
125
150
Distance (m)
Observed
Manual Calibration
Seq. Pest Calibration
Sim. Pest Calibration

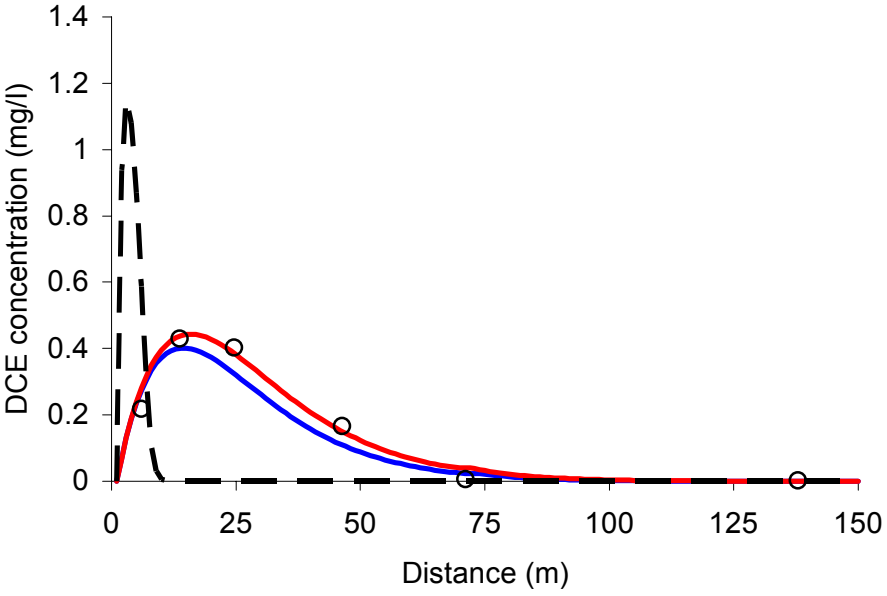
DCE concentration (mg/l)
1.4
1.2
1
0.8
0.6
0.4
0.2
0
0
25
50
75
100
125
150
Distance (m)

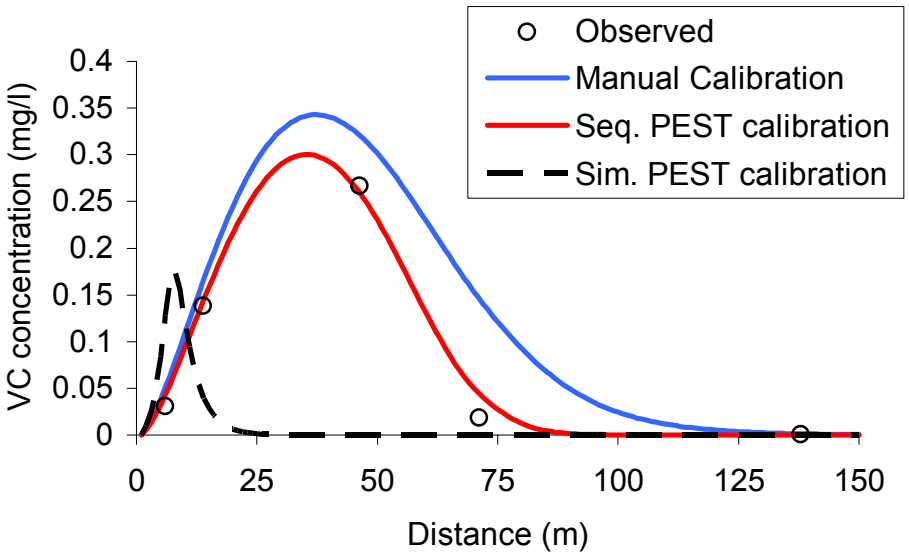

Figure 3.12. Optimization outcome for the Pensacola site model using manual calibration, sequential and simultaneous PEST optimization.

3.4. CONCLUSIONS

Tests on the optimization methodology showed that it was successful in optimizing SEAM3D model parameter. A comparison of parameter estimation techniques showed that a sequential estimation of the model parameters was better than a simultaneous estimation for cases of multi-component reactive solute transport. The kinetic state of the model was shown to have no effect on the quality of parameter estimate technique. The technique seemed to be robust against any kinetic state. The same can be said about the effect of noisy observations. The optimization technique proved to work satisfactory despite the presence of perturbations in the observations. The study on the effect of the observation weights showed that keeping the weights at a value of one for all the observations was advantageous over the case were weights were applied. It was observed that even though the optimized parameters provided simulation results similar to the observed concentrations, the optimized parameter values themselves may or may not be regenerated in a synthetic setting. This is due to the non-uniqueness in the model solution, because multiple sets of parameters may yield the exact same model outcome.

This is a common issue in groundwater models (Poeter and Hill, 1997). In the real world application, the Pensacola site, the generated plumes using the automated parameter estimation proved to match field observations even better than those generated using manual calibration. This proves a clear advantage of the automated calibration using inverse modeling over the manual calibration both in terms of accuracy and time.

Overall, this optimization process using PEST proved to be an efficient way for calibrating more sophisticated models like SEAM3D, where multiple reactive species and multiple kinetic states can be simulated. Further tests are needed to assess the robustness of this methodology under various situations of mixed oxidative reductive environments, and to statistically validate the results reached from the previous tests. The results of those studies are shown in the next chapter of this dissertation were studies are made on a multiple redox zone model and numerous tests are performed to ensure statistical significance of the findings.

Chapter 4

Multiple Redox Zone Model

4.1. INTRODUCTION

Calibration of input parameters for a groundwater flow and contaminant transport model is crucial for accurate simulation and prediction of plume behavior at contaminated sites. Automated optimization of the model parameters is becoming more appealing with advancements in computational tools. Multi-species models, however, with nonlinear reaction terms, such as Monod kinetics, present a challenge for automated groundwater model calibration. This is in part due to the high computational cost for each optimization simulation, the complexity of the processes those models simulate, and the interaction between the various parameters of each compound. The situation gets even more complex when the oxidation-reduction environments change within the ground-water system where the contamination resides. Therefore, introducing multiple biodegradation processes is an added layer of complication that will be accounted for in the model.

In this chapter the use of a nonlinear parameter optimization algorithm for calibrating a multi-redox solute transport model that uses Monod kinetics for simulating the transport of a chlorinated ethenes plume is presented. Multiple tests were performed to develop a methodology for achieving the purpose mentioned above. A methodology will be recommended for calibrating models of chloroethene-contaminated sites. The site that will be modeled and calibrated in this study has two zones of different reducing conditions; one zone of sulfate-reduction near the contaminant source area, and another zone of Fe(III) reduction further down gradient. This phenomenon has been observed at various chloroethene-contaminated sites.

Sensitivity analysis on the model parameters was performed for the purpose of isolating the high influence parameters. A test was designed afterwards to assess the statistical advantage, if any, for optimizing a subgroup of the parameters that has the highest sensitivity coefficient over that with lower sensitivity coefficients. Another test was then designed to come up with the best way of undertaking model calibrations. Three ways

were tested and recommendations were made. Another test was then performed to assess the need for assigning weights to the observations. These tests yielded the best-calibrated model achievable for the site under consideration and helped set up the methodology for calibrating models of such sites. A series of additional tests were performed to assess the contribution of the anaerobic direct oxidation process to the biodegradation of chlorinated ethenes.

4.2 METHODS, TESTING TECHNIQUES AND SITE DESCRIPTOPN

4.2.1 Sensitivity analysis

The sensitivity analysis was performed using a parameter perturbation method. A total of 30 parameters in the SEAM3D model were put to test including eight parameters for the direct oxidation process. The goal of this test was to isolate the parameters with the highest influence on the model outcome in order to focus the efforts on them in the calibration process. The parameters used in the study are listed in Table 4.1.

Table 4.1. Parameters used in the sensitivity analysis and the max sensitivity coefficient values.

		Maximum Sensitivity coefficient			
		PCE	TCE	DCE	VC
1	Inhibition coefficient of PCE by Fe(III) ($k_{PCE,FeIII}$)	0.000	0.000	0.000	0.000
2	Inhibition coefficient of PCE by sulfate ($k_{PCE,SO4}$)	0.012	0.094	0.034	0.014
3	Inhibition coefficient of TCE by Fe(III) ($k_{TCE,FeIII}$)	0.000	0.002	0.000	0.000
4	Inhibition coefficient of TCE by sulfate ($k_{TCE,SO4}$)	0.000	0.045	0.022	0.012
5	Inhibition coefficient of TCE by PCE ($k_{TCE,PCE}$)	0.002	0.357	0.206	0.097
6	Inhibition coefficient of DCE by Fe(III) ($k_{DCE,FeIII}$)	0.000	0.000	0.001	0.000
7	Inhibition coefficient of DCE by sulfate ($k_{DCE,SO4}$)	0.000	0.001	0.724	0.212
8	Inhibition coefficient of DCE by PCE ($k_{DCE,PCE}$)	0.000	0.000	0.000	0.000
9	Inhibition coefficient of DCE by TCE ($k_{DCE,TCE}$)	0.000	0.001	0.333	0.247
10	Inhibition coefficient of VC by Fe(III) ($k_{VC,FeIII}$)	0.000	0.000	0.000	0.000
11	Inhibition coefficient of VC by sulfate ($k_{VC,SO4}$)	0.000	0.000	0.003	0.011
12	Inhibition coefficient of VC by PCE ($k_{VC,PCE}$)	0.000	0.000	0.000	0.000

13	Inhibition coefficient of VC by TCE ($k_{VC,TCE}$)	0.000	0.000	0.001	0.004
14	Inhibition coefficient of VC by DCE ($k_{VC,DCE}$)	0.000	0.000	0.015	0.059
15	Half saturation Coefficient of PCE ($\overline{K}^{e}_{PCE}$)	0.534	1.237	0.822	0.283
16	Half saturation Coefficient of TCE ($\overline{K}^{e}_{TCE}$)	0.002	4.387	3.981	0.596
17	Half saturation Coefficient of DCE ($\overline{K}^{e}_{DCE}$)	0.000	0.001	4.041	0.237
18	Half saturation Coefficient of VC ($\overline{K}^{e}_{VC}$)	0.000	0.000	0.051	0.297
19	Maximum specific rate of PCE ($v^{\max}_{PCE}$)	0.942	1.335	0.645	0.321
20	Maximum specific rate of TCE ($v^{\max}_{TCE}$)	0.002	2.539	1.098	0.853
21	Maximum specific rate of DCE ($v^{\max}_{DCE}$)	0.000	0.001	1.485	0.292
22	Maximum specific rate of VC ($v^{\max}_{VC}$)	0.000	0.000	0.066	0.365
23	Maximum specific rate of direct oxidation of DCE by Fe(III) reducers ($v^{\max}_{DCE,FeIII}$)	0.000	0.000	0.007	0.003
24	Maximum specific rate of direct oxidation of VC by Fe(III) reducers ($v^{\max}_{VC,FeIII}$)	0.000	0.000	0.040	0.003
25	Maximum specific rate of direct oxidation of DCE by sulfate reducers ($v^{\max}_{DCE,SO4}$)	0.000	0.014	0.645	0.151
26	Maximum specific rate of direct oxidation of VC by sulfate reducers ($v^{\max}_{VC,SO4}$)	0.000	0.003	0.303	0.336
27	Half saturation Coefficient of DCE by Fe(III) reducers ($\overline{K}^{e}_{DCE,FeIII}$)	0.000	0.000	0.005	0.004
28	Half saturation Coefficient of VC by Fe(III) reducers ($\overline{K}^{e}_{VC,FeIII}$)	0.000	0.000	0.051	0.013
29	Half saturation Coefficient of DCE by sulfate reducers ($\overline{K}^{e}_{DCE,SO4}$)	0.001	0.012	0.684	0.103
30	Half saturation Coefficient of VC by sulfate reducers ($\overline{K}^{e}_{VC,SO4}$)	0.000	0.003	0.228	0.328

The starting parameter values were obtained by multiplying the parameter values resulting from the preliminary manual calibration by a random number between 0 and 1.0. This insured a random set of starting parameter values.

The sensitivity study was performed by perturbing the parameter set by 50%. The sensitivity coefficient is calculated by taking the absolute value of the normalized difference in the model output divided by the normalized difference in the parameter value. Mathematically, the sensitivity coefficient formula takes the following form:

$$Sensitivity\ coefficient = \left| \frac{\frac{O_p - O_b}{O_b}}{\frac{P_P - P_b}{P_b}} \right| \tag{4.1}$$

where O_p is the model output after perturbing the input parameter, O_b is the model output for original (base) set of parameters, P_p is the perturbed parameter, P_b is the base parameter.

The higher the value of the sensitivity coefficient of a certain parameter, the more influence that parameter has on the ultimate model output. Therefore, a subgroup of parameters was identified based on the results of the sensitivity analysis and was used in subsequent optimization. It is worth noting that some parameters for the daughter compounds were chosen despite the fact that they don't have the highest sensitivity coefficient. These input parameters were chosen based on having the highest sensitivity coefficient among the group of daughter compound parameters while, at the same time, having no effect on the simulated parent compound concentrations. Further discussion can be found at the results and discussion section.

4.2.2 Parameter optimization

The parameter optimization process is done using the nonlinear estimation technique: the Gauss-Marquardt-Levenberg method. This is the method used in the parameter estimation software PEST. The mathematics of PEST have been discussed previously in Chapters 2 and 3 and further details are located in Appendix A.

The site being considered is different from the problem considered in the previous chapter. In this case, two different zones of redox conditions along the ground-water flow path are taken into consideration: sulfate-reducing conditions in and around the source zone and iron-reducing conditions further down gradient. Contaminant concentration in ground water as well as laboratory microcosm experiments suggest a decrease in the rates of degradation due to reductive dechlorination coincides with this change in the redox conditions (Chapelle et al., 2003). In addition, a second attenuation

mechanism, anaerobic oxidation of cis-DCE and VC, can be expected in iron-reducing ground-water systems. Therefore, before attempting to calibrate a chlorinated ethenes model one needs to ensure the accuracy of the redox component calibration. Because of the difference in energy yield of the various electron acceptors and the sequential use over space and time, it is proposed to calibrate the biodegradation component of the model in a sequential manner. In this case, calibration of Fe(III), the electron acceptor with the highest energy yield, was performed first, followed by calibration of sulfate, and then methane (methanogensis).

To provide for a comprehensive study and reach solid recommendations about the best methodology for performing chlorinated ethenes parameter optimization and model calibration, several tests were designed to answer the following research questions:

A. Which is better; optimize all the possible input parameters or only the ones that the model is most sensitive to (only 13 parameters)?

B. For the better of the two scenarios above, which of these three cases yields better results? :
    1. Optimizing the model parameters of each compound alone in a sequential manner starting with PCE and ending with VC.
    2. Optimizing the model parameters of each compound alone in a sequential manner while using the observations from the compound of interest as well as its daughter compounds.
    3. Optimizing the model parameters of all the compounds simultaneously using the observations from all the compounds.

C. What influence does assigning observation weights other than one have on the quality of parameter estimate?

D. What is the contribution of the anaerobic direct oxidation degradation process to chloroethene attenuation and mass loss relative to reductive dechlorination?

Full versus partial parameter model

Two groups of tests were performed to address the first research question. One test contains a model calibrated by optimizing all the possible parameters (referred to as full parameter model), while the other test contains a model calibrated by optimizing a subgroup of all the parameters (referred to as a partial parameter model). This subgroup is identified from the sensitivity coefficient values obtained using the previous study. The

quality of parameter optimization is assessed using the Sum of Squares of Residuals (SSR) between the optimized model outcome and the measured concentrations for each compound. However, for the purpose of statistical validation, the test was performed multiple times for each group.

For each group nine optimization runs were performed. The first group consisted of nine optimization runs with the full parameter model, and the other group consisted of nine optimization runs with the partial parameter model. Each one of these nine runs was different from the rest in its starting parameter values used in the optimization, nine different sets of starting parameter values were generated by multiplying a base set by a random number between 0 and 2. The Sum of squared residual for each optimization test was calculated yielding nine SSR values for each of the two groups. The normality of each group of SSR values was tested using normal probability plot, then the SSR resulting from one group is compared to the other using a statistical two sample t-test assuming unequal variances.

In addition, for the average model outcome from each scenario, a 90% confidence interval plumes were generated; this would give a visual indication for the quality of fit. This, along with the statistical results, would give solid grounds for making a recommendation for the best possible scenario for performing model parameter optimization.

Sequential versus simultaneous estimation of model parameters

Three optimization groups for the same model were preformed to address the second research question. In the first group (case B1), the parameters for the first compound (PCE) were optimized, the optimization was performed by comparing the optimized model output with the concentrations of the compound being considered alone (without any consideration to the concentrations of the daughter compounds). Once the parent compound parameters were optimized its daughter compound parameters are optimized and so on.

In the second group (case B2), the parameters for the first compound (PCE) were optimized, the optimization was performed by comparing the optimized model output with the concentrations of the compound being considered along with its daughter compounds. So for example in the PCE optimization process, the concentration of TCE, DCE and VC play a role in calculating the objective function which directs the optimization process. The third group (case B3), all the parameters for the four compounds were optimized simultaneously, so a single optimization run is needed for all the parameters.

Again, for statistical validation, multiple runs of each group were needed. Nine runs for each group were performed, the SSR for each one of these runs was calculated and two sample t-test was performed. 90% confidence interval plumes were generated around the average plume as well.

Observation weight influence

Difference in the order of magnitude of the observation values used in the optimization process makes it important to study the effect (if any) of having an observations weighing mechanism applied during optimization. The two approaches for assigning the weights are similar to the ones used in Chapter 3. The first approach is based on the work of Anderman and Hill (1999), in which the weights are produced using formula listed in Chapter 3

$$W_i = 1 / (C_v C_i)^2 \qquad (4.2)$$

where W_i = is the weight to be assigned for the concentration C_i, C_v = is the coefficient of variation which is set to a value of 0.25. The second approach is to keep the default weight of one for all the observations.

The first weighing mechanism is designed so that no single observation would have a significantly greater influence over the optimization process than the rest. In the other case, where the weights were kept at values of one, the concentration values only have

impact on the direction of the optimization process. In the weighted concentrations case, the concentration-weight product dictates the optimization direction.

For the purpose of statistical validation, nine runs for each case were performed. The SSR for each one of these runs was calculated and two sample t-tests were performed, 90% confidence interval plumes were generated around the average plume as well.

Contribution of anaerobic direct oxidation

Anaerobic direct oxidation process (DOx.) was modeled as a contributor to the degradation of chlorinated ethenes. This group of tests was designed to assess the contribution of this process to the overall degradation of the chlorinated ethenes in the site under consideration. To do this, seven runs of the model were performed; the difference between them was the processes being considered for degrading the chlorinated ethenes. The first case was that were degradation was due to reductive dechlorination (RD) only, no anaerobic direct oxidation took place, this was achieved by setting the maximun specific rate of direct oxidation for both DCE and VC to zero. The second case was with the degradation process being the reductive dechlorination only in the sulfate dominant region, the RD on the Fe(III) zone was shut down by reducing the inhibition coefficient of both DCE and VC by the presence of Fe(III) to a small value of 0.01, and this insured minimizing the effect of RD in the Fe(III) zone. The third case was the default case of both RD and DOx. acting together for degrading the chloroethene plume, all the other cases are compared to this case. The fourth case is a case where RD is active and DOx. in the Fe(III) region only is active. The fifth case is where RD in the sulfate region along with DOx. in the Fe(III) region are active. The sixth case is where the RD in the sulfate and DOx. in the Fe(III) for VC only are active. The seventh and final case is where RD in the sulfate region and DOx. for VC are the only active process of degradation. The plumes generated from modeling the seven cases were plotted and compared, and the quality of match with the observed concentrations was assessed.

4.2.3 Site description: Kings Bay, GA

The site under consideration is a U.S Department of Navy facility in North-Central Camden County, Georgia. The interest in this site started in January 1992 when volatile organic contaminants (VOCs) were detected in ground water. The origin of these contaminants was a landfill located in the Naval Submarine Base (NSB) in Kings Bay. It was used as a municipal waste disposal landfill that operated in the mid 1970s to 1980 era. The landfill received solvent municipal wastes that were disposed using the trench method wherein trenches were dug, backfilled with waste, and covered with fill (EPA, 2000).

The NSB lies in the southeastern Camden County, Georgia, bounded from the north by krooked river state park, to the east by Krooked River and Cumberland sound, to the south by corporate boundary of St. Marys, GA, and to the west by Georgia state highway. It has been found through a series of investigations that the general trend of ground water movement is to the North West direction. Figure 4.1 shows a schematic of the overall location of the site and chloroethenes plume:

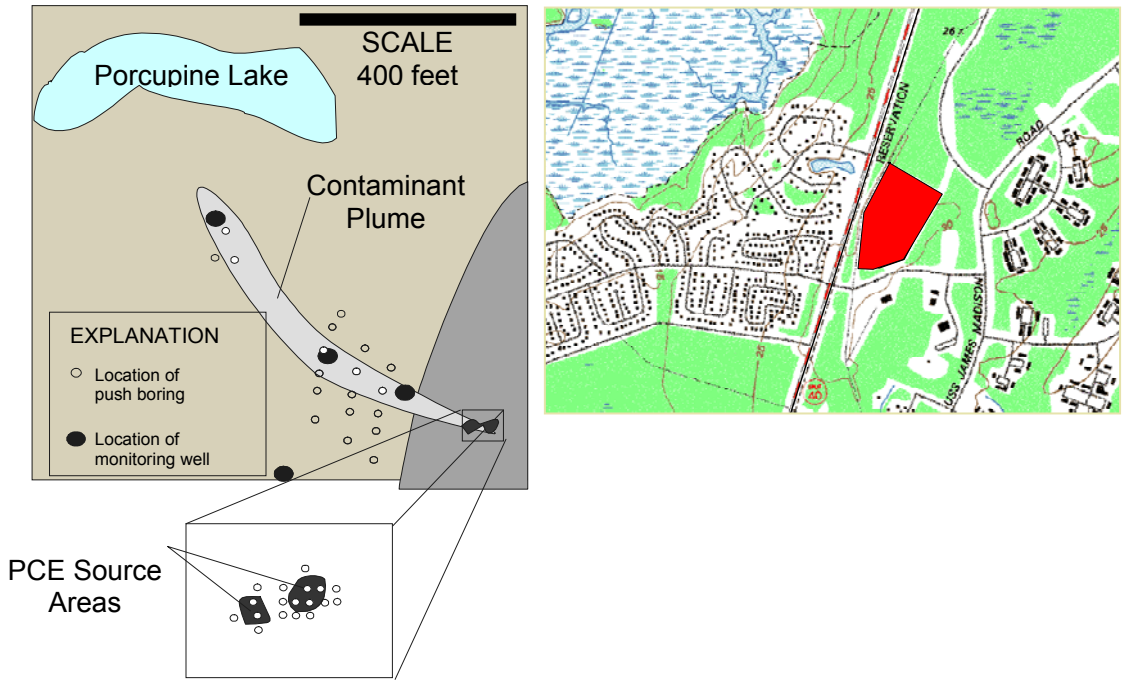

Figure 4.1. Schematic of the Kings Bay landfill location and the chloroethenes plume

The redox data at the site indicate the presence of an sulfate-reducing zone near the source zone that gradually grades to an Fe(III)-reducing zone down gradient (Chapelle et al., 2003). The contaminant concentration data indicate a distinct change in the biodegradation rates for total chlorinated ethenes that coincide with the change in the rodox conditions (Chapelle et al., 2003). The observed concentration values along the centerline of the plume are shown in the Figure 4.2:

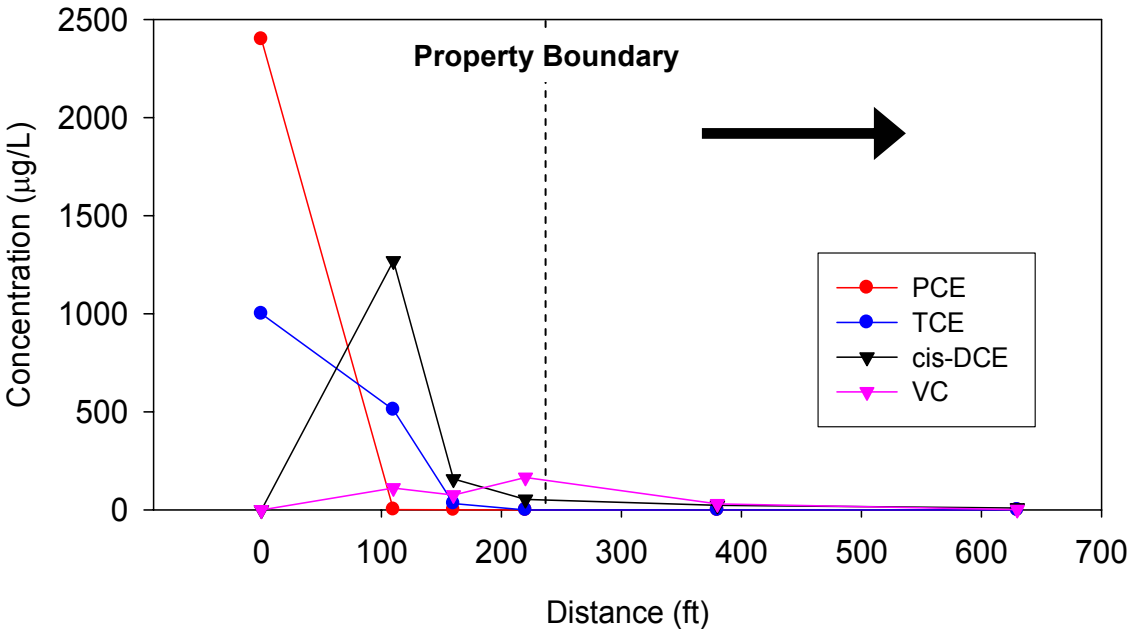

Figure 4.2. Concentration values along the centerline of the chloroethenes plume in Kings Bay

The chloroethene plume at this site was modeled using MODFLOW for the flow model and SEAM3D for the solute transport model. It was composed of a single layer of 45 model rows and 20 model columns totaling 900 model cells. Each cell is 5 meter in dimension for all the rows but three. These three cells are near the source zone and are different than the rest to better capture the plume behavior in the source zone region. Homogeneity is assumes, therefore, the hydraulic conductivity was set to a single value throughout the model of 10 m/d, and the porosity to a value of 0.3. A down gradient boundary condition was defined by setting a single row of cells as a constant flow boundary. The average groundwater velocity is approximately 5 cm/d which is the value that tracer studies at the site suggest. The simulation was run in a steady state mode for a

period of 20 years which is a reasonable time period between what is believed to be a time of contamination and a time of the start of the clean up and remediation efforts.

The contaminant in the source zone was modeled using a constant concentration cell for PCE and TCE. The longitudinal dispersivity was set to 5 m while the transverse horizontal /longitudinal ratio was 0.01. The main biodegradation processes simulated were reductive dechlorination and anaerobic direct oxidation.

4.3 RESULTS AND DISCUSSION

4.3.1 Sensitivity analysis

Thirty parameters were subject to the sensitivity analysis study, the parameters and the maximum sensitivity coefficient values obtained are listed in Table 4.1.

The sensitivity analysis resulted in identifying a subgroup of the 30 parameters listed earlier to have the higher influence on the model outcome. This subgroup consisted of 13 parameters, some of which were chosen for having the highest sensitivity coefficient values while others were chosen for having the highest sensitivity coefficient while, at the same time, having no effect on the simulated parent compound concentrations. For example, upon doing the sensitivity analysis for DCE, the test resulted in a higher sensitivity coefficient for parameter number 16 which is listed in the table above as $\overline{K}^{e}_{TCE}$, a parameter of DCE's parent compound, TCE, however manipulating this parameter would affect it's parent parameter and probably throw it's calibration off. Therefore, the parameter chosen instead was number 17 which is $\overline{K}^{e}_{DCE}$, this parameter ranks number two for DCE yet was chosen to be optimized because its effect is on the compound of interest, DCE, and its daughter compound VC. The 13 parameters chosen for further testing and model calibration are listed in Table 4.2.

Table 4.2. The group of high sensitivity coefficient parameters along with their sensitivity coefficients

Parameter	Max. Sensitivity Coefficient
Half saturation Coefficient of PCE ($\overline{K}^{e}_{PCE}$)	1.237
Half saturation Coefficient of TCE ($\overline{K}^{e}_{TCE}$)	4.387
Half saturation Coefficient of DCE ($\overline{K}^{e}_{DCE}$)	4.041
Maximum specific rate of VC ($v^{\max}_{VC}$)	0.365
Inhibition coefficient of PCE by sulfate ($k_{PCE,SO4}$)	0.045
Inhibition coefficient of TCE by PCE ($k_{TCE,PCE}$)	0.357
Inhibition coefficient of DCE by TCE ($k_{DCE,TCE}$)	0.333
Inhibition coefficient of DCE by sulfate ($k_{DCE,SO4}$)	0.724
Inhibition coefficient of VC by DCE ($k_{VC,DCE}$)	0.059
Maximum specific rate of direct oxidation of DCE by Fe(III) reducers ($v^{\max}_{DCE,FeIII}$)	0.007
Maximum specific rate of direct oxidation of VC by Fe(III) reducers ($v^{\max}_{VC,FeIII}$)	0.040
Maximum specific rate of direct oxidation of DCE by sulfate reducers ($v^{\max}_{DCE,SO4}$)	0.645
Maximum specific rate of direct oxidation of VC by sulfate reducers ($v^{\max}_{VC,SO4}$)	0.336

It was observed that the concentration of daughter compounds (DCE and VC) is sensitive to many more parameters than their parent compounds PCE and TCE. This is due to the fact that rates of generation and accumulation of these daughter compounds are impacted by natural biodegradation of their parent compounds. Therefore, the parameters influencing the daughter compounds are indirectly those of their parent compounds. This observation suggested that any model calibration of the parent compound needs to take into account the effect on the daughter compounds. Therefore, one of the tests described in parameter optimization section of this chapter was designed to compare a calibration exercise where the parent compounds were calibrated without any consideration to the daughter compounds with another exercise where the parent compound was calibrated keeping in mind the effect on the daughter compounds. The results of the sensitivity analysis study are summarized in Figures 4.3 through 4.6, the parameter names corresponding to the numbers are listed in Table 4.1.

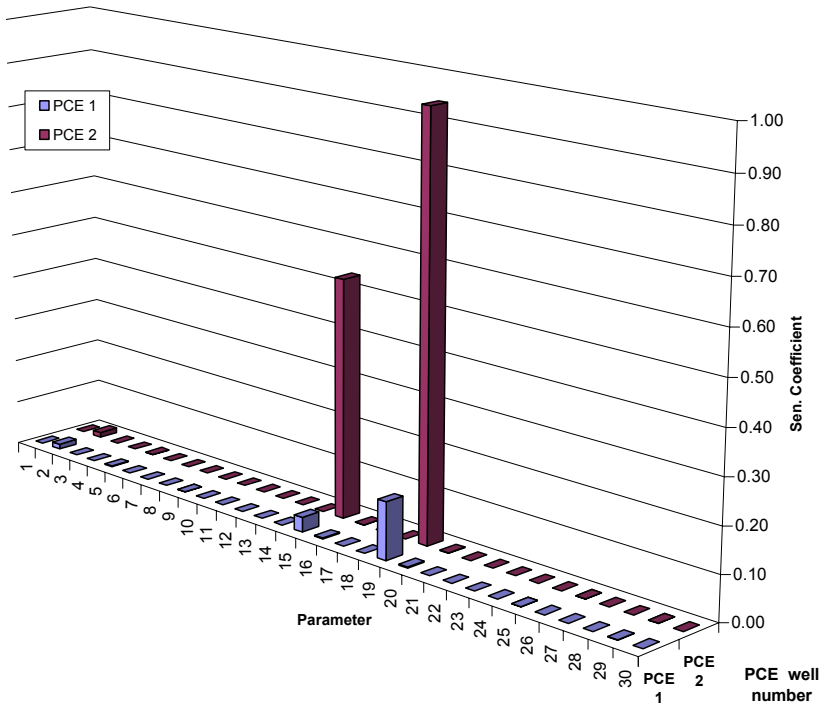

Figure 4.3. PCE Sensitivity coefficient values

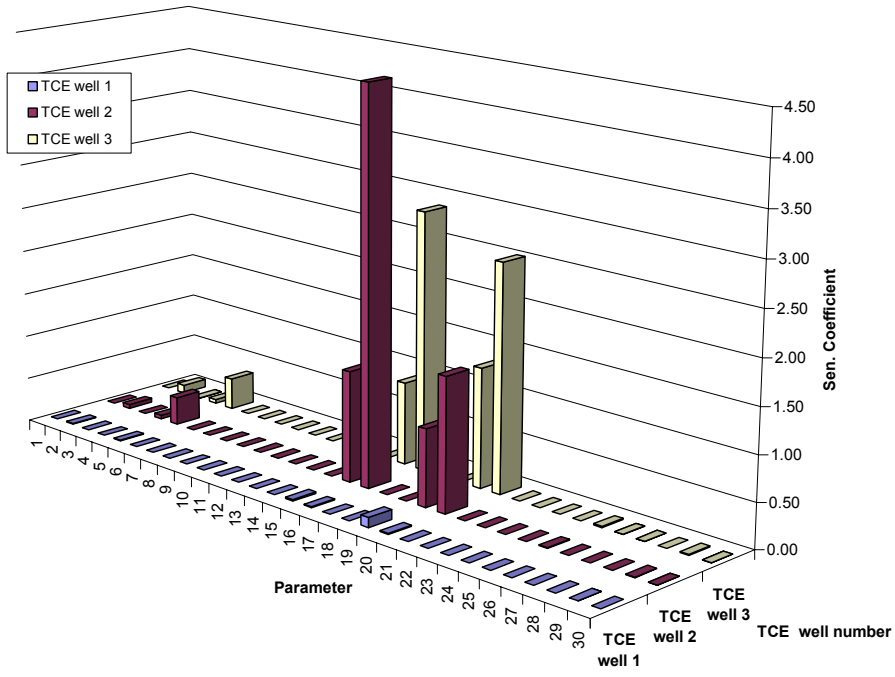

Figure 4.4. TCE Sensitivity coefficient values

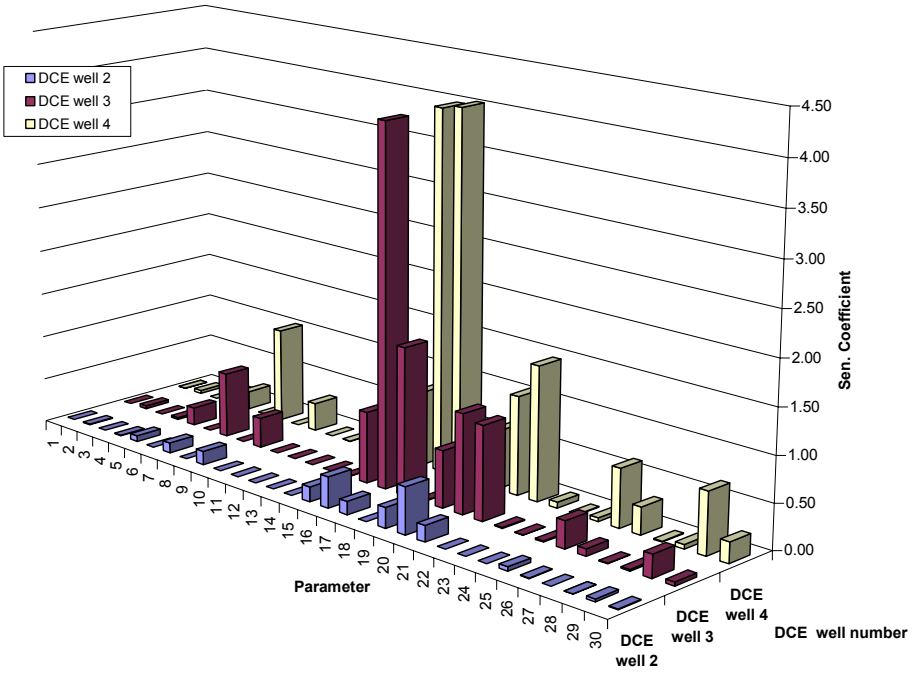

Figure 4.5. DCE Sensitivity coefficient values

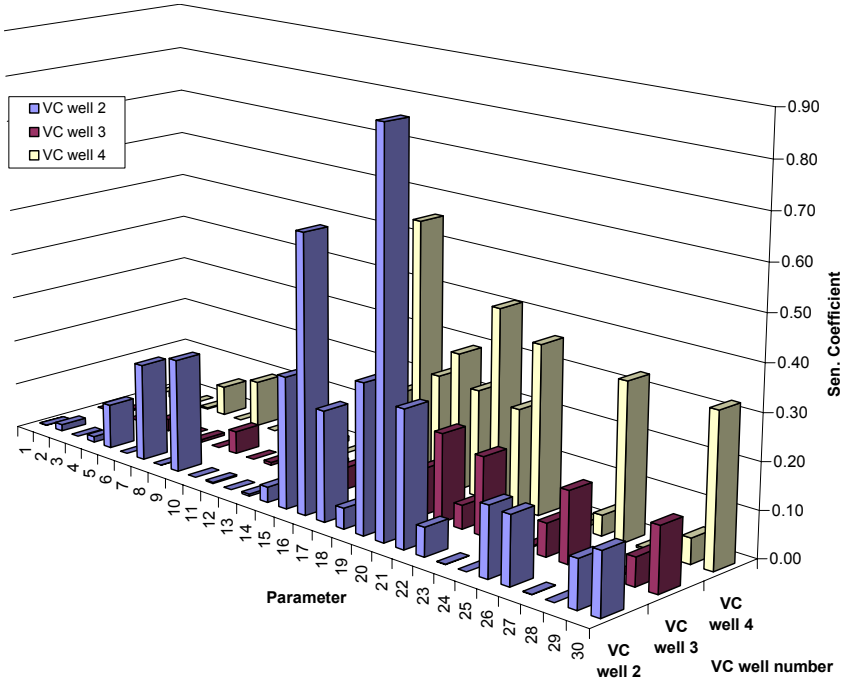

Figure 4.6. VC Sensitivity coefficient values

4.3.2 Anaerobic oxidants calibration

As mentioned before, an anaerobic oxidant calibration is a prerequisite to performing chlorinated ethenes model calibration. The first step is to calibrate the model to the Fe(II) observed data since the use of lower energy yielding electron acceptors is inhibited by the presence of the higher energy yielding electron acceptors. So once that calibration is satisfactory the second in the list of strong oxidants is calibrated, which is sulfate, and then methane. The parameters used for the optimization are listed in Table 4.3.

Table 4.3. Input parameters used in the anaerobic oxidant calibration

Parameter	Optimized value
Maximum specific rate of substrate utilization with Fe(III) as electron acceptor	0.0800
Maximum specific rate of substrate utilization with CO2 as electron acceptor	0.7683
Sulfate yield coefficient	0.0380
Fe(II) generation coefficient	0.0025
Methane generation coefficient	6.3539

The calibration yielded satisfactory results. The general trend of plume behavior in the three compounds was simulated.

The results of the calibration of anaerobic oxidants are shown in Figures 4.7, 4.8, and 4.9:

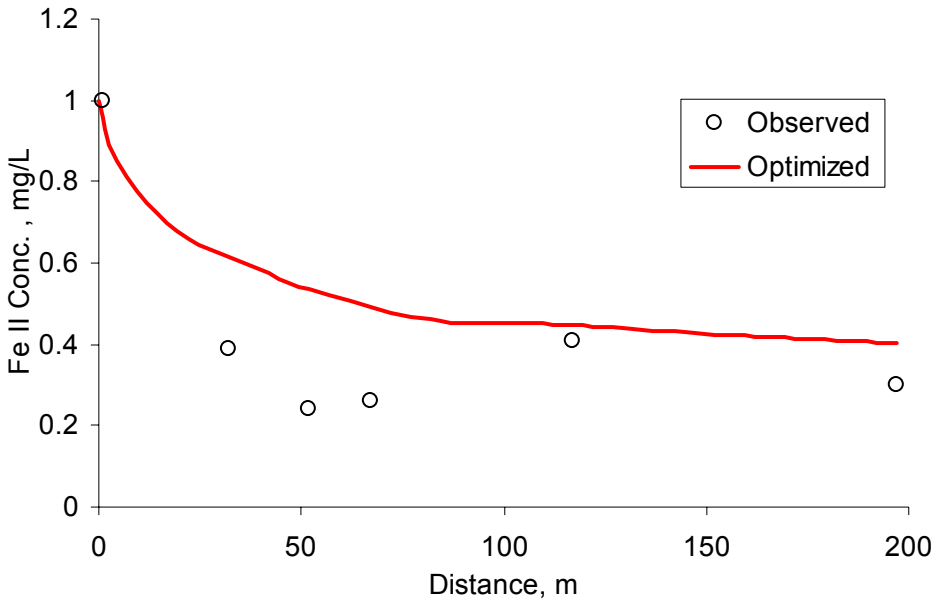

Figure 4.7. Calibrated model of the Fe(II) plume.

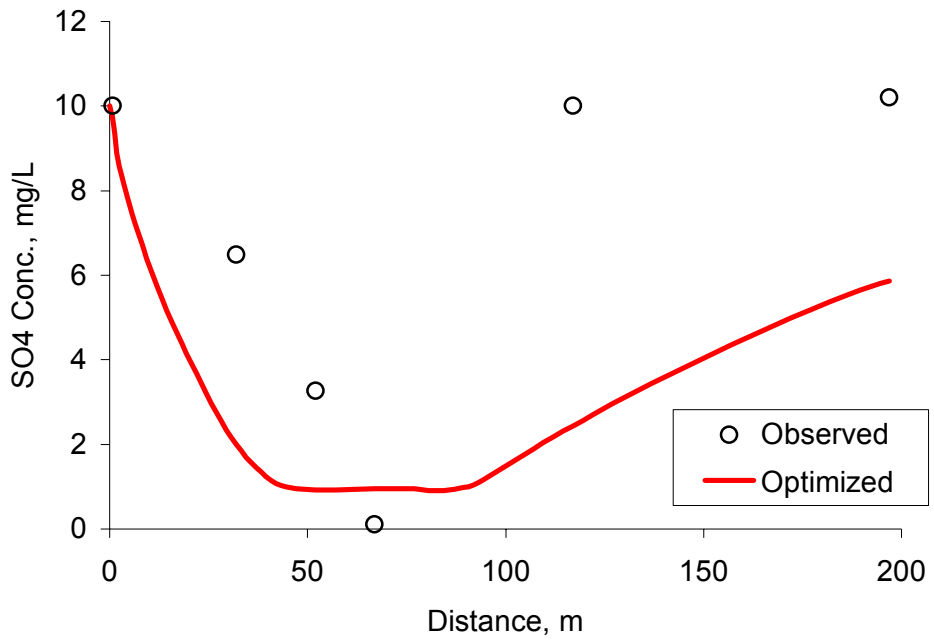

Figure 4.8. Calibrated model of the sulfate data.

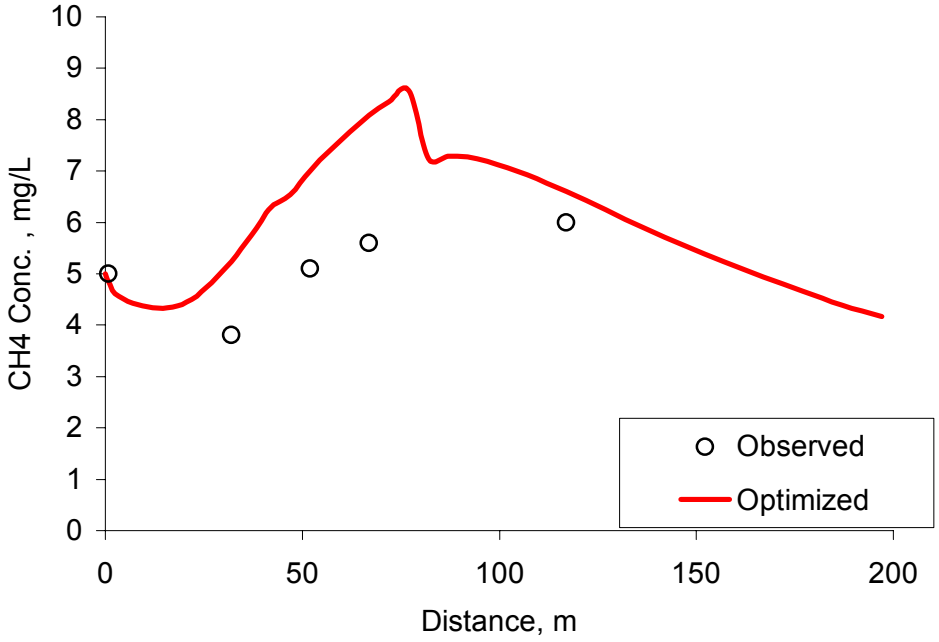

Figure 4.9. Calibrated model of the methane plume.

4.3.3 Full versus partial parameter model

In general, the partial parameter model that had only a subgroup of the parameters optimized performed better than the full parameter model that had all the possible parameters optimized. This result can be statistically verified in two of the four compounds. In the other two, the results support the conclusion mentioned above without having the statistical significance. With the partial group of parameters, the optimization algorithm has access to the highly sensitive parameters, this partial set of parameters have the greatest influence on the model outcome, and therefore, optimizing these parameters focuses the computational effort in a productive manner. In addition to the advantage of the partial model in terms of the overall SSR, there is another advantage in terms of the lesser variance in the optimization outcome, that can be seen through the 90% confidence intervals around the average plume which seem to be narrower in the case of the partial model than it is in the case of full parameter model. The average SSR values obtained from the nine optimization runs as well as an analysis of significance is summarized in Table 4.4.

Table 4.4. Summary of the optimization outcome for the full and partial models along with the statistical significance analysis

Compound	Full Model Avg. SSR	Partial model avg. SSR	Statistical advantage for the partial over full parameter model
PCE	0.30	0.16	Yes
TCE	0.67	0.30	No
DCE	0.75	0.19	Yes
VC	0.05	0.04	No

Before performing a t-test on the SSR values, the normality of the sample need to be checked. That was performed using the normal probability plot. The closer the data points are to the center line the more the evidence there is that the data is normally distributed. An example for one of the tests performed before a t-test study is shown in Figure 4.10. The outcome of this test for each compound is shown in Figures 4.11 through 4.14.

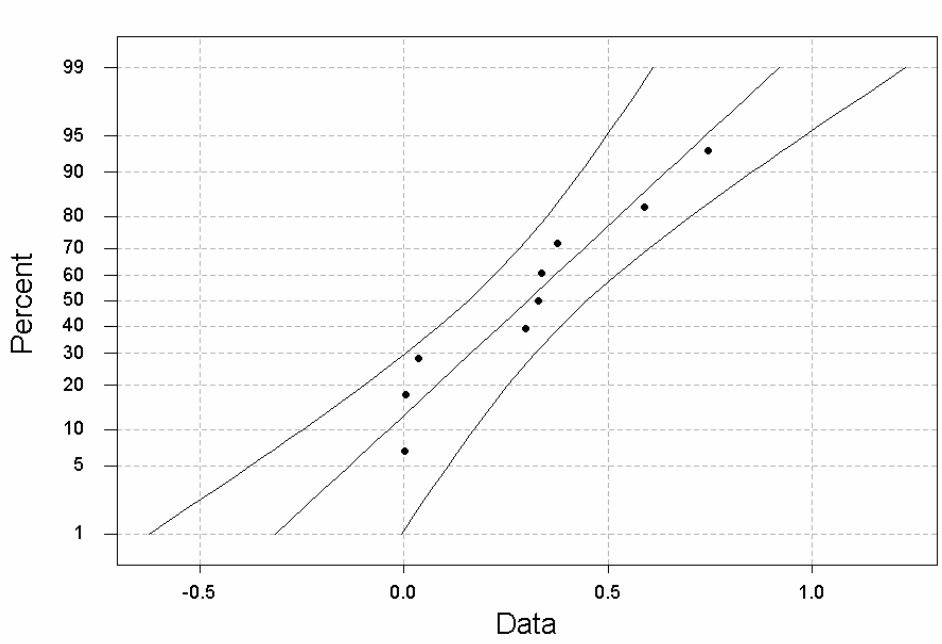

Figure 4.10. A sample of the normal probability plots used to check normality of values of SSR used in statistical t-testing for PCE full parameter model, the confidence interval lines shown are 90% C.I.

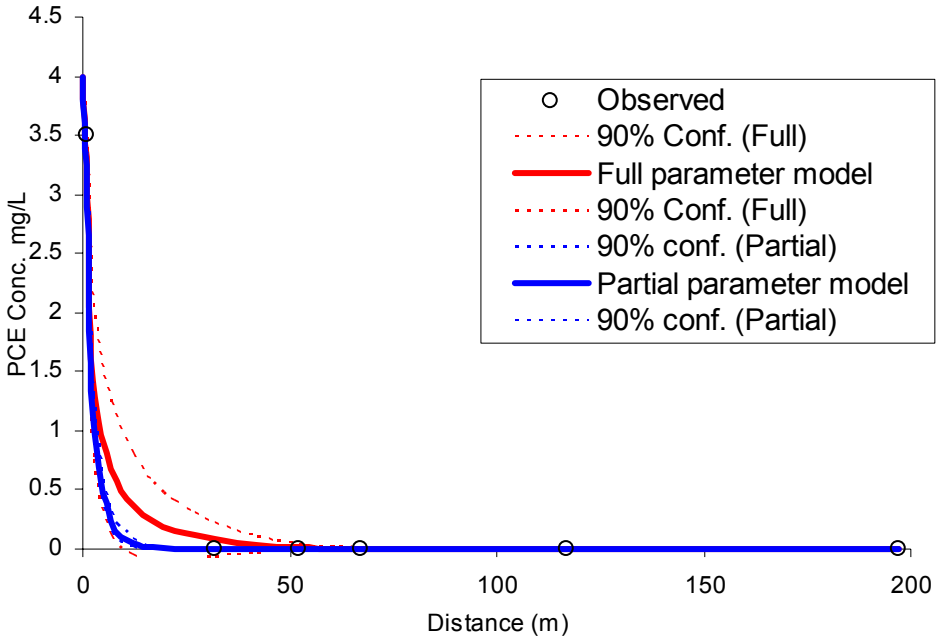

Figure 4.11. PCE plumes generated using a model where all the parameters are optimized (Full parameter model) and another where a partial set only was optimized (partial parameter model).

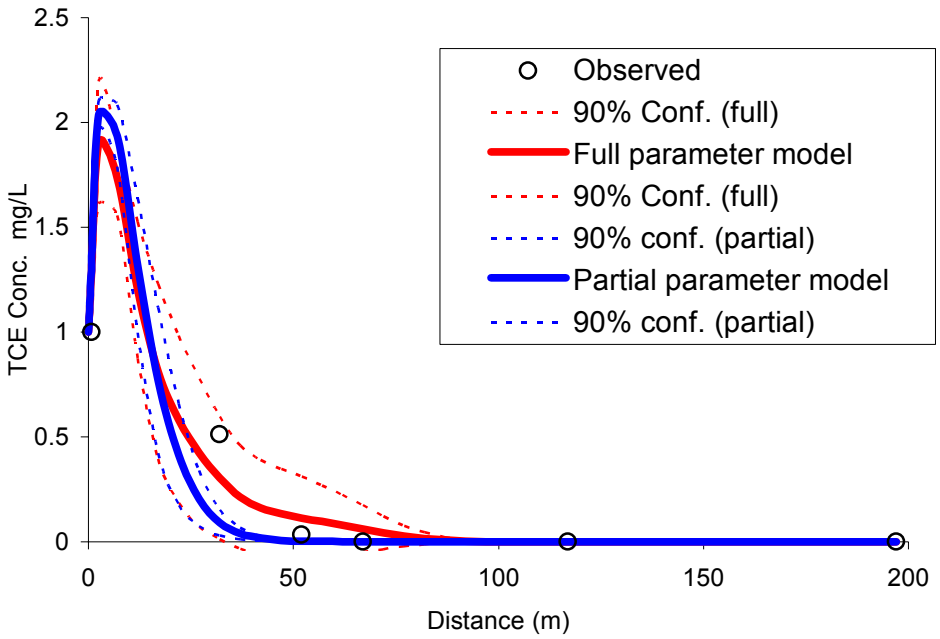

Figure 4.12. TCE plumes generated using a model where all the parameters are optimized (Full parameter model) and another where a partial set only was optimized (partial parameter model).

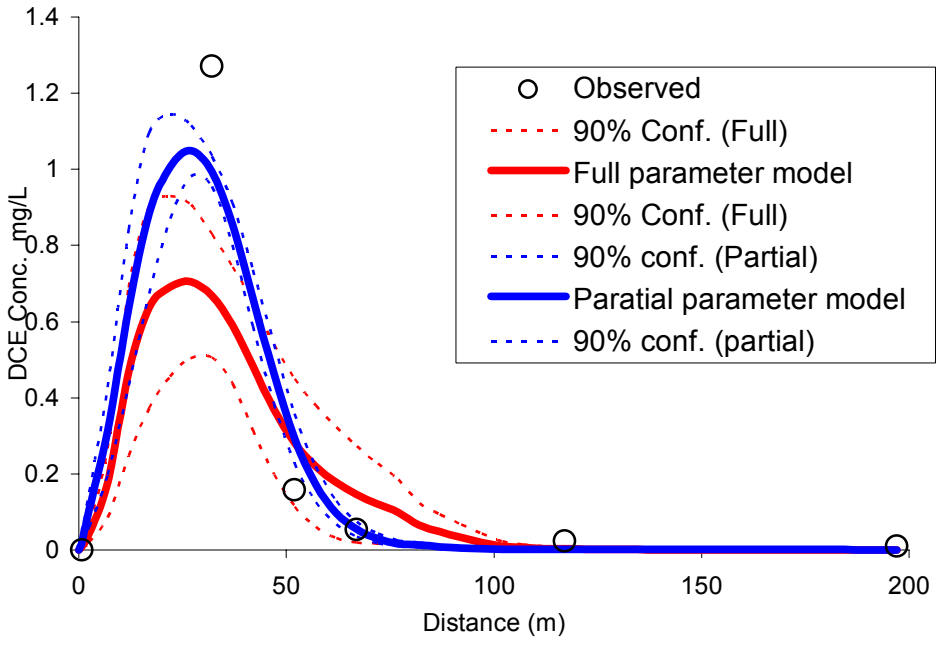

Figure 4.13. DCE plumes generated using a model where all the parameters are optimized (Full parameter model) and another where a partial set only was optimized (partial parameter model).

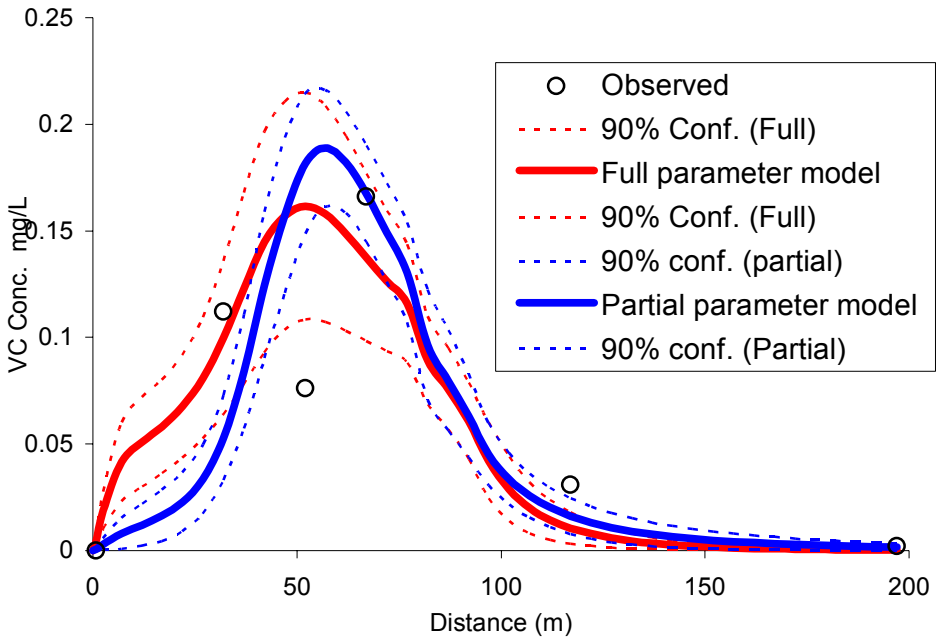

Figure 4.14. VC plumes generated using a model where all the parameters are optimized (Full parameter model) and another where a partial set only was optimized (partial parameter model).

4.3.4 Sequential versus simultaneous estimation of the model parameters

The first test indicated that using the partial parameter model in the optimization process yields a better overall fit; therefore, this partial parameter model will be compared against the two other cases. The first test is a case where the parameters for the source compound (PCE) were optimized first. This optimization was performed by comparing the optimized model output with the observed concentrations of the compound being considered alone (without any consideration to the observed concentrations of the daughter compounds). Once the input parameters for the parent compound were optimized, the parameters for daughter compounds are sequentially optimized. This is referred to as case B1.

In the second case (case B2), the parameters for the source compound (PCE) were optimized by comparing the optimized model output with the observed concentrations along with the concentrations of the immediate daughter compound. The third case (case

B3) is the case where all the parameters for the four compounds were optimized simultaneously.

Nine optimization runs of each case were performed, each one of these nine runs started with a different set of starting parameter values. In order to eliminate any source of variability, the starting parameter values were the same for the same run in all the three cases. For example, the starting parameter values for the fourth optimization run in all the three cases were the same, those for fifth optimization run were different than the fourth but the same for the three cases.

The average concentrations for each case were plotted, and 90 % confidence intervals around the average were calculated and plotted to assess the variability in the optimization outcome, the SSR for each of the nine runs was calculated and compared to the nine SSR for the other cases. The hypothesis of no difference between the means of the SSR values was tested.

Overall the second case (case B2) were the parameters were optimized sequentially taking into account the effect on the daughter compounds, yielded a better match between the observed and model predicted concentrations than the other two cases. This advantage was statistically significant in many cases, even in the cases of where it wasn't statistically significant the advantage can still be seen by looking at the average SSR values as well as the plume profiles. The 90% confidence intervals are narrower in the B2 case suggesting a less variable optimization outcome. Table 4.5 provides a summary of this test's results. Figures 4.15 to 4.18 show the results of this study

Table 4.5. Summary of the optimization outcome for the three optimization methods B1, B2 and B3 along with the statistical significance test results

Comp.	B1 Avg. SSR	B2 Avg. SSR	B3 Avg. SSR	Stat. sig. advantage of B2 over B1	Stat. Sig. advantage of B2 over B3
PCE	0.004	0.001	0.166	No	Yes
TCE	0.424	0.260	0.292	No	No
DCE	1.520	0.079	0.191	Yes	Yes
VC	0.027	0.032	0.044	No	Yes

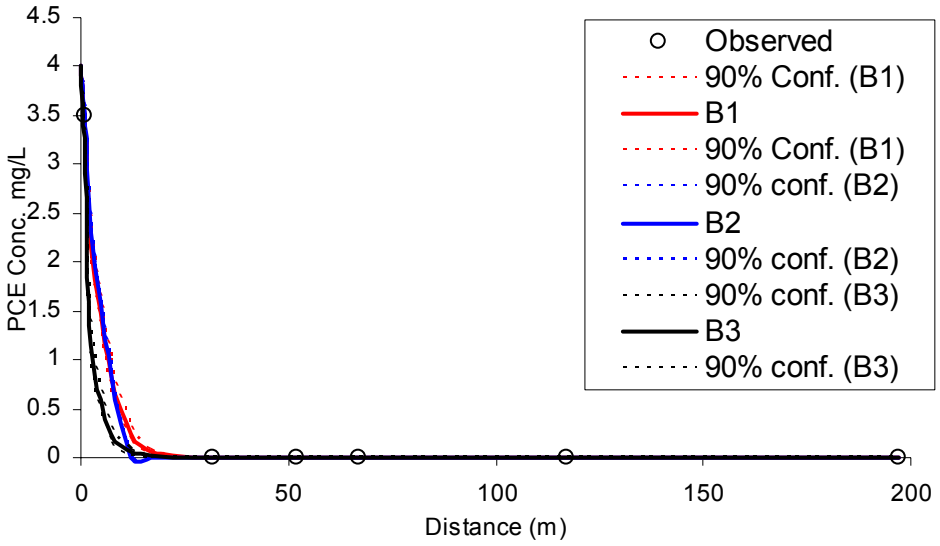

Figure 4.15. PCE plumes generated using the three methods: B1, where the optimization is sequential without consideration for the daughter compounds, B2 where the optimization is sequential with consideration for the daughter compounds and B3 where the optimization is simultaneous

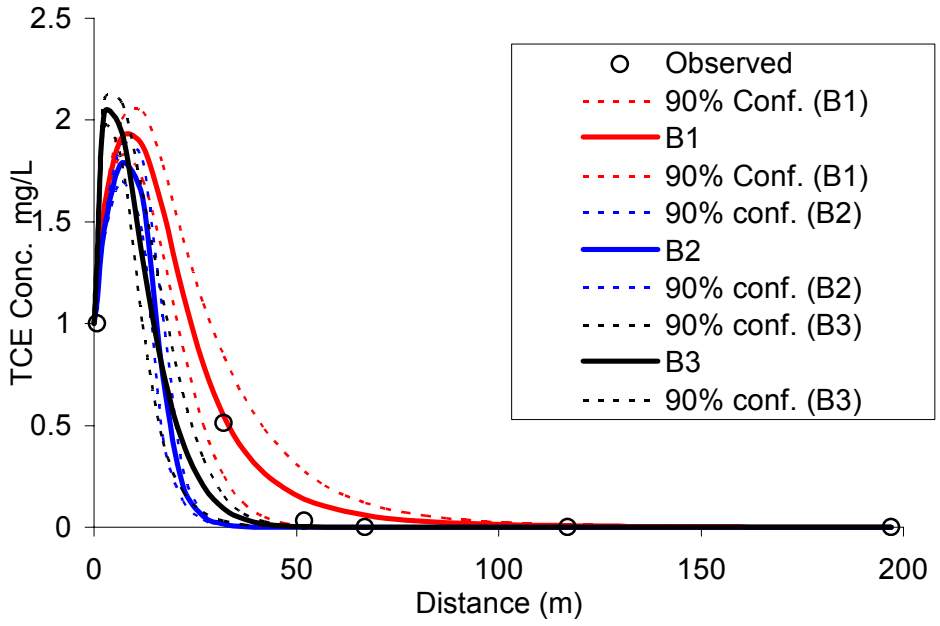

Figure 4.16. TCE plumes generated using the three methods: B1, where the optimization is sequential without consideration for the daughter compounds, B2 where the optimization is sequential with consideration for the daughter compounds and B3 where the optimization is simultaneous

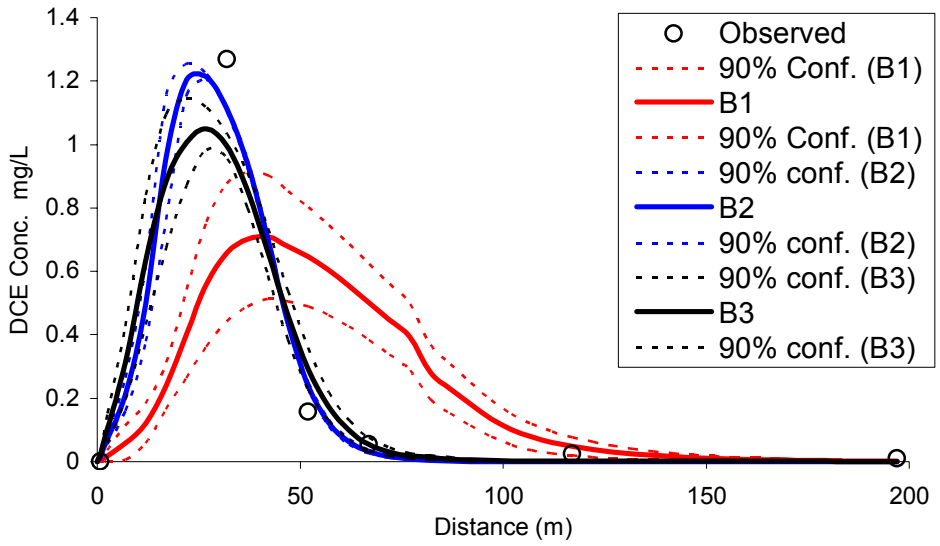

Figure 4.17. DCE plumes generated using the three methods: B1, where the optimization is sequential without consideration for the daughter compounds, B2 where the optimization is sequential with consideration for the daughter compounds and B3 where the optimization is simultaneous

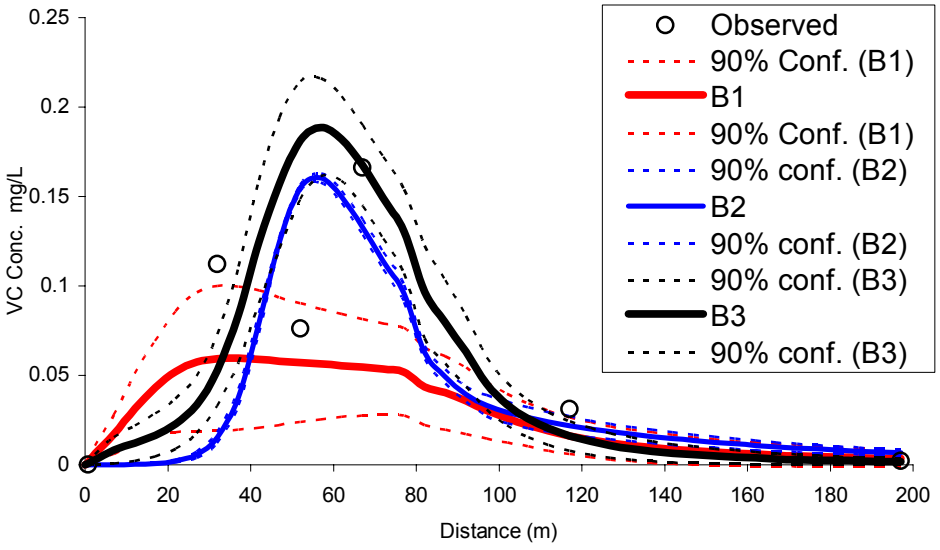

Figure 4.18. VC plumes generated using the three methods: B1, where the optimization is sequential without consideration for the daughter compounds, B2 where the optimization is sequential with consideration for the daughter compounds and B3 where the optimization is simultaneous

4.3.5 Observation weight influence

The two scenarios tested were one with the observation weights set to 1.0 regardless of their value, the other with the observation weights being a function of the of the observation value and coefficient of variation, the coefficient of variation was set to 0.25 because of the lack of detailed information about the sampling and measurements process. The first scenario naturally puts more emphasis on matching the observations with higher values; the higher the value of the observations is the more it directs the optimization process. In the second scenario, however, the smaller observation concentrations have a comparable impact to larger observation concentrations on the optimization process due to the higher weight they have. The smaller the observation, the larger the weight is, and therefore, all the observations have somewhat of a similar impact on the optimization process.

Table 4.6. Summary of the optimization outcome for the two weighing mechanisms, one where the weights are set to one and another with assigned weights other than one

Compound	Wt. = 1.0 SSR	Weighed observations SSR	Statistical significance
PCE	0.0005	0.0019	No
TCE	0.2607	0.0472	Yes for weighed obs.
DCE	0.0795	1.0837	Yes for Wt. =1
VC	0.0321	0.0162	Yes for weighed obs.

The resulting average SSR for the two cases can be summarized in Table 4.6. The results of this test were not very conclusive, for the parent compound (PCE), the SSR for the model in the wt. = 1.0 scenario was less than that for the weighed observation model. This advantage however wasn't found to be statistically significant. The model with the weighed observations yielded better match than that with the wt. = 1.0 for the TCE compound this was statistically significant, the plume plot also supports this finding. On the other hand, for DCE, the model in which all the concentrations are set to one yielded a much better match than that with weighed parameters. Despite the numbers that suggest a better match for the weighed observation model of VC, the plume matches the observations better in the case of wt. =1.0 than it does in the weighed observation case. It was also observed that the variance in the model outcome is higher in the cases of weighed observation models than it is for wt. =1.0 models, particularly for the VC,

suggesting higher confidence in the predictions of the wt. =1.0 models. This suggests that even though this test's results were not very conclusive, it suggests that keeping the observation weights at their default value of one is better in matching the overall trend of the chlorinated ethenes plume, particularly for the daughter compounds DCE and VC. Naturally, there is more confidence in the measurement of higher concentration then there is in smaller concentration, therefore a more reliable model can be calibrated when the higher concentration values dictate the optimization process; the case of wt. =1.0.

Figures 4.19 through 4.22 show the results of observation weight influence test:

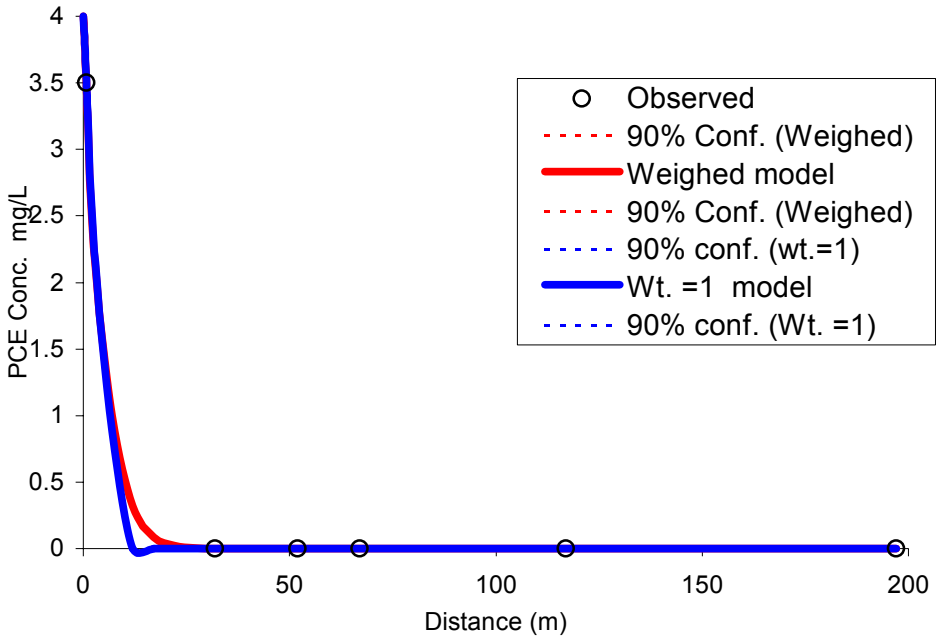

Figure 4.19. PCE plumes generated using the parameters optimized with both weighed observations and observations with a weight of one.

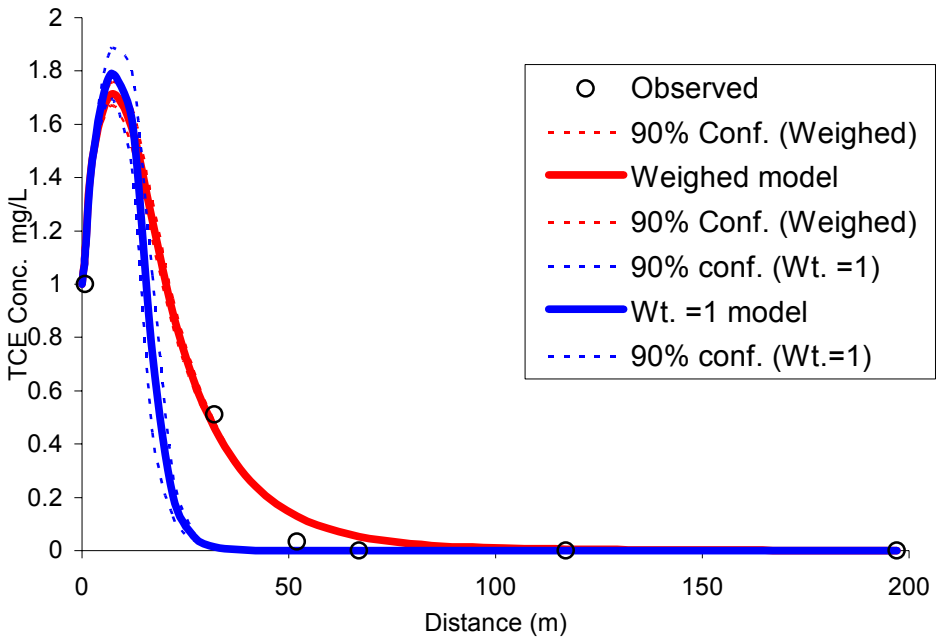

Figure 4.20. TCE plumes generated using the parameters optimized with both weighed observations and observations with a weight of one.

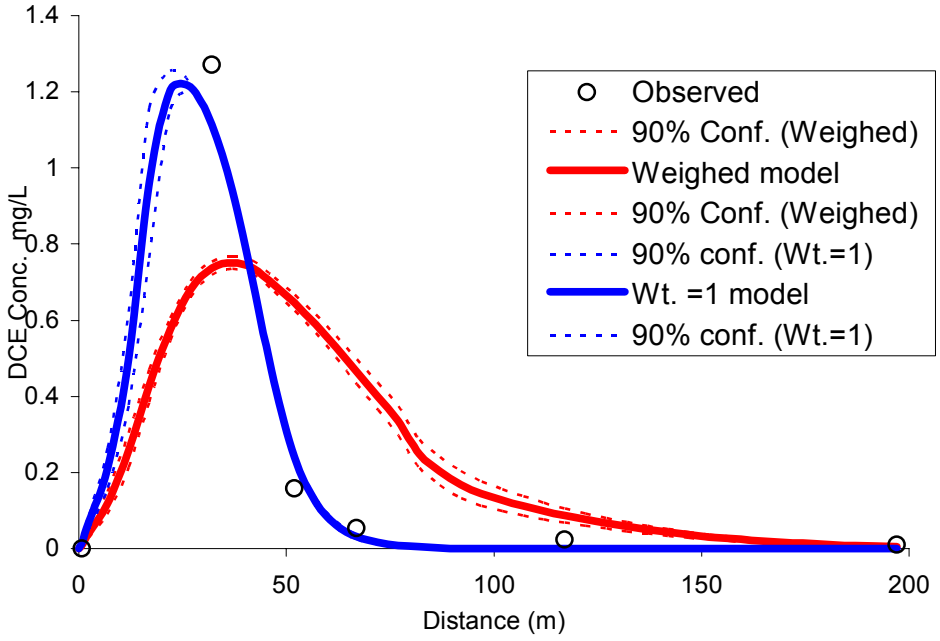

Figure 4.21. DCE plumes generated using the parameters optimized with both weighed observations and observations with a weight of one.

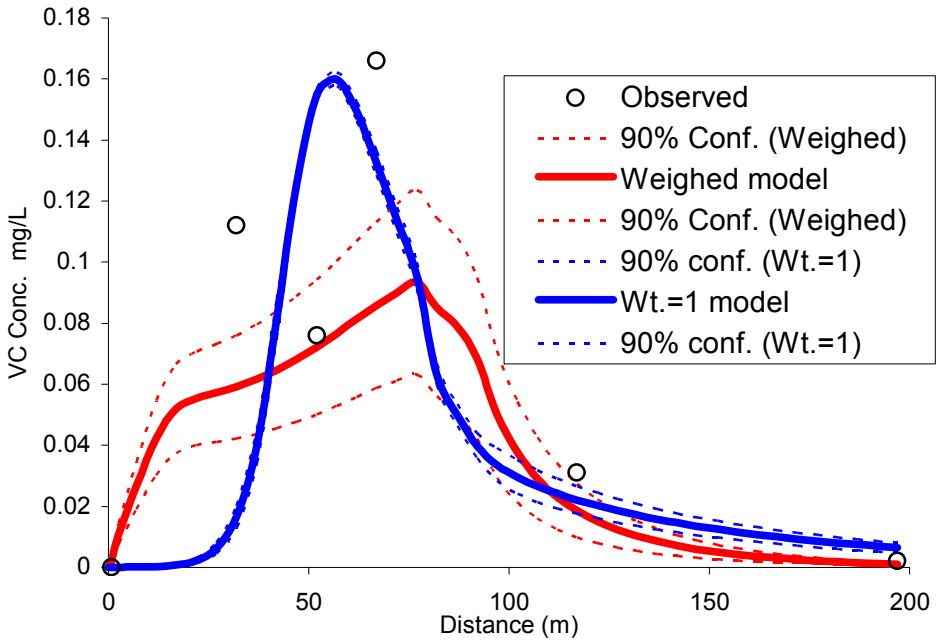

Figure 4.22. VC plumes generated using the parameters optimized with both weighed observations and observations with a weight of one.

4.3.6 Contribution of anaerobic direct oxidation

Overall, this test illustrated the contribution of the anaerobic direct oxidation to the degradation of chlorinated ethenes. As mentioned before, a total of seven model runs were performed each different in the combination of the degradation process. The third run is the one where both direct oxidation and reductive dechlorination are simulated. It is the case that yielded the lowest SSR (best model fit between the observed and simulated data). The other cases where only reductive dechlorination is simulated, or a partial combination of reductive dechlorination and direct oxidation yielded a poor match relative to the full combination of the two, Table 4.7 lists the details of each case and the resulting SSR for both cis-DCE and VC.

Table 4.7. Summary of the results obtained from assessing the contribution of anaerobic oxidation to the degradation of chlorinated ethenes

Case #	Description	DCE SSR	VC SSR
1	Reductive dechlorination (RD) only	0.073	0.024
2	RD in the sulfate zone	0.085	0.023
3	RD and Direct Oxidation (DOx.)	0.032	0.017

4	RD and DOx. in the Fe(III) zone	0.071	0.021
5	RD in the sulfate zone and DOx. in the Fe(III) zone	0.071	0.024
6	RD in the sulfate zone and DOx. in the Fe(III) zone for VC only	0.085	0.023
7	RD in the sulfate zone and DOx for VC only	0.035	0.017

The results suggest the incapability of the reductive dechlorination process alone to fully capture the plume behavior relative to other cases where both reductive dechlorination and direct oxidation are both simulated. It is worth noting that the seventh case performed almost as good as the third case; the seventh case is a sub group of the third case in which reductive dechlorination in the sulfate zone alone is considered and direct oxidation plays a role in degrading VC. The slightly poorer prediction in the DCE case may suggest the need for a contribution of the direct oxidation for degrading DCE as well. The predicted concentrations of PCE and TCE are not affected by the presence or absence of the anaerobic direct oxidation process. Reductive dechlorination is the dominant process of degradation for these two compounds. Figure 4.23 shows the results of this test for the DCE and VC compounds.

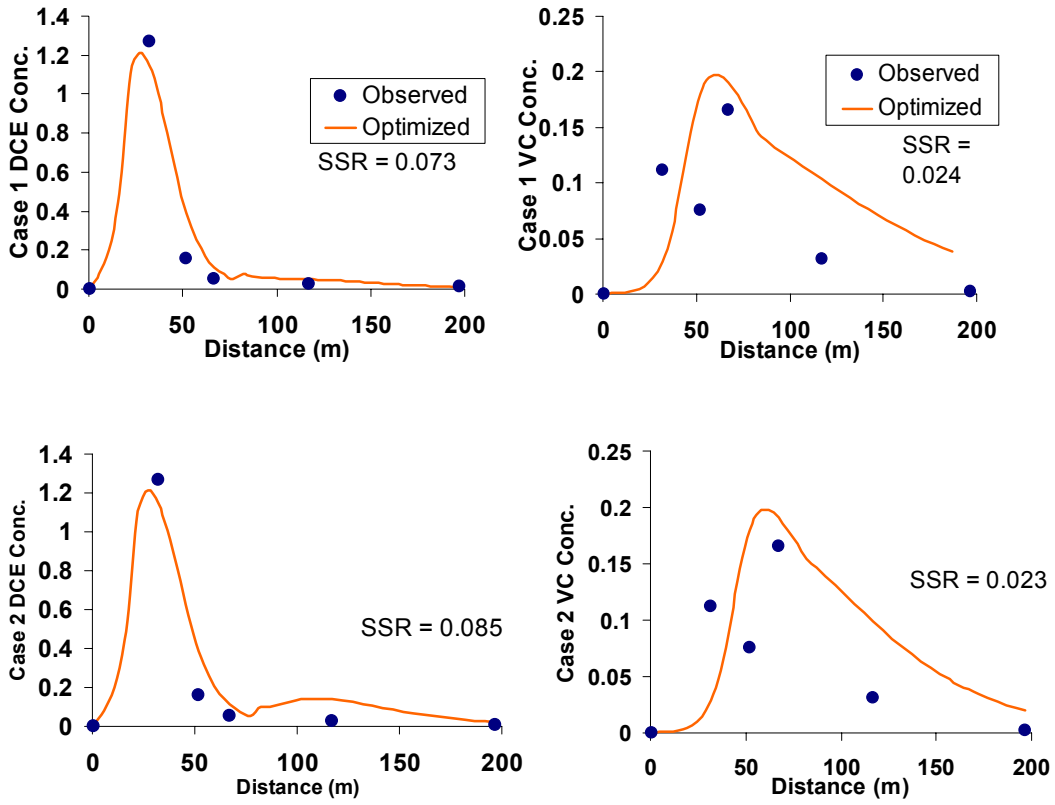

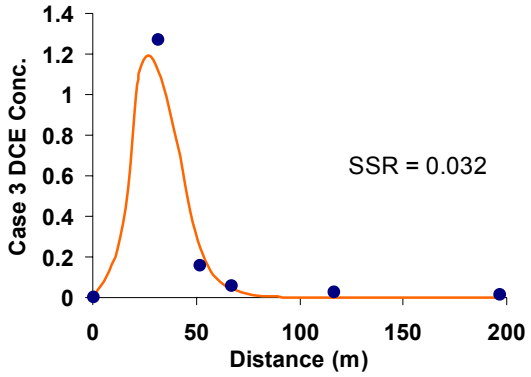
Case 3 DCE Conc.
1.4
1.2
1
0.8
0.6
0.4
0.2
0
0
50
100
150
200
Distance (m)
SSR = 0.032

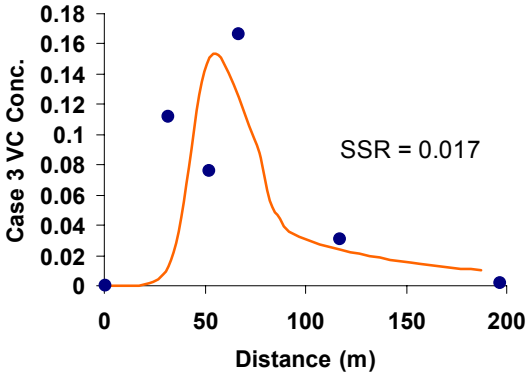
Case 3 VC Conc.
0.18
0.16
0.14
0.12
0.1
0.08
0.06
0.04
0.02
0
0
50
100
150
200
Distance (m)
SSR = 0.017

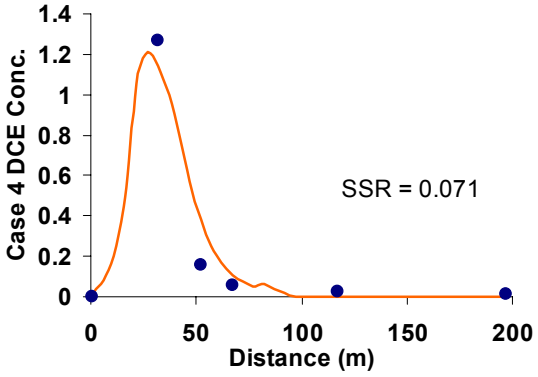
Case 4 DCE Conc.
1.4
1.2
1
0.8
0.6
0.4
0.2
0
0
50
100
150
200
Distance (m)
SSR = 0.071

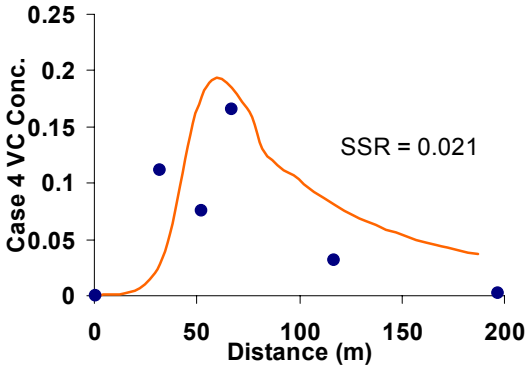
Case 4 VC Conc.
0.25
0.2
0.15
0.1
0.05
0
0
50
100
150
200
Distance (m)
SSR = 0.021

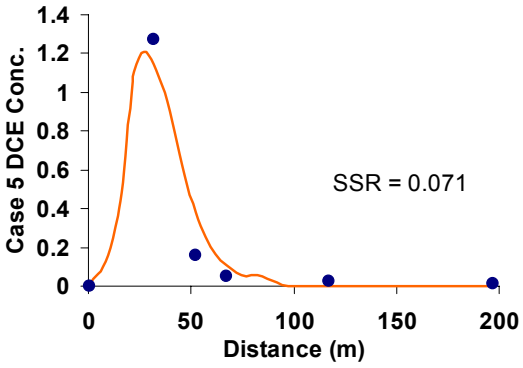
Case 5 DCE Conc.
1.4
1.2
1
0.8
0.6
0.4
0.2
0
0
50
100
150
200
Distance (m)
SSR = 0.071

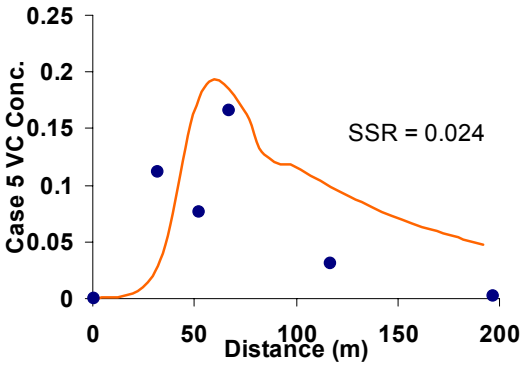
Case 5 VC Conc.
0.25
0.2
0.15
0.1
0.05
0
0
50
100
150
200
Distance (m)
SSR = 0.024

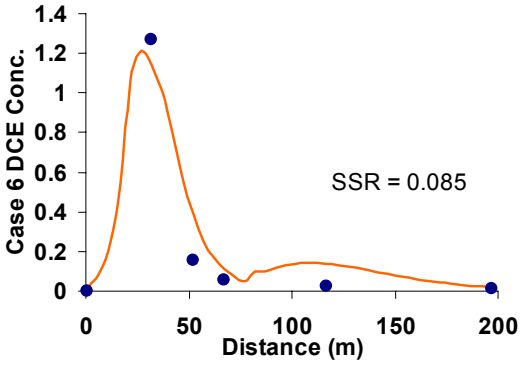
Case 6 DCE Conc.
1.4
1.2
1
0.8
0.6
0.4
0.2
0
0
50
100
150
200
Distance (m)
SSR = 0.085

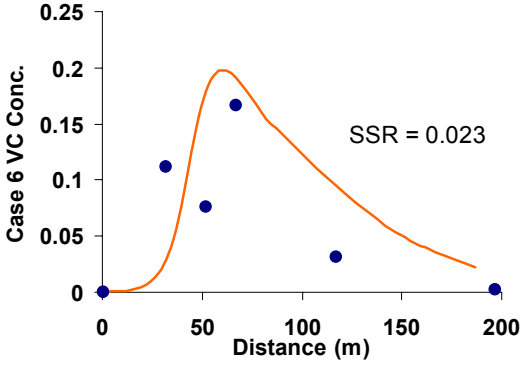
Case 6 VC Conc.
0.25
0.2
0.15
0.1
0.05
0
0
50
100
150
200
Distance (m)
SSR = 0.023

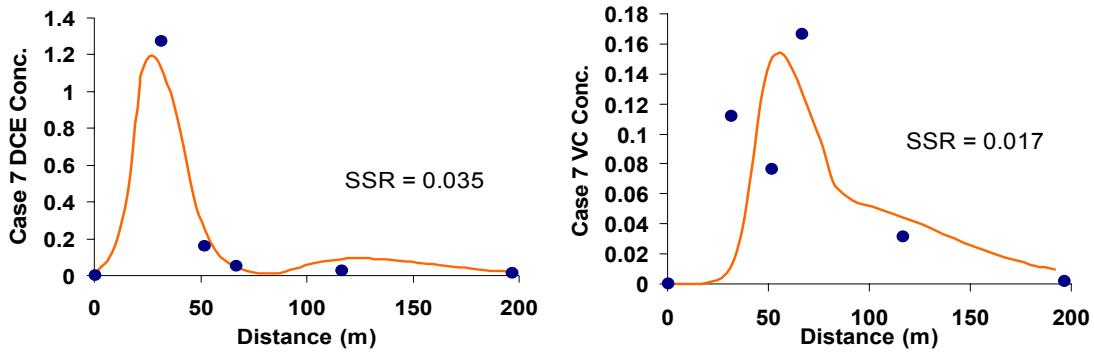

Figure 4.23. DCE and VC plumes resulting form different case studies designed to assess the contribution of anaerobic direct oxidation.

A comparison was made between the cases where the only reductive dechlorination (case 1) and where both reductive dechlorination and direct oxidation are simulated (case 3). This was done to assess the added effect direct oxidation had on the overall degradation process. The two cases were compared to a situation where no biodegradation was simulated; this was done to assess the liquid phase concentration reduction due to the two degradation mechanisms.

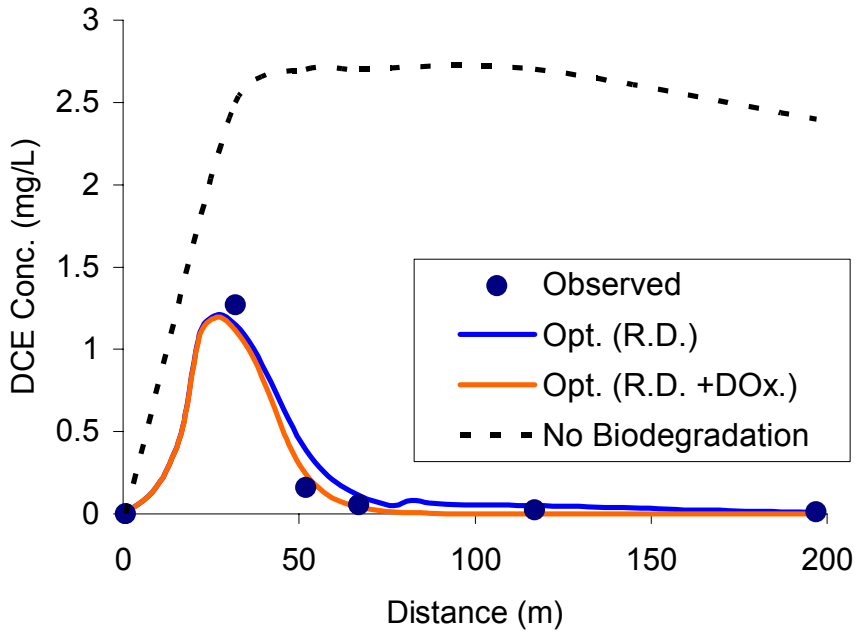

Figure 4.24. DCE concentration profiles in three cases, 1) with R.D. only simulated, 2) with both R.D. and DOx., and 3) when no biodegradation is simulated.

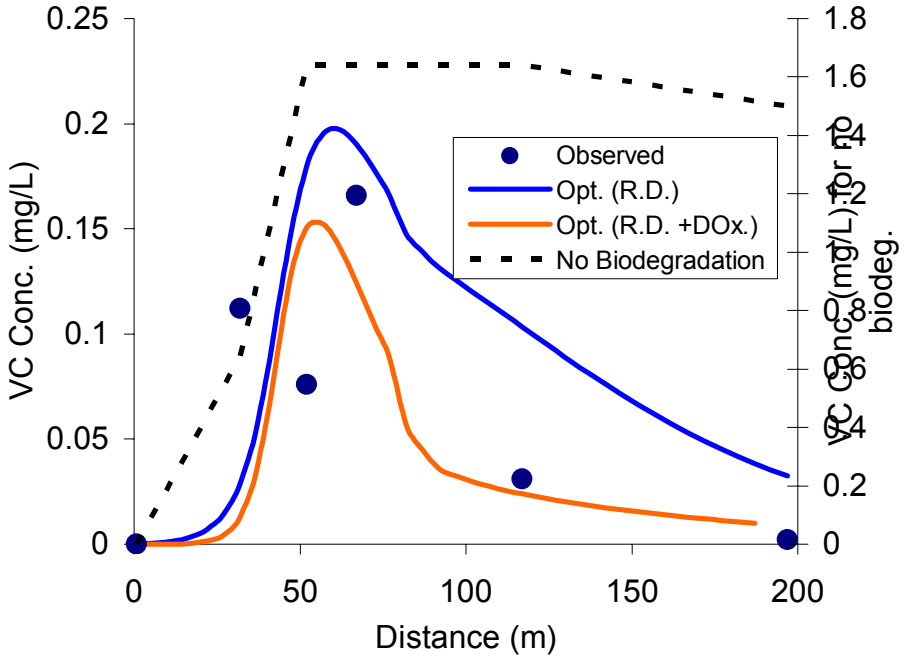

Figure 4.25. VC concentration profiles in three cases, 1) with R.D. only simulated, 2) with both R.D. and DOx., and 3) when no biodegradation is simulated.

Table 4.8 below shows the outcome of the analysis done on the two cases presented in Figures 4.24 and 4.25:

Table 4.8. The SSR and the % reduction due to adding the direct oxidation process, along with the liquid phase concentration removal due to the two degradation process

	R.D.	R.D +DOx.	% Red.
DCE (SSR)	0.073	0.032	56%
VC (SSR)	0.024	0.017	29%
DCE Conc. removal	87%	89%	
VC Conc. removal	93%	95%	

4.3.7 Calibrated Kings Bay model outcome

Figures 4.26 to 4.29 show the calibrated Kings Bay model predictions for the concentrations of the four chlorinated ethenes compounds. The concentration profiles were generated using the model calibrated by applying the proposed methodology for using a non linear parameter estimation technique for estimating the parameters of a reactive multi-solute transport model. Table 4.9 lists the associated SSR values.

Table 4.9. Average SSR for the C.E concentration profiles generated using the calibrated Kings Bay model

Comp.	Average SSR
PCE	0.001
TCE	0.260
DCE	0.079
VC	0.032

The general trend was properly simulated. The modeled rate of degradation of TCE was higher than the observed rate, as evident by Figure 4.27 and the relatively high SSR value. That high rate, however, was essential for capturing the DCE concentration profile in which the second well concentration was measured to be 1.2 mg/L. The calibrated model matched particularly well with the measured concentration for DCE and VC.

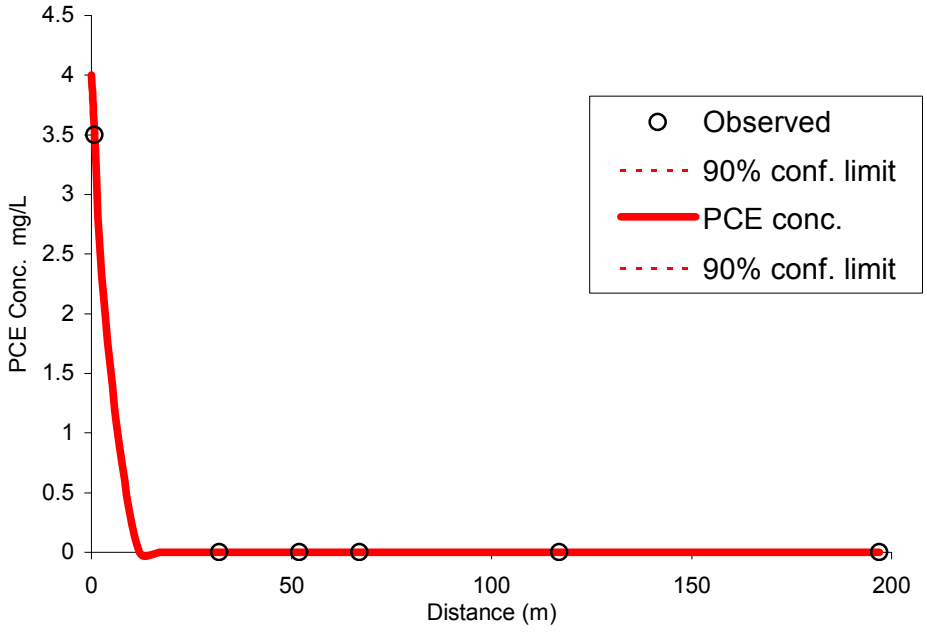

Figure 4.26. Concentration profile yielded from the calibrated PCE model

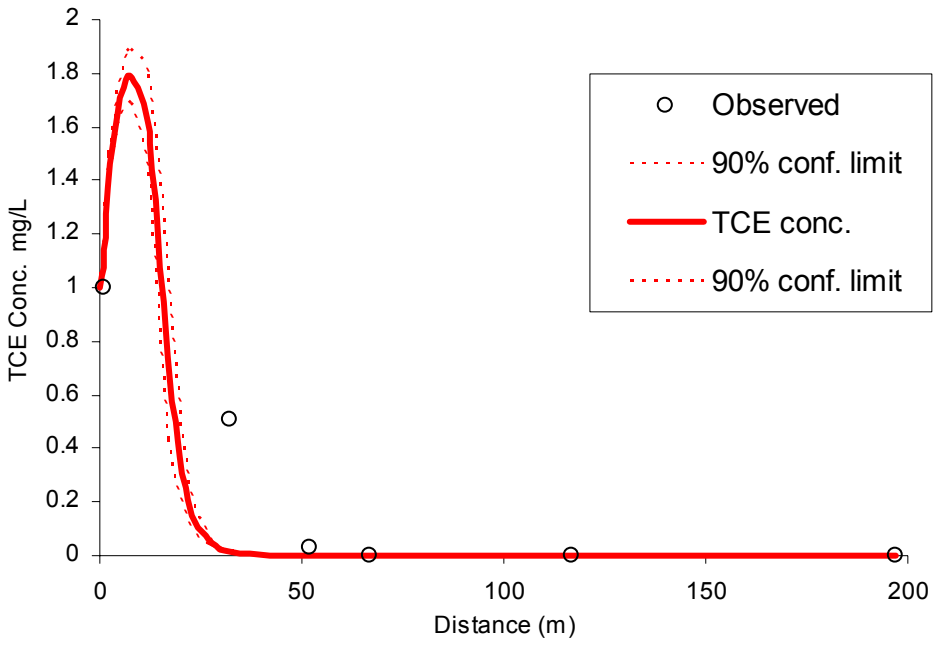

Figure 4.27. Concentration profile yielded from the calibrated TCE model

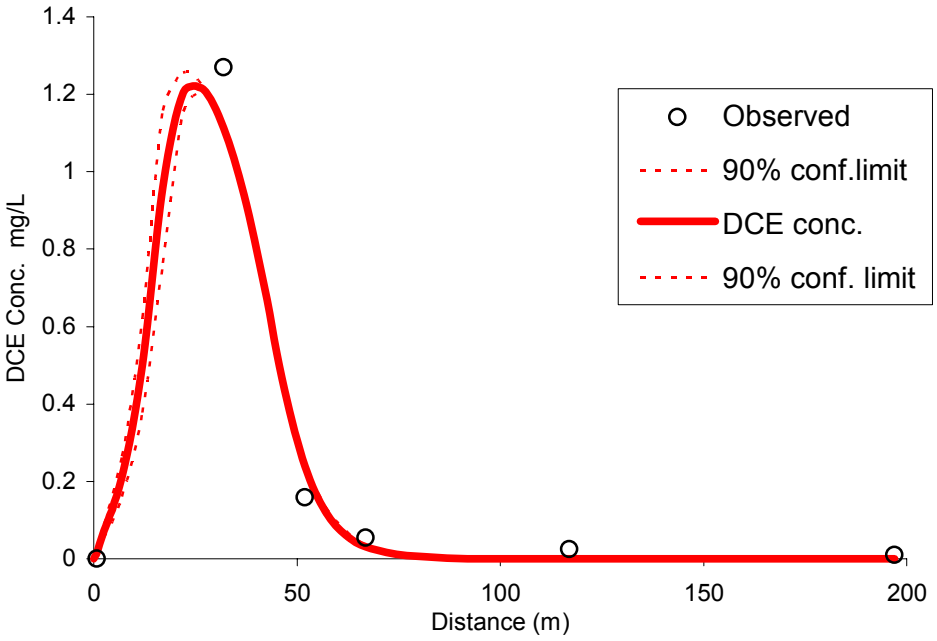

Figure 4.28. Concentration profile yielded from the calibrated DCE model

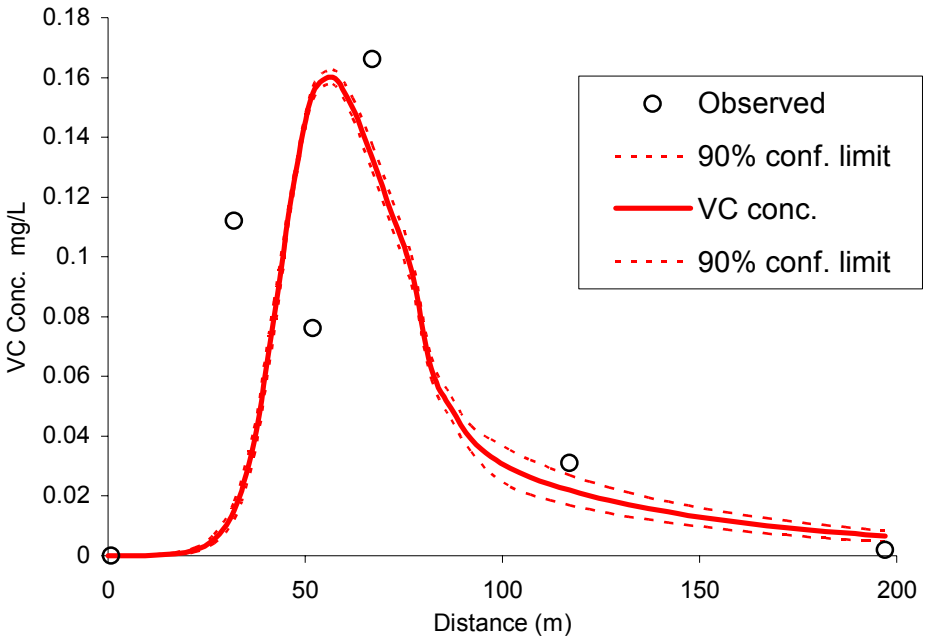

Figure 4.29. Concentration profile yielded from the calibrated VC model

4.4 SUMMARY

The series of tests mentioned before were performed to better design the methodology for undertaking automated parameter estimation for chlorinated ethenes contaminant models. It was observed that a sensitivity analysis study is essential to isolate the most sensitive parameters. This needed to be done once the model was built and all the high confidence parameters (the ones that the modeler has a good idea about their values based on field studies of previous experience) were fed to the model, and the model is ready for the final calibration. The sensitivity analysis study will yield a subgroup of the most influential parameters. This subgroup was found to be more efficient if used in calibrating the model than if all the possible parameters were used. The choice of the weighing mechanism is left the modeler and the specific needs of the project. However, it is recommended to keep the observation weights at values of one. This proved to be a good starting point for calibration, if the optimization outcome is poor, then other weighing mechanisms can be applied.

The optimization for multi-species reactive solute transport models (chlorinated ethenes models for example) was found to be better performed in a sequential manner, taking into account the impact of optimization of a certain compound on it's daughter products concentrations. These guidelines produced the best achievable calibration for the Kings Bay site model.

Chapter 5

Summary and Conclusions

The methodology for model calibration using the automated parameter optimization (inverse modeling) developed in this study was successful in yielding well calibrated groundwater and solute transport models. Several tests were performed to develop and refine the methodology. Some of these tests were inspired from previous research published in the literature while others are unique to the problem investigated in this study. A series of tests were performed initially on a synthetic model setup that was developed to provide a simple testing platform in which observations can be generated as needed. The methodology was then tested on a chlorinated ethenes contaminated site model of single redox conditions (Pensacola site). Then tested even further on anther chlorinated ethenes contaminated site model of multiple redox conditions (Kings Bay site). Multiple tests were performed on the Kings Bay site model to insure statistical significance of the test findings.

The main focus of this research was to develop the methodology for estimating the parameters of multi species reactive solute models. Therefore, one of the tests on the synthetic system involved studying the advantage, if any, for estimating the model parameters sequentially over estimating them simultaneously. The tests performed on the model with chlorinated ethenes being the contaminants of concern showed that sequential optimization of the model parameters has an advantage over the simultaneous optimization. This can be anticipated when looking at the sequential nature of degradation for chlorinated ethenes. A detailed discussion of this test and its results can be found in Chapter 3. Another test performed on the synthetic system was the study of the impact of the kinetic state on the quality of the parameter estimate. It was found that regardless of the site/ model kinetic state, the optimization methodology performed well. A Third test looked at the effect that noisy observations have on the quality of the parameter estimation process. The results showed limited impact noise has on the optimization process, overall, the optimization method performed satisfactorily. The weighting mechanism of the observations was also investigated; the tests showed that the

best optimization outcome was achieved when the weights to the observations were all set to one.

The first chlorinated ethenes contaminated site looked at was in Pensacola, FL. The site has a single redox zone and the numerical model was built accordingly. The findings and recommendations resulting from the testing on the synthetic system were followed upon calibrating and optimizing the parameters of the Pensacola model. The model was calibrated using the inverse modeling technique with observation weights set to one. The parameters were optimized in a sequential manner; starting with the PCE parameters and ending with the VC parameters. The parameters to be optimized were identified from a sensitivity analysis study performed before the actual calibration of the model. The results of the inverse modeling calibration of the Pensacola site model were very encouraging and the model yielded concentration profiles that were more in match with the measured observation than those yielded by the manually calibrated model.

The results and recommendations yielded from the testing on the synthetic system and the single redox zone Pensacola model had to be tested even further. The second chlorinated ethenes contaminated site; the Kings Bay site was modeled. This site has two distinct redox zones, so it was necessary before attempting to calibrate the chlorinated ethenes model to calibrate the anaerobic oxidants components. The model had a sulfate reducing zone at and around the source zone and an Fe(III) reducing zone further down gradient. The parameters of the two compounds were optimized and the model outcome was compared to the observed concentrations. The parameter optimization was done using PEST. Once the redox components were optimized, the chlorinated ethenes model was optimized. A number of tests were performed on this model as well. Those tests were designed to provide statistical evidence for the results and recommendations of the previous tests done on both the synthetic model and the Pensacola site model. Here again, a sensitivity analysis study was performed before attempting the chlorinated ethenes parameter optimization.

The sensitivity coefficients of thirty of the model parameters were calculated. From which a subgroup of 13 parameters were identified as high sensitivity parameters. A test

was performed on this subgroup, it aimed at testing the statistical significance of the hypothesis that optimizing a partial group of the model parameters has an advantage over optimizing the full group of parameters. The results of the tests showed that indeed there is statistical advantage in optimizing the partial group of high sensitivity parameters for two of the 4 compound of chlorinated ethenes, the other two still showed an advantage but not strong enough to be statistically significant. So overall there is confidence in the process of optimizing a partial group of the parameters. Another test performed on the Kings Bay site model was to test the statistical significance of the hypothesis that sequential optimization of the chlorinated ethenes parameters has an advantage over the simultaneous optimization of the parameters of the 4 compounds. The results of the test also showed a significant advantage of the sequential optimization in many of the studied cases. Even in those cases where it wasn't statistically significant, there was still an advantage as evident from the average SSR values. Again there is an overall confidence that the sequential optimization of the model parameters is advantageous to the simultaneous optimization. Another test performed on the Kings Bay site model was to test the statistical significance of the hypothesis that performing optimization while keeping the observation weights at values of one has an advantage over applying weights to the observations. The result of the test showed no decisive statistical evidence that the either mechanism is better than the other. However, looking at the generated concentration profiles and the 90% confidence limits shows that the optimization process with the weights set to a value of one yields better plume profiles than the other weighing mechanism. So the recommendation would be to start the optimization process while setting the weight values to one. If the predicted concentration values were very different than the observed, other weighing mechanisms can be used. The last test performed on the Kings Bay site model was a test of the contribution of the anaerobic direct oxidation process to the overall degradation of the chlorinated ethenes compounds. The calibrated model was run 7 times with 7 different configurations of degradation process. The results of that test showed that the process shown to actually capture the observed behavior of the plume is a combination of both reductive dechlorination and anaerobic direct oxidation. The other cases in general produced poorer match with the observed set of concentration.

All the tests performed earlier helped in developing and refining the methodology for using automated parameter estimation for optimizing the parameters of multi-compound reactive solute transport models. The proposed methodology can be outlined as follows:

1. A conceptual model of the site needs to be developed, based on which a numerical model is built. The parameters of the numerical model are not calibrated at this point and are assigned values based on previous modeling experience or site investigation information.

2. Sensitivity analysis is performed on the model parameter values assigned before. Sensitivity coefficients for all the parameters are calculated using parameters perturbation and the parameters with highest sensitivity coefficients for each compound are isolated.

3. The model has to be calibrated so that oxidation-reduction species are properly simulated; this is done by performing optimization on the parameters of the oxidant / reducer model. It is important to calibrate the model of the strongest oxidant first then the model of the next in line. For example, the model of nitrate (if present) has to be calibrated before the Fe(III) model, and the Fe(III) model has to be calibrated before the sulfate model.

4. The high sensitivity parameters are optimized for the first (parent) compound in the multi-compound reactive solutes (chlorinated ethenes in this study) using the nonlinear optimization method in PEST. This optimization process may be repeated multiple times using different starting parameter values to obtain more confidence in the model predictions. The optimized parameters resulting from the optimization process of the first (parent) compound are updated in the second (daughter) compound's model. In case of multiple optimization runs, the parameters of the run that yields a sum of squared residual (SSR) similar to the average SSR are chosen to be updated in the daughter compound's model. Upon assessing the quality of match between the model predicted and the observed concentrations, the concentration of all the daughter compounds have to be taken into consideration. Therefore the PEST files have to be designed such that the

observations used in calculating the SSR are those of the parent compound as well as those of all it's daughter compounds. During the optimization process, all the observation weights are set to one, and the results of the optimization are monitored. If it was felt that a different set of observation values was necessary, then the optimization can be repeated with the new set of observation weights.

5. The process in 4 above is repeated for all the species. The parameters of each parent species are optimized then updated in the daughter compound's model and so on, until all the parameters for all the species are optimized. The overall match between the observed and optimized concentration profile is assessed using criteria such as the sum of squared residuals and the visual resemblance.

Future Work:

The methodology suggested from this study has to be tested further with as many site models as possible. The more sites this methodology is tested on the more confidence is gained in the methodology and consequently the more refined the methodology gets. This methodology could also be tested on other classes of reactive species such as petroleum hydrocarbons contaminated site. This is important since the biodegradation processes for petroleum hydrocarbons are rather different from those of chlorinated ethenes. So testing it on the petroleum hydrocarbons contaminated sites will investigate the applicability of this methodology to other solutes.

Once there is enough confidence in the methodology, it can be incorporated with the SEAM3D model. This way the optimization algorithm becomes an integral part of the SEAM3D model instead of being an external tool that has to be linked to the model. This will add convenience and ease of use to the process and will make it more accessible to modelers with limited exposure to ptimization techniques. Inverse modeling has been linked to groundwater flow models within the same interface such as the case with MODFLOW and PEST in the Groundwater Modeling System (GMS), but to the author's best knowledge has not been linked within the same interface to a solute transport model. So with the guidelines suggested by this study and the acquired experience after applying

the methodology to other sites, enough experience can be gained to include the optimization process within the SEAM3D interface.

References

Anderman, E.R. and Hill, M.C., 1999. A new multistage groundwater transport inverse method:Presentation, evaluation, and implications. Water resources research, 35(4): 1053-1063.

Bekins, B.A., Warren, E. and Godsy, E.M., 1998. A comparison of zero-order, first-order, and Monod biotransformation models. Ground Water, 36(2): 261-268.

Bennett, G.D. and Zheng, C., 2002. Simulation of non equilibrium processes and reactive transport in Applied contaminant transport modeling, 2nd ed. wiley Intersciences.

Bradley, P.M., 2000. Microbial degradation of chloroethenes in groundwater systems. Hydrogeol, J., 8: 104-111.

Breukelena, B.M., J.G., Roling, W.F.M. and van Verseveld, H.W., 2004. Reactive transport modelling of biogeochemical processes and carbon isotope geochemistry inside a landfill leachate plume. Journal of Contaminant Hydrology, 70: 249– 269.

Chapelle, F.H. and Bradley, P.M., 1998a. Selecting remediation goals by assessing the natural attenuation capacity of groundwater systems Bioremediation Journal 2(3&4): 227-238.

Chapelle, F.H. and Bradley, P.M., 1998b. Selecting remediation goals by assessing the natural attenuation capacity of groundwater systems Bioremediation Journal, 2(3&4): 227-238.

Chapelle, F.H., Brauner, J.S., Widdowson, M.A., Mendez, E. and Casey, C.C., 2003. Methodology for Estimating Times of Remediation Associated with Monitored Natural Attenuation. 03-4057, USGS, Colombia, SC.

Clement, T.P., Sun, Y., Hooker, B.S. and Petersen, J.N., 1998. Modeling multi-species reactive transport in groundwater aquifers. Ground Water Mon. Rem., 18(2): 79-92.

Dai, Z. and Samper, J., 2004. Inverse problem of multicomponent reactive chemical transport in porous media: Formulation and applications. Water resources research, 40.

Doherty, J., 2004. PEST, Model independent parameter estimation user manual, 5th ed. , Watermark Numerical Computing.

EPA, 1998. Technical Protocol for Evaluating Natural Attenuation of Chlorinated Solvents in Groundwater.

EPA, 2000. Cost and performance summary report, in situ chemical oxidation using Fenton's reaget at Naval Submarine Base Kings Bay , Site 11, Camden County, Georgia U.S. Environmental Protection Agency, Office of Solid waste and Emergency response technology innovation office

Essaid, H.I. and et al. , 2003. Inverse modeling of BTEX dissolution and biodegradation at the Bemidji, MN crude-oil spill site. Journal of Contaminant Hydrology, 67: 269-299.

Harrouni, K. E. Ouazar, D., Waiters, G.A. and Cheng, A.H.-D., 1996. Groundwater optimization and parameter estimation by genetic algorithm and dual reciprocity boundary element method. Engineering Analysis with Boundary Element, 18: 287-296.

Hill, M.C., 1998. Methods and guidelines from effective model calibration. USGS Water resources investigations report 98-4005, Denver, Colorado.

Jakeman, A.J., Letcher, R.A. and Norton, J.P., 2006a. Ten iterative steps in development and evaluation of environmental models. Environmental Modelling & Software 21(5): 602-614

Jakeman, A.J., Letcher, R.A. and Norton, J.P., 2006b. Ten iterative steps in development and evaluation of environmental models. Environmental Modelling & Software, 21(5): 602-614

Leijnse, A., Pastoors, M.J.H. and Roelofsen, F.J., 2002. The effect of weighting the observations on parameter estimates in groundwater modeling. In: K. Kovar (Editor), Calibration and reliability in groundwater modelling, a few steps closer to reality. IAHS, Czech republic., pp. 204- 211

Ling, M. and Rafai, H.S., 2003. Assessing Uncertainty in Groundwater Model Predictions at a Chlorinated Solvents Contaminated Site. In: S. Mishra (Editor), Groundwater Quality Modeling an Management Under Uncertainty. ASCE, Philadelphia, PA.

Maymo-Gatell, X., Tandoi, V., Gossett, J.M. and Zinder, S.H., 1997. Isolation of bacterium the reductively dechlorinates tetrachloroethene to ethene. Science, 276(1568-1571).

Mugunthan, P., Shoemaker, C.A. and Regis, R.G., 2005. Comparison of function approximation, heuristic, and derivative-based methods for automatic calibration of computationally expensive groundwater bioremediation models. Water resources research, 41.

Poeter, E., 2006. 2006 Darcy Lecture: All Models Are Wrong: How Do We Know Which Are Useful?, pp. http://www.mines.edu/~epoeter/DarcyLecture2006/index.shtml.

Poeter, E. and Anderson, D., 2005. Multimodel Ranking and Inference in Ground Water Modeling. Ground water, 43(4): 597–605.

Poeter, E.P. and Hill, M.C., 1997. Inverse models : A necessary next step in ground-water modeling. Ground water, 35(2): 250 - 260.

Reed, P., Minsker, B., and Valocchi, A.J., 2000. Cost-effective long-term groundwater monitoring design using a genetic algorithm and global mass interpolation. Water resources research, 36(12): 3731-3741.

Ritzel, B.J., Ehart, J.W. and Ranjithan, S., 1994. Using genetic algorithms to solve a multiple objective groundwater pollution containment problem Water resources research, 30(5): 1589-1603.

Sciortino, A., Harmon, T.C. and Yeh, W.W.G., 2000. Inverse modeling for locating dense nonaqueous pools in groundwater under steady flow conditions. Water resources research, 35: 1723–1735.

Suarez, M.P. and Rifai , H.S., 1999. Biodegradation rates for fuel hydrocarbons and chlorinated solvents in groundwater. Bioremediation Journal, 3(4): 337-362.

Sun, Y., Petersen, J.N., Clement, T.P. and Skeen, R.S., 1999. Development of analytical solutions for multispecies transport with serial and parallel reactions. Water Resour. Res., 35(1): 185-190.

Suna, Y., Petersen, J.N. and Bearc, J., 2001a. Successive identification of biodegradation rates for multiple sequentially reactive contaminants in groundwater. Journal of Contaminant Hydrology, 51: 83-95.

Suna, Y., Petersen, J.N. and Bearc, J., 2001b. Successive identification of biodegradation rates for multiple sequentially reactive contaminants in groundwater. Journal of Contaminant Hydrology 51: 83-95.

Tebes-Stevens, C.L., Espinoza, F. and Valocchi, A.J., 2001. Evaluating the sensitivity of a subsurface multicomponent reactive transport model with respect to transport and reaction parameters. Journal of Contaminant Hydrology, 52: 3-27.

Tebes-Stevens, C.L. and Valocchil, A.J., 2000a. Calculation of reaction parameter sensitivity coefficients in multicomponent subsurface transport models. Advances in Water Resources, 23 (2000): 591 - 611.

Tebes-Stevens, C.L. and Valocchil, A.J., 2000b. Calculation of reaction parameter sensitivity coefficients in multicomponent subsurface transport models. Advances in Water Resources, 23 591 - 611.

Widdowson, M.A., 2004. Modeling natural attenuation of chlorinated ethenes under spatially varying redox conditions. Biodegradation Journal, 15: 435-451.

Widdowson, M.A. and Waddill, D.W., 1998. Modeling intrinsic bioremediation of chlorinated solvents in groundwater. Battelle Press, Columbus, OH, 225-236 pp.

Widdowson, M.A. and Waddill, D.W., 2000. SEAM3D: A Numerical Model for Three-Dimensional Solute Transport and Sequential Electron Acceptor-Based Biodegradation in Groundwater, U.S. Army Engineer Research and Development Center Technical Report ERDC/EL TR-00-X.

Willis, M.B. and Shoemaker, C.A., 2000. Engineered PCE dechlorination incorporating competitive biokinetics: Optimization and transport modeling. Battelle Press, Columbus, OH, 1311-1318 pp.

Wu, J., Zheng, C., Chien, C.C. and Zheng, L., 2006. A comparative study of Monte Carlo simple genetic algorithm and noisy genetic algorithm for cost-effective sampling network design under uncertainty. Advances in Water Resources, 29(2006): 899–911.

Yager, R.M., 2000. Simulated Transport and Biodegradation of Chlorinated Ethenes in a Fractured dolomite Aquifer near Niagara Falls, New York. Water-Resources Investigations Report 00-4275, USGS.

Yeh, W.W.G., 1986. Review of parameter identification proceedures in groundwater hydrology: the inverse problem. Water resources research 22: 95-108.

Zheng, C. and Bennett, G.D., 2002. A framework for model applications in Applied contaminant transport modeling, 2nd ed. wiley Intersciences.

Appendices

Appendix A: DETAILED DISCUSSION OF THE MATHEMATICS OF INVERSE MODELING

Mathematical models in general can be classified into linear and non-linear models. Linear models are those in which the processes are presented using a set of linear Equations of the form:

$$a\vec{X} = \vec{b} \tag{A.1}$$

with *a* representing an *m x n* matrix of variables (*m* rows and *n* columns), *m* is the number of observations and *n* is the number of parameters, $\vec{X}$ being a vector of order *n* which holds the system parameters; and $\vec{b}$ being a vector of size *m* representing the system response to a set of excitations in the matrix a.

The idea of inverse modeling is to find a set of parameters (components of *X*) that would yield specific values of model outcomes that match the observed or measured values. Therefore, a term Φ (Objective function) is introduced. It is the sum of squared deviations between model-generated outcome and experimental observations or measurements. The smaller the objective function values are, the better the match is between the model output and observations. The objective function can be represented mathematically as follows:

$$\Phi = (b - aX)^T Q(b - aX) \tag{A.2}$$

where T indicates the transpose of the matrix, *Q* is a square diagonal matrix whose ith diagonal element is the square of the weight attached to the ith observation. This weight factor is introduced to account for the difference in orders of magnitude between the various parameters due to unit differences. The elements of *X* vector that minimize Φ can be shown to be:

$$X = (a^T a)^{-1} a^T Qb \tag{A.3}$$

the formula above assures a unique solution to the parameter estimation problem provided that the number of observations *m* equals or exceeds the number of parameters *n*.

In non-linear systems, which most of the environmental systems are, the situation is rather different. The relation between the parameters and the observations controlled by a certain non-linear function *M* in the following form:

$$M(X) = b \tag{A.4}$$

Assuming that an initial set of parameters X_o is fed to the system, the resulting outcome is:

$$M(X_o) = b_o \tag{A.5}$$

If we change the parameter values to *X,* the resulting change in the response *b* could be presented according to Taylor's theorem in the following linear form:

$$b = b_0 + J(X - X_0) \tag{A.6}$$

where *J* is the Jacobian matrix, which is a diagonal matrix in which each diagonal element represents the change in the response values relative to change in one of the parameters. The calculation of the Jacobian matrix is one of the key steps in nonlinear inverse modeling (Dai and Samper 2004). There are three approaches for computing its components (sensitivity coefficients): finite difference, sensitivity Equation, and adjoint state. The finite difference approach is the most practical now that the numerical models complexity has increased dramatically. The above formula makes the task of inverse modeling much easier since it approximates that nonlinear system with a linear one. Therefore, tools similar to the linear system tools for inverse modeling could be used to calculate the parameter values in a non-linear system. The weighted objective function in this case takes the following form:

$$\Phi = \left(b - b_o - J\left(X - X_o\right)\right)^T Q\left(b - b_o - J(X - X_o\right) \tag{A.7}$$

The idea with non-linear system parameter estimation is to keep adjusting the set of parameters and testing the resulting objective function. This can be achieved by

introducing a parameter upgrade vector that gives a set of new parameter values based on the sensitivity of the model outcome to the parameter values. Once these new values are obtained, the model is run once again, and the objective function is calculated. This process is repeated until one of pre-specified stopping criteria of the objective function is achieved. The parameter upgrade vector in non-linear systems is presented by:

$$u = (J^T Q J)^{-1} J^T Q (b - b_o) \tag{A.8}$$

For better numerical performance, the above formula can be adjusted by introducing a parameter named the Marquardt parameter and a scaling matrix. The Marquardt parameter (α) helps in preventing a phenomenon called "hemstitching" in which the parameter set jumps from one side of a valley of minimum Φ to another without actually reaching a minimum. The scaling matrix (*S*) is a diagonal matrix that takes care of the vast difference in the magnitudes of the components of the Jacobian matrix due to difference in the types of the parameters. This magnitude difference introduces great round off errors in the parameter upgrade vector. The scaling matrix is a function of the Jacobian matrix (*J*) and the (*Q*) matrix discussed earlier. The final form of the parameter upgrade vector after adjusting for the two previous factors, which is equivalent but far numerically superior to the previous form is:

$$S^{-1}u = \left((JS)^T QJS + \alpha S^T S\right)^{-1} (JS)^T Q(b - b_o) \tag{A.9}$$

where the elements of the diagonal scaling matrix take the form:

$$S_{ii} = \left(J^T Q J\right)_{ii}^{-1/2} \tag{A.10}$$

where the largest element of the term $\alpha S^T S$ is denoted as (λ) the "Marquardt Lambda".

The calculation of the derivatives (the components of the Jacobian matrix) is the most time consuming step in the optimization process. Finite difference techniques are the typically used to approximate the actual values of the derivatives. Forward difference techniques in which the value of the model outcome is calculated as a response to a fine increase in one of the model parameters, the ratio of the model response change to change in the parameter value represents an approximation of the derivative called forward difference.

Another technique that can be used is the central difference in which a decrease in the parameter value is made. The model response is recorded, then an increase in the parameter value is made and the response value is recorded. This method uses three points instead of two, it adds accuracy to the derivative approximation but increases the computational demand since three model runs are required instead of two. In complex numerical models (which most of the environmental and groundwater models are), however, the accuracy of estimate has precedence over computational times since round off errors could easily be carried over from one calculation iteration to another, therefore the use of central difference as well as high number of significant figures is a must for accurate optimization outcome. Figure A.1 summarizes the process of SEAM3D parameter optimization using PEST:

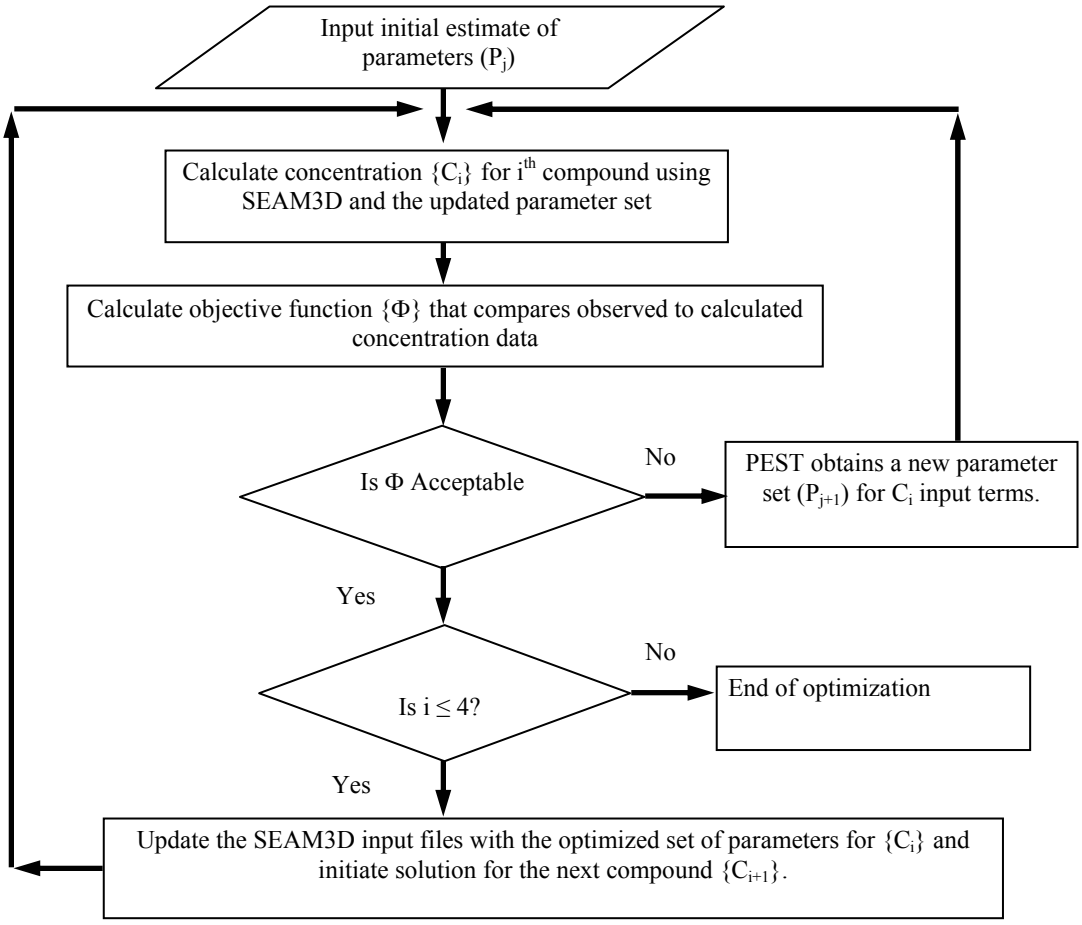

Figure A.1. Optimization process of the SEAM3D parameters using PEST

Appendix B: CHLORINATED ETHENES BIODEGRADAION PROCESSES

Chlorinated ethenes are the category of contaminants used in this research as a case study of multi-component reactive solute transport in the subsurface. Both PCE and TCE are cited as two of the most frequently detected contaminants in groundwater systems. The use of these compounds is wide spread because of their characteristics as solvents especially in industrial degreasing and in the dry cleaning industry. Many contaminated sites have been identified due to accidental spills or due to improper discharge of the solvents in the ground. A very important component in natural attenuation of the chlorinated ethenes is the biodegradation process. Depending on the environmental conditions, microorganisms can transform chlorinated ethenes into environmentally innocuous compounds such as carbon dioxide, ethene and chloride (Chapelle et al. 2003).

In chlorinated ethenes, four biodegradation processes have been identified as mechanisms of biodegradation; reductive dechlorination, aerobic oxidation, anaerobic oxidation, and aerobic cometabolism (Chapelle 2001). Reductive dechlorination is thought to be the dominant process for attenuating chlorinated ethenes in anaerobic groundwater systems, but there is considerable controversy on the role of anaerobic direct oxidation. The availability of certain electron acceptors is what triggers the strength of a certain process over the others. Therefore, one of the most challenging tasks in modeling chlorinated ethenes is determining which of the above process are the most prevailing. Three biodegradation processes relevant to monitored natural attenuation of chlorinated ethenes (reductive dechlorination, aerobic oxidation and anaerobic oxidation) are discussed below:

Reductive dechlorination

Due to the oxidized nature of the chlorinated ethenes, these compounds can act as electron acceptors in the presence of a suitable electron donor and catalyst. Studies in the early nineties showed that certain types of microorganisms were capable of using the chlorinated ethenes as terminal electron acceptors. The process of replacing the chlorine

ion with a hydrogen ion is what is called reductive dechlorination. When the parent compound is PCE, it is degraded to yield TCE, which then degrades primarily to cis-dichloroethene (cis-DCE). Under strongly-reducing conditions, cis-DCE degrades to VC, which then degrades to ethene.

It was observed that the tendency for a chlorinated ethene to undergo reductive dechlorination decreases as the number of chlorine ions decreases (Chapelle et al. 2004). PCE with four chlorine ions readily undergoes reductive dechlorination except in aerobic aquifers. On the other hand the reduction from TCE to cis-DCE requires at least Fe (III) conditions. The reduction of cis-DCE to VC requires at least sulfate (SO_4) reducing conditions, but proceeds more readily in methanogenic environment. Due to this behavior, the reductive dechlorination of the chlorinated ethenes is often incomplete and yields accumulation of cis-DCE and VC.

Reductive dechlorination is driven by molecular hydrogen (H_2), and the efficiency of the degradation process is directly related to the availability of H_2. The strength of the reducing conditions (CO_2>SO_4>Fe (III)>NO_3) is due to the abundance of the H_2 molecule in the environment (Chapelle 2001).

Aerobic oxidation

In a manner opposite to the situation in reductive dechlorination, as the tendency to undergo reductive dechlorination decreases, the tendency to undergo aerobic oxidation increases, resulting in a strong tendency for VC to serve as an electron donor. Many studies have shown that VC can be used as a primary substrate for microbial oxidation under aerobic conditions. Studies have concluded that the effect of aerobic oxidation is often limited to the edges of the contaminant plume where the oxygen reserve was not depleted completely by the microbial population (Chapelle 2001).

Anaerobic oxidation

It was discovered back in 1996 that microorganisms can oxidize VC to CO_2 under anaerobic conditions if sufficiently strong oxidant is available to drive microbial

degradation (Chapelle 2001). Fe (III) oxides are known to be strong oxidants. The efficiency of biodegradation changes according to the present terminal electron acceptor. Oxygen typically is the most thermodynamically favored. Among the rest of electron acceptors, the oxidation potential decreases in the order of energy yield, starting with nitrate, NO_3 > Fe (III) > Sulfate > CO_2 (Methanogenic) (Chapelle et al. 2004). The importance of anaerobic oxidation is that it, along with reductive dechlorination, provides a path which guarantees complete degradation of chlorinated ethenes; where the later process would degrade PCE and TCE and the former is responsible of cis-DCE and VC mineralization to CO_2 (Chapelle et al. 2004).

Redox conditions play a major role in identifying the chloroethenes path of degradation. For example, the dechlorination of PCE and TCE to DCE occurs under mildly reducing conditions such as NO_3 or Fe (III). Whereas transformation from cis-DCE to VC needs more strong reducing conditions such as methanogenesis or SO_4.

Appendix C: SENSITIVITY AND UNCERTAINITY ANALYSES

Sensitivity analysis is an integral component of the model calibration process. Identifying the most sensitive model parameters and assessing the confidence a modeler has in the parameters values will give indications about model output uncertainty. (Zheng and Bennett 2002) identified sensitivity analysis as one of three methods quantifying uncertainty in a model output. Two of the methods are deterministic, which are sensitivity analysis and first order analysis, while the third is probabilistic which is the Monte Carlo method. Below is a brief discussion of each of these methods:

Sensitivity analysis

This can be defined as a study of the effect of changing one parameter on the model outcome. So the sensitivity of a model dependent variable to a model input parameter is the partial derivative of the dependent variable with respect to that parameter (Zheng and Bennett 2002).

$$X_{i,k} = \frac{\partial \hat{y}_i}{\partial a_k} \tag{C.1}$$

where $X_{i,k}$ is the sensitivity coefficient of the model dependent variable $\hat{y}$ with respect to the k^{th} parameter a_k at the i^{th} observation point.

There are many forms of the sensitivity coefficient; some of which have the units of the dependent variable (the parameter term is normalized). Others are completely unitless (both the dependent variable and parameter terms are normalized). A third form links the objective functions change (change in how near the model predictions are to the actual measured or observed values) to a change in the parameter value. The partial derivative term in the formula above can be approximated using a difference term.

The form of the sensitivity coefficient where that has the units of dependent variables in solute transport applications (concentrations) with the partial derivatives approximated by differences is as follows:

$$X_{i,k} = \frac{C_{i,k\,new} - C_{i,k\,old}}{\left(\frac{k_{new} - k_{old}}{k_{old}} \right)} \qquad \text{(C.2)}$$

in which $C_{i,k\,new}$ is the new concentration at location i after changing the parameter value to k_{new}. $C_{i,k\,old}$ is the concentration at location i resulting from the initial (old) parameter value $k_{old.}$

To perform a sensitivity analysis, a simulation is run with the best available values of the parameters. During the consequent runs one of the parameters is varied from the base value by a certain percentage while the others are kept constant. The process is repeated until all the parameters are perturbed. The result of each of the runs is compared to that of base value and the sensitivity coefficient is calculated. The larger the sensitivity coefficient is, the larger the effect of that parameter on the overall model output. Therefore the sensitivity coefficient serves as an indicator of the contribution of uncertainty of one model parameter the uncertainty in the calculated results.

The advantage of the sensitivity analysis is in its simplicity. It can be calculated simply by conducting multiple model runs. One of the disadvantages, on the other hand, is that it assumes the parameters to be completely uncorrelated. In reality this is hardly ever true; many of the parameters are either physically or mathematically correlated. Another problem in using sensitivity coefficient is that it assumes linear relation between parameters and the model output. Therefore, the sensitivity coefficient value is a function of the initially selected parameter values and change percentages. The third drawback is that it is a deterministic measure that does not take into consideration the probabilistic nature of the parameters. Despite these problems, sensitivity analysis is still considered extremely practical and powerful tool for rapid assessment of the model sensitivity (Zheng and Bennett 2002).

First order analysis

This method studies the propagation of uncertainty from the input parameters to the model outcome. It is based on the Taylor series expansion with all the terms higher than the first order term neglected, yielding the format:

$$y - y^0 \approx \sum_{i=1}^{n} (x_i - x_i^{\,0}) \left[\frac{\partial y}{\partial x_i} \right]_{x^0} \tag{C.3}$$

where y is the model outcome, y^0 is the average model outcome when all the parameters are average, n is the number of parameters, x_i is parameter i, x_i^0 is the average value of the parameter. Therefore it can be shown that the uncertainty in model outcome as characterized by its variance can be approximated by the sum of the variances of the input variables multiplied by their respective sensitivity coefficients, as presented in the formula:

$$Var[y] = \sum_{i=1}^{n} Var[x_i] \left[\frac{\partial y}{\partial x_i} \right]_{x^0} \tag{C.4}$$

The drawback of this method is that it is approximate; the higher order terms in the Taylor expiation can only be canceled when the coefficients of variation of model input parameters are small, therefore the use of this method is limited.

Monte-Carlo method

This may be by far the most commonly used method for uncertainty analysis associated with complex numerical methods (Zheng and Bennett 2002). The method considers each model input parameter x_i as a random variable defined by a probability density function (pdf) or cumulative density function (cdf). A large number of input parameter values are generated using a computer random number generator according to the parameter distribution curve. The process is repeated for every parameter and multiple model runs with a random mix of all the parameters are conducted. The outcome of all the runs is presented in the form of a histogram, from which the probability of the model outcome being larger (or smaller) than a specified value can easily be obtained.

This method has the advantages of the conceptual simplicity, general applicability and ability to accurately quantify the uncertainty in the model output. On the other hand the obvious difficulty in using the method is in identifying the distributions for various parameters, since choosing the right distribution is crucial to the accuracy of the parameter estimate. A second disadvantage is the extensive computational demand of this method where a typical study may need hundreds if not thousands of runs to have statistically meaningful outcome.

Appendix D: STATISTICAL TESTING CALCULATION SAMPLE

The research presented in chapter four; the Kings Bay site model, was designed taking the statistical testing into consideration. In order to produce data sufficient for statistical testing the optimization had to be performed multiple times (9 times in most tests) with different starting parameter values The starting parameter value groups were made different by multiplying the components of the base set by a series of randomly generated numbers between 0 and 2. The resulting concentration profile from each optimization run was exported to an Excel spreadsheet, and the sum of squared residual (SSR) was calculated by comparing the model predictions to the measured observations. This process was repeated 9 times for the outcome of each optimization run. The nine generated SSR values were grouped together and compared against another group of nine SSR values generated from the optimization runs of another method.

An example to this can be seen in the test performed to investigate the effect of optimizing all the model parameters as apposed to optimizing a selected group. The optimization was run 9 times for the first case where all the model parameters and the SSR values for all of those were calculated. Then the optimization was performed 9 times for the second case where only a subgroup of the model parameters was optimized, and the SSR for all was calculated. So with these two groups of 9 SSR values each the hypothesis of no difference in the means of each of the two SSR groups can be tested. The normality of the SSR was tested first using a normal probability plot then the hypothesis was tested using a two sample t-test assuming unequal variances. The statistical software MINITAB was used for checking the normality of the SSR values and plotting the normal probability plot. The data analysis tool pack in Excel was used for performing the two sample t-test. In addition to that, 90% confidence intervals were calculated around the average concentration profile for every case, the 90% confidence intervals were calculated for each concentration point (42 points composed the concentration profile representing almost 210 meters in the field).

The upper and lower limits of the 90% confidence intervals can be calculated using the following formula

$$\left(\overline{X} - 1.645 \times \frac{\sigma}{\sqrt{n}}, \overline{X} + 1.645 \times \frac{\sigma}{\sqrt{n}} \right) \tag{D.1}$$

where $\overline{X}$ is the average value of the concentrations at a certain location, σ is the sample standard deviation, n is the number of values in the sample. The formula above was entered into a spread sheet and a confidence limit around each of the concentration values was calculated. A sample calculation for the PCE two sample t-test for the test mentioned before is presented below:

The sum of squares residuals (SSR) generated from the 9 optimization runs for each of the two cases; full parameter optimization and partial parameter optimization along with some statistics are shown in Table D.1 below

Table D.1. SSR for the full vs. partial parameter estimation test.

SSR		
Full	Partial	
0.337	0.150	
0.035	0.179	
0.001	0.196	
0.744	0.080	
0.004	0.130	
0.375	0.109	
0.328	0.127	
0.589	0.362	
0.299	0.162	
0.301	0.166	Average
0.067	0.007	Variance
9	9	Observations

The degrees of freedom for the two samples can be calculated using the formula

$$v = \frac{\left(\frac{s_1^2}{m} + \frac{s_2^2}{n} \right)^2}{\frac{\left(s_1^2 / m \right)^2}{m-1} + \frac{\left(s_2^2 / n \right)^2}{n-1}} \tag{D.2}$$

where s_1 and s_2 represent the standard deviations of the first and second samples respectively, m and n are the numbers of the first and second samples respectively, plugging in our numbers yield degrees of freedom of 9.

At a 90% confidence level, the t-statistic can be calculated according to the following formula:

$$t = \frac{\bar{x} - \bar{y} - \Delta_o}{\sqrt{\frac{s_1^2}{m} + \frac{s_2^2}{n}}} \tag{D.3}$$

where Δ_o is the hypothesized mean difference = 0 in our case. This value depends on the alternative hypothesis; in our case the null hypothesis was that of no difference in the means, therefore, the alternative hypothesis was that the mean of the full parameter optimization model is larger than the partial parameter optimization model (one tailed test). Plugging in our numbers yield a value for the t-statistic of 1.49.

This t-statistic value is compared to a t-critical value. If the t-statistic is larger (more extreme) then there is enough evidence to reject the null hypothesis, i.e. the full parameter optimization model is statistically different from the partial. The t-critical can be obtained from the t curve tail areas tables that can be found in any standard statistics book. For a 90% confidence level and 9 degrees of freedom the value of the t-critical is 1.383. Since the t-statistic is larger than the t-critical, the null hypothesis can be rejected. Therefore, the SSR resulting from the method where all the possible parameters are optimized (full parameter model), is significantly higher that the SSR resulting from the method were only a subgroup of the parameters are used in the optimization process. This means that the partial parameter method is better in producing a calibrated model than the full parameter method (lower overall SSR)

This statistical testing procedure is repeated for all the tests in the 4th chapter and the results are summarized in the results and discussion section.

Appendix E: DISCUSSION OF THE PEST SOFTWARE

Parameter estimation software (PEST) is a number of executable files that use the Levenberg- Marquardt algorithm. It is a derivative based optimization algorithm for optimizing a set of parameters. In addition to the executables, multiple input files need to be prepared for PEST to perform parameter optimization. These include the PEST control file, the PEST instruction file and the PEST template file. These input files can be written using a regular text editor and saved with special extensions that are described in the PEST manual. The PEST control file contains all the information needed for running the Levenberg- Marquardt algorithm and for running PEST. These parameters include but not limited to the number of parameters, number of observations, Marquardt lambda, the optimization stopping criteria, a list of the names of all the files needed by PEST to perform the optimization process, the name of the executable for the model to be optimized, and many other necessary parameters. The detailed description of the components of any of the PEST files can be found in the PEST manual (Doherty, 2004). The other type of files needed by PEST is the instruction files. Those give PEST the information as to where to search in the model output files (SEAM3D in our case) for the model output data (concentrations). This file includes the line number and the location within the line in which the necessary output information can be found. The third type is the PEST template file; this gives PEST a template for writing the model input files after calculating a new set of parameters. Template files are composed of the model original input files with the parameter location identified by a certain symbol so that PEST could overwrite the original model input file with a new one after updating the parameter values. This new input file is used instead of the old one and the model is rerun again. The process is repeated until the optimal set of parameters is found.

The PEST necessary executables and input files need to be in the same folder where the model is. Upon running the PEST executable it calls the model, runs it with the set of initial parameter values listed in the PEST control file, reads the output concentrations in the model output file, and then runs it again after finely perturbing the parameters and the output concentrations are also recorded. The output concentrations, along with the

parameter perturbation ratio, are sufficient for calculating the finite difference terms needed for knowing the sensitivity of each parameter. This sensitivity value is needed by the Levenberg-Marquardt algorithm for calculating the parameter upgrade vector used in updating the parameter value set to a new set. Once the parameter value set is upgraded, the process is repeated again and a new parameter set is calculated. The process is repeated until one of the pre-specified stopping criteria is reached. At that point, the model is run one last time with the optimal set of parameters, and the optimization output files (the PEST record and sensitivity files) are produced and saved. Figure E.1 illustrates the process of optimization as performed by the algorithm used by PEST; u in the figure refers to the parameter upgrade vector shown in Equation (A.8), and Φ being the objective function shown in Equation (A.7).

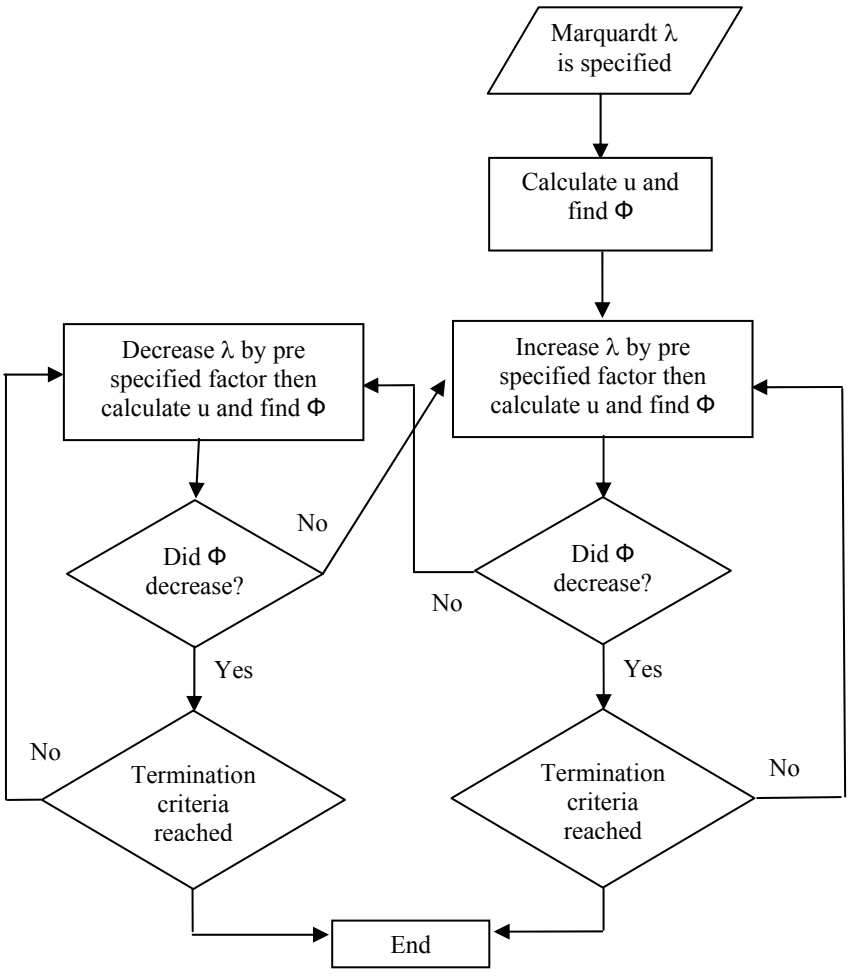

Figure E.1. A diagram of the PEST optimization process

Figures E.3 to E.5 are screen captures of a sample of the PEST control, instruction and template files used in the study:

```
pcf
* control data
restart  estimation
    2     24     2     0     1
    1     4 double point   1   0   0
  5.0   5.0   0.3  0.01    10
  0.75 5.0 0.001  0
  0.1
   30  0.001     3     3  0.01     3
    1     1     1
* parameter groups
HSCPCE       relative 0.01  0.0  switch  2.0 parabolic
ICPCESO4       relative 0.01  0.0  switch  2.0 parabolic
* parameter data
HSCPCE      none relative   0.329362    0.00000001         100.00000    HSCPCE         1.0000         0.0000      1
ICPCESO4      none relative   52.2681   0.00000001         100.00000    ICPCESO4       1.0000         0.0000      1
* observation groups
obsgroup
* observation data
PCEKBA-34               3.5000          1.0  obsgroup
PCEUSGS-2               0.002           1.0  obsgroup
PCEKBA-11-13A           0.0005          1.0  obsgroup
PCEUSGS-5               0.0     1.0  obsgroup
PCEUSGS-10              0.0     1.0  obsgroup
PCEKBA-11-37            0.0     1.0  obsgroup
TCEKBA-34               1.000           1.0  obsgroup
TCEUSGS-2               0.511           1.0  obsgroup
TCEKBA-11-13A           0.033           1.0  obsgroup
TCEUSGS-5               0.0001          1.0  obsgroup
TCEUSGS-10              0.0001          1.0  obsgroup
TCEKBA-11-37            0.0001          1.0  obsgroup
DCEKBA-34               0.000           1.0  obsgroup
DCEUSGS-2               1.270      1.0  obsgroup
DCEKBA-11-13A           0.158     1.0  obsgroup
DCEUSGS-5               0.054     1.0  obsgroup
DCEUSGS-10              0.024     1.0  obsgroup
DCEKBA-11-37            0.010     1.0  obsgroup
VCKBA-34               0.000           1.0  obsgroup
VCUSGS-2               0.112      1.0  obsgroup
VCKBA-11-13A           0.076           1.0  obsgroup
VCUSGS-5              0.166     1.0  obsgroup
VCUSGS-10            0.031     1.0  obsgroup
VCKBA-11-37          0.002     1.0  obsgroup
* model command line
sishell
* model input/output
PCE.tpl  model.chl
PCE.ins  mt3d007.obs
TCE.ins  mt3d008.obs
DCE.ins  mt3d009.obs
VC.ins   mt3d010.obs
* prior information
```

Figure E.2. Screen capture of a sample PEST control file

```
pif $

156 $7300.0$ (PCEKBA-34)22:34 (PCEUSGS-2)35:49 (PCEKBA-11-13A)50:63
(PCEUSGS-5)64:77 (PCEUSGS-10)78:91 (PCEKBA-11-37)92:106
```

Figure E.3. Screen capture of a sample PEST instructions file

```
ptf #
 T          0
******* Chlorinated Compound Minimum Concentrations *******
0.0
0.0
0.0
0.0
0.0
0.0
******* Biomass Starting Concentrations *******
       100          0          (16E14.5)         -1
2.50000E-01   2.50000E-01   2.50000E-01   2.50000E-01   2.50000E-01   2.50000E-01   2.50000E-01   2.50000E-01   2.50000E-01
2.50000E-01   2.50000E-01   2.50000E-01   2.50000E-01
2.50000E-01   2.50000E-01   2.50000E-01   2.50000E-01   2.50000E-01   2.50000E-01   2.50000E-01   2.50000E-01   2.50000E-01
2.50000E-01   2.50000E-01   2.50000E-01   2.50000E-01
2.50000E-01   2.50000E-01   2.50000E-01   2.50000E-01   2.50000E-01   2.50000E-01   2.50000E-01   2.50000E-01   2.50000E-01
2.50000E-01   2.50000E-01   2.50000E-01   2.50000E-01
2.50000E-01   2.50000E-01   2.50000E-01   2.50000E-01   2.50000E-01   2.50000E-01   2.50000E-01   2.50000E-01   2.50000E-01
2.50000E-01   2.50000E-01   2.50000E-01   2.50000E-01
2.50000E-01   2.50000E-01   2.50000E-01   2.50000E-01   2.50000E-01   2.50000E-01   2.50000E-01   2.50000E-01   2.50000E-01
2.50000E-01   2.50000E-01   2.50000E-01   2.50000E-01
2.50000E-01   2.50000E-01   2.50000E-01   2.50000E-01   2.50000E-01   2.50000E-01   2.50000E-01   2.50000E-01   2.50000E-01
2.50000E-01   2.50000E-01   2.50000E-01   2.50000E-01
2.50000E-01   2.50000E-01   2.50000E-01   2.50000E-01   2.50000E-01   2.50000E-01   2.50000E-01   2.50000E-01   2.50000E-01
2.50000E-01   2.50000E-01   2.50000E-01   2.50000E-01
2.50000E-01   2.50000E-01   2.50000E-01   2.50000E-01   2.50000E-01   2.50000E-01   2.50000E-01   2.50000E-01   2.50000E-01
2.50000E-01   2.50000E-01   2.50000E-01   2.50000E-01
2.50000E-01   2.50000E-01   2.50000E-01   2.50000E-01   2.50000E-01   2.50000E-01   2.50000E-01   2.50000E-01   2.50000E-01
2.50000E-01   2.50000E-01   2.50000E-01   2.50000E-01
2.50000E-01   2.50000E-01   2.50000E-01   2.50000E-01   2.50000E-01   2.50000E-01   2.50000E-01   2.50000E-01   2.50000E-01
2.50000E-01   2.50000E-01   2.50000E-01   2.50000E-01
2.50000E-01   2.50000E-01   2.50000E-01   2.50000E-01   2.50000E-01   2.50000E-01   2.50000E-01   2.50000E-01   2.50000E-01
2.50000E-01   2.50000E-01   2.50000E-01   2.50000E-01
2.50000E-01   2.50000E-01   2.50000E-01   2.50000E-01   2.50000E-01   2.50000E-01   2.50000E-01   2.50000E-01   2.50000E-01
2.50000E-01   2.50000E-01   2.50000E-01   2.50000E-01
2.50000E-01   2.50000E-01   2.50000E-01   2.50000E-01   2.50000E-01   2.50000E-01   2.50000E-01   2.50000E-01   2.50000E-01
2.50000E-01   2.50000E-01   2.50000E-01   2.50000E-01
2.50000E-01   2.50000E-01   2.50000E-01   2.50000E-01   2.50000E-01   2.50000E-01   2.50000E-01   2.50000E-01   2.50000E-01
2.50000E-01   2.50000E-01   2.50000E-01   2.50000E-01
2.50000E-01   2.50000E-01   2.50000E-01   2.50000E-01   2.50000E-01   2.50000E-01   2.50000E-01   2.50000E-01   2.50000E-01
2.50000E-01   2.50000E-01   2.50000E-01   2.50000E-01
2.50000E-01   2.50000E-01   2.50000E-01   2.50000E-01   2.50000E-01   2.50000E-01   2.50000E-01   2.50000E-01   2.50000E-01
2.50000E-01   2.50000E-01   2.50000E-01   2.50000E-01
2.50000E-01   2.50000E-01   2.50000E-01   2.50000E-01   2.50000E-01   2.50000E-01   2.50000E-01   2.50000E-01   2.50000E-01
2.50000E-01   2.50000E-01   2.50000E-01   2.50000E-01
2.50000E-01   2.50000E-01   2.50000E-01   2.50000E-01   2.50000E-01   2.50000E-01   2.50000E-01   2.50000E-01   2.50000E-01
2.50000E-01   2.50000E-01   2.50000E-01   0.00000E+00
0.001
******* Yield Coefficients *******
0.0
0.0
0.0
0.0
******* Chlorinated Ethene Inhibition Terms *******
******* Inhibition of PCE *******
10
18.931100
#ICPCESO4#
******* Inhibition of TCE *******
10
46.474200
44.269600
.00111624
******* Inhibition of DCE *******
10
10.295700
.26800700
.00260490
4.8790E-4
******* Inhibition of VC *******
10
4.17156000
9.86095000
.064825800
.075045100
.192996000
******* Chlorinated Ethene Stoichiometric Factors *******
0.79230000
0.21410000
0.73790000
0.27020000
0.64470000
0.36620000
0
0.44890000
0.56800000
******* Half Saturation Constants for Reductive Dechlorination *******
# HSCPCE #
10.1698375
7.42937142
5.96998127
******* Maximum Specific Rate of Reductive Dechlorination *******
0.06598788
0.30042609
0.40823166
0.00459259
```

Figure E.4. Screen capture of a sample PEST template file